AD-A156 463 USE OF THE WAVENUMBER TECHNIQUE WITH THE LLOYDS MIRROR FOR AN ACOUSTIC DOUBLET(U) NAVAL POSTGRADUATE SCHOOL MONTEREY CA P B KING MAR 85 1/2

UNCLASSIFIED F/G 17/1 NL

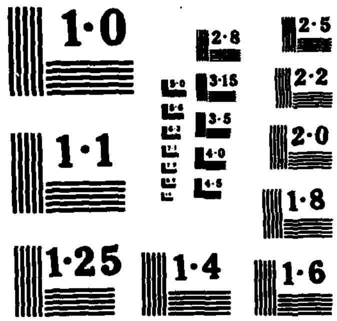

NATIONAL BUREAU OF STANDARDS
MICROCOPY RESOLUTION TEST CHART

UNCLASSIFIED

SECURITY CLASSIFICATION OF THIS PAGE (When Data Entered)

REPORT DOCUMENTATION PAGE		READ INSTRUCTIONS BEFORE COMPLETING FORM
1. REPORT NUMBER	2. GOVT ACCESSION NO. AD-A156 463	3. RECIPIENT'S CATALOG NUMBER
4. TITLE (and Subtitle) Use of the Wavenumber Technique With the Lloyds Mirror For an Acoustic Doublet		5. TYPE OF REPORT & PERIOD COVERED Master's Thesis March 1985
		6. PERFORMING ORG. REPORT NUMBER
7. AUTHOR(s) Portia Baird King		8. CONTRACT OR GRANT NUMBER(s)
9. PERFORMING ORGANIZATION NAME AND ADDRESS Naval Postgraduate School Monterey, California 93943		10. PROGRAM ELEMENT, PROJECT, TASK AREA & WORK UNIT NUMBERS
11. CONTROLLING OFFICE NAME AND ADDRESS Naval Postgraduate School Monterey, California 93943		12. REPORT DATE March 1985
		13. NUMBER OF PAGES 112
14. MONITORING AGENCY NAME & ADDRESS(if different from Controlling Office)		15. SECURITY CLASS. (of this report)
		15a. DECLASSIFICATION/DOWNGRADING SCHEDULE

16. DISTRIBUTION STATEMENT (of this Report)

Approved for Public Release; Distribution is Unlimited.

17. DISTRIBUTION STATEMENT (of the abstract entered in Block 20, if different from Report)

18. SUPPLEMENTARY NOTES

19. KEY WORDS (Continue on reverse side if necessary and identify by block number)

Lloyds Mirror; Underwater Acoustics; Fast Fourier Transform; Wavenumber Technique; Pressure Spectrum; Source Depth Determination; Acoustic Propagation; ~~ASW~~, Isospeed Environment

20. ABSTRACT (Continue on reverse side if necessary and identify by block number)

This thesis examines a method to determine the depth of a point source in an isospeed ocean environment. Using the Fourier Transform on the acoustic pressure field in the range domain results in the attainment of the acoustic pressure spectrum in the wavenumber domain and a characteristic nodal spacing unique to the source-receiver depths. Quantitative examination of a magnitude plot of the spectrum and use of simple mathematical formulae yield the source depth. The debilitative effects of narrowband

DD FORM 1 JAN 73 1473 EDITION OF 1 NOV 65 IS OBSOLETE

S N 0102-LF-014-6601

UNCLASSIFIED

SECURITY CLASSIFICATION OF THIS PAGE (When Data Entered)

noise and surface roughness on the pressure spectrum are also examined. The pressure spectrum is recognizable in noise after the pressure field in the range domain has been lost in the noise field. The effect of surface gravity waves on the pressure spectrum is similar to that on the pressure field in the range domain: the characteristic nodal spacing is suppressed as the height of the surface waves increases.

Approved for public release; distribution is unlimited.

Use of the Wavenumber Technique
With the Lloyds Mirror
For an Acoustic Doublet

by

Portia B. King
Lieutenant Commander, United States Navy
B.S., Louisiana State University in New Orleans, 1971

Submitted in partial fulfillment of the
requirements for the degree of

MASTER OF SCIENCE IN SYSTEMS TECHNOLOGY
(Antisubmarine Warfare)

from the

NAVAL POSTGRADUATE SCHOOL
March 1985

Dist A-1

Author: Portia B. King
Portia B. King

Approved by:
A. B. Coppens, Thesis Advisor

C. R. Dunlap, Thesis Advisor

R. N. Forrest, Chairman,
Antisubmarine Warfare Academic Group

David A. Schrady,
Academic Dean

ABSTRACT

This thesis examines a method to determine the depth of a point source in an isospeed ocean environment. Using the Fourier Transform on the acoustic pressure field in the range domain results in the attainment of the acoustic pressure spectrum in the wavenumber domain and a characteristic nodal spacing unique to the source-receiver depths. Quantitative examination of a magnitude plot of the spectrum and use of simple mathematical formulae yield the source depth. The debilitative effects of narrowband noise and surface roughness on the pressure spectrum are also examined. The pressure spectrum is recognizable in noise after the pressure field in the range domain has been lost in the noise field. The effect of surface gravity waves on the pressure spectrum is similar to that on the pressure field in the range domain: the characteristic nodal spacing is suppressed as the height of the surface waves increases.

TABLE OF CONTENTS

LIST OF TABLES

LIST OF FIGURES

LIST OF SYMBOLS

A	Amplitude
c	Sound Speed
e	2.718281828...
FFT	Fast Fourier Transform
FFT^{-1}	Inverse Fast Fourier Transform
f	Frequency
$\underset{\sim}{f}(r)$	Generic Function of Range
$\underset{\sim}{g}(\gamma)$	Spectral Density of $\underset{\sim}{f}(r)$
H_0	Hankel Function
i	Square Root of -1
J_0	Bessel Function of the First Kind
k	Wavenumber
M	Surface Roughness Factor
m	Index of Calculations or Null Number in the Range Domain
N	Number of Points in the Wavenumber Spectrum

n	Index of Calculations or Null Number in the Wavenumber Spectrum
$\underset{\sim}{n}$	Complex Narrowband Noise Field
$\underset{\sim}{P}$	Time Independent Factor of Complex Pressure
$\underset{\sim}{P}_s$	Complex Pressure of the Source
$\underset{\sim}{P}_i$	Complex Pressure of the Reflection
$\underset{\sim}{P}_N$	Complex Pressure in the Presence of Noise
$\underset{\sim}{P}(k)$	Pressure Field in the Wavenumber Spectrum
$\underset{\sim}{p}$	Time Dependent Factor of Complex Pressure
R_1	Distance of the Direct Wave Path
R_2	Distance to the Image (Reflected Path)
RCVR	Receiver
r	Range Between Source and Receiver
SRC	Source
t	time factor
W	Hanning Window
Y_0	Bessel Function of the Second Kind
Z_S	Source Depth

z_r	Receiver Depth
Δr	Range Increment
β	Vertical Component of the Wavenumber
$\Delta\beta$	Vertical Wavenumber Increment
γ	Horizontal Component of the Wavenumber
$\Delta\gamma$	Horizontal Wavenumber Increment
θ	Angle of Grazing Incidence at the Surface
λ	Wavelength
π	3.14159265...
φ	Phase Angle
ψ_R	Surface Reflection Coefficient
ω	Angular Frequency
$\sqrt{}$	Square Root Operator
$\int$	Integration Operator

ACKNOWLEDGEMENTS

Contrary to popular opinion, this part of the thesis was the hardest to write because, for several reasons, it is the most important part of this entire undertaking. I encountered many difficulties during the course of this research; solutions to all the myriad problems were found eventually. Let me express heartfelt gratitude for the help and guidance of three experts in the field of acoustics: Dr. A. B. Coppens, Dr. T. Gabrielson, and Dr. Suk Wang Yoon, for the support of Professor C. R. Dunlap, for the help of Dr. DeWayne White of N.O.R.D.A in understanding the FFT, and the relatively minor but ever-so-important helpful hints and good wishes of my peers and fellow officers in the class of IX-33. Most of the mathematics and much of the direction for the research came from Professors Coppens and Gabrielson. Indeed, this thesis would not have been written without Professor Coppens' patience and leadership. Each person played a role, whether major or minor, in getting this thesis done. Without them, this paper would remain just another unfulfilled wish.

And, last but not least, I wish to thank a very special person for his support, cajolery, laughter, faith and other expressions of his love for me - my husband, Dr. David Benton King. Whenever I look back at what went into the writing of this paper, I shall always remember that I met him for the first time at the start of all the research that has gone into it. I shall also remember that, if I had never come to the Naval Postgraduate School, I would never have met him. And for that, I shall always be grateful to the United States Navy.

I. HISTORY AND INTRODUCTION

This thesis is the third in a series of investigations into a proposal put forth by R. Lauer of Naval Underwater Systems Center, New London, CT, in 1979. In his memorandum [Ref. 1], Lauer describes a "new" way to analyze sound propagation in the ocean and two applications of the method, which he named the "Wavenumber Technique," or W.T. In his proposal, Lauer stated that a source of sound in the ocean could be pinpointed in both depth and range by a single omnidirectional hydrophone provided the source is generating a continuous wave tone.

The W.T. was initially described by F. DiNapoli [Ref. 2] as an intermediary step in his development of a speedier computer algorithm used in analyzing sound propagation as a function of range. DiNapoli and Lauer proposed converting the pressure as a function of range $\underset{\sim}{p}(r)$ to the pressure spectrum as a function of the wavenumber $\underset{\sim}{p}(k)$. The conversion is accomplished by taking a weighted Fourier transform of the pressure field $\underset{\sim}{p}(r)$. Once the pressure spectrum is obtained, analysis of the pressure field can be accomplished in a manner analogous to that presently used in signal processing.

Lauer proposed two uses for his "Wavenumber Technique:"

1. determination of the depth of the acoustic source, an ability which has obvious tactical applications;
2. use of the W.T. to evaluate the accuracy of existing, and future, acoustic models such as P.E. and F.A.C.T., by breaking the generated pressure field down into ray path "families," such as bottom-bounce, refracted-surface-reflected, and surface-ducted families, thus giving a quantitative read-out of what

proportion of the total acoustic energy is being channelled through the various ray paths.

For both uses, a knowledge of the acoustic environment is necessary.

It is the intended purpose of this thesis to investigate the validity of the first application of Lauer's wavenumber technique by using it in conjunction with an acoustic phenomenon that is well-known and for which accurate results can be calculated with precision; this phenomenon is the LLoyds Mirror for an Acoustic Doublet. Using several source/receiver combinations, this investigator intends to compare actual source depth with that predicted by the W.T. If Lauer's technique is cogent, the source depths calculated via the two methods should be equal, or very close within a statistically acceptable degree.

As mentioned in the beginning of this thesis, two prior investigators, B. Stamey and J. Blanchard, looked into applying the W.T. to determining source depth. Stamey's investigation [Ref. 3] utilized a parabolic equation computer model developed by H.K. Brock, the Split Step Fast Fourier Transform, or SSFFT, to generate the pressure fields. He qualitatively compared the model to a Normal Mode model and a P. E. Finite Difference model, both range dependent, and to DiNapoli's Fast Field Program model, a range independent model. Stamey concluded that the W.T. showed promise as an analysis tool and that further investigations were warranted.

J. Blanchard carried Stamey's researches one step further [Ref. 4]. Using two Parabolic Equation computer algorithms, Brock's Split Step Fast Fourier Transform and Jaeger's Implicit Finite Difference, as his pressure field generators, he examined the use of the spacing between nulls of the pressure spectrum to determine source depth. His results are interesting and support the need for further investigation.

The author was not satisfied with Stamey's and Blanchard's findings. Both individuals acknowledged shortcomings in their respective studies, especially with regard to the mutual presence of the "U-shaped phenomenon" encountered in the pressure spectrum. One should remember, however, that their theses were preliminary studies only and were produced within a highly restricted time frame. Also, they used existing computer algorithms specifically designed to approximate acoustic propagation in a velocity-variant medium. However, the environmental settings used by both gentlemen were that of the Lloyds Mirror for an Acoustic Doublet which requires a constant sound speed throughout the water column; thus, the approximations, assumptions and "fudge factors" used by these models make their results for an isospeed medium highly artificial and somewhat suspect. Fortunately, however, there exists for the Lloyds Mirror a simple, geometric solution specifically designed for an isospeed environment [Ref. 5]. Since the pressure fields for varying source and receiver depths and, therefore, the corresponding pressure spectra, can be precisely calculated, it was thought this model would be a good check on the operational applicability of Lauer's proposed technique.

Secondary considerations of this study were to examine what effect, if any, the introductions of, firstly, surface waves and, secondly, noise would have on the pressure spectrum. The first objective was simulated by use of mathematical formulae given in reference 5; for the second objective, it was thought that complex noise, random in both amplitude and phase and similar to a Rician distribution [Ref. 6: p. 189], would provide a simple but reasonable approximation of an ocean noise field. This investigator intends to gradually intensify the surface waves and the noise field, separately, until the original pressure spectrum is no longer recognizable. In this manner, it should

be possible to make a qualitative assessment of their respective debilitating effects under the carefully controlled conditions found in the Lloyds Mirror phenomenon.

Section II sets forth in more detail the theoretical development of each point described in this introduction. Section III summarizes the investigator's results and the conclusions drawn from those results. Section IV contains a listing of the computer algorithms utilized.

II. THEORY

This chapter presents the mathematical basis of the wavenumber technique.

A. THE LLOYDS MIRROR PHENOMENON

A diverging monofrequency spherical pressure wave [Ref. 5: p.112] can be written in complex form as

$$\underset{\sim}{p}(R,t) = \underset{\sim}{P}(R)e^{-i\omega t} = \frac{A}{R}e^{i(kR-\omega t)} \qquad \text{(eqn 2.1)}$$

where $\underset{\sim}{P}(R)$ is the spatial factor. Referring to Figure 2.1, R_1 is the range from the source to the receiver and R_2 is the range from the image to the receiver. For convenience in all that follows, we shall set A to unit magnitude. The following equations apply to the acoustic waves propagating directly out from the source $\underset{\sim}{p}_s$ and from the apparent image $\underset{\sim}{p}_i$ (which is actually the wave reflected from the surface):

$$\underset{\sim}{p}_s(R,t) = \underset{\sim}{P}_s(R)e^{-i\omega t} = \frac{1}{R_1}e^{i(kR_1-\omega t)}$$

$$\underset{\sim}{p}_i(R,t) = \underset{\sim}{P}_i(R)e^{-i\omega t} = \frac{-1}{R_2}e^{i(kR_2-\omega t)} \qquad \text{(eqn 2.2)}$$

where $\underset{\sim}{p}$, $\underset{\sim}{p}_s$, and $\underset{\sim}{p}_i$ are complex functions of horizontal range r, vertical depth Z and time t; the minus sign in the equation for $\underset{\sim}{p}_i$ is derived from the surface reflection coefficient, $\psi_R = -1$, for a smooth surface. Inspection of Figure 2.1 reveals that

$$R_1 = \sqrt{(z_r - z_s)^2 + r^2}, \qquad R_2 = \sqrt{(z_r + z_s)^2 + r^2},$$

and $\Delta r = \left| R - R_{1,2} \right|$

And so the total field can be written as

$$\underset{\sim}{p}_s - \underset{\sim}{p}_i = \underset{\sim}{P}(R)e^{-i\omega t} = \frac{e^{i(kR_1 - \omega t)}}{R_1} - \frac{e^{i(kR_2 - \omega t)}}{R_2} \qquad \text{(eqn 2.3)}$$

Since $\underset{\sim}{p}_s$ and $\underset{\sim}{p}_i$ both have the same time factor, $\exp(-i\omega t)$, we can retain just the spatial factors and equations 2.3 reduce to

$$\underset{\sim}{P}(R) = \left[\frac{e^{ikR_1}}{R_1} - \frac{e^{ikR_2}}{R_2} \right] \qquad \text{(eqn 2.4)}$$

Equation 2.4 is a form of the complex pressure as a function of range used in the computer algorithm shown in Appendix I.

Inspection of Figure 2.1 reveals that, for $R \gg Z_s$ and θ very small,

$$r \approx R$$

or

$$\sin\theta \approx \frac{Z_r}{R}$$

or

$$\Delta r \approx \frac{Z_r Z_s}{R} \qquad \text{(eqn 2.5)}$$

and the pressure amplitude can be approximated by

$$\underset{\sim}{P}(R) \approx \frac{2}{R} \left| \sin\left(\frac{kZ_r Z_s}{R}\right) \right| \qquad \text{(eqn 2.6)}$$

Looking at just the formula for the pressure amplitude, we can see that as

$$\left(\frac{k z_r z_s}{R}\right) \longrightarrow n\pi \,, \quad n=0,1,2,3,\ldots \qquad \text{(eqn 2.7)}$$

the pressure amplitude goes to zero, producing the classic $|P(R)|$ vs R curve shown in Figure 2.2

B. THE RELATIONSHIP BETWEEN K, γ, AND β

In his description of the Wavenumber Technique [Ref. 1: p. 5-6], Lauer utilizes the horizontal and vertical components of the wavenumber, k. The general relationship amoung these three terms is illustrated in Figure 2.3 and can be written mathematically as

k = the wavenumber $\doteq 2\pi f/c$

γ = the horizontal component of k = $k \cos\varphi$

β = the vertical component of k = $k \sin\varphi$

or

$$k = \sqrt{\gamma^2+\beta^2} \qquad \text{(eqn 2.8)}$$

C. THE WAVENUMBER TECHNIQUE AND THE LLOYDS MIRROR

Given a point source in free space, the monofrequency pressure field at the receiver, $\underset{\sim}{P}(R)$, can be expressed as a spherical wave (time factor suppressed),

$$\underset{\sim}{p}(R) = \frac{e^{ikR}}{R} \qquad \text{(eqn 2.9)}$$

where, from Figure 2.1,

$$R^2 = r^2 + Z_r^{\ 2}\ , \text{ for } Z_r > Z_s$$

or

$$R^2 = r^2 + Z_s^{\ 2}\ , \text{ for } Z_r < Z_s \qquad \text{(eqn 2.10)}$$

In integral form, $\underset{\sim}{p}(R)$ can be written as [Ref. 7: p. 127]

$$\underset{\sim}{p}(R) = \frac{e^{ikR}}{R} = \int_0^\infty \frac{J_0(\gamma r)\, e^{\pm i\beta|z_r - z_s|}}{i\beta}\, \gamma\, d\gamma \qquad \text{(eqn 2.11)}$$

which is taken from the Fourier-Bessel Transform Pair [Ref. 7: p. 126],

$$\underset{\sim}{f}(r) = \int_0^\infty \underset{\sim}{g}(\gamma)\, J_0(\gamma r)\, \gamma\, d\gamma$$

$$\underset{\sim}{g}(\gamma) = \int_0^\infty f(r)\, J_0(\gamma r)\, r\, dr \qquad \text{(eqn 2.12)}$$

where $\underset{\sim}{f}(r)$ represents the acoustic pressure function in the range domain, and $\underset{\sim}{g}(\gamma)$ is the acoustic pressure spectrum in the wavenumber domain. The sign of the exponential function in the integral is based on which of Z_s and Z_r is greater. For the case of receiver depth being greater than source depth so that waves from both image and source are travelling downward at the receiver depth, the total pressure at the receiver can be expressed as

$$\underset{\sim}{p}(R) = \int_0^\infty \frac{e^{i\beta(z_r - z_s)} - e^{i\beta(z_r + z_s)}}{i\beta}\, J_0(\gamma r)\, \gamma\, d\gamma \qquad \text{(eqn 2.13)}$$

Use of Euler's Identity reduces Equation 2.13 to

$$\mathcal{P}(R) = -2\int_0^\infty \frac{e^{i\beta z_r}\sin(\beta z_s)}{\beta} J_0(\gamma r)\gamma\, d\gamma \qquad \text{(eqn 2.14)}$$

Using the relationship between the Hankel functions [Ref. 5: p. 449],

$$H_0^{(1)}(\gamma r) = J_0(\gamma r) + iY_0(\gamma r)$$

and

$$H_0^{(2)}(\gamma r) = J_0(\gamma r) - Y_0(\gamma r) \qquad \text{(eqn 2.15)}$$

one can re-write the Bessel function in equation 2.14 as

$$J_0(\gamma r) = \frac{1}{2}\left[H_0^{(1)}(\gamma r) + H_0^{(2)}(\gamma r)\right] \qquad \text{(eqn 2.16)}$$

so that

$$2\underset{\sim}{g}(\gamma) = \int_0^\infty \underset{\sim}{f}(r) H_0^{(1)}(\gamma r) r\, dr + \int_0^\infty \underset{\sim}{f}(r) H_0^{(2)}(\gamma r) r\, dr \qquad \text{(eqn 2.17)}$$

Letting r' = -r and looking at the second term on the right hand side of equation 2.17,

$$\int_0^{-\infty} \underset{\sim}{f}(-r') H_0^{(2)}(-\gamma r') r'\, dr' = \int_{-\infty}^0 \underset{\sim}{f}(-r) H_0^{(1)}(\gamma r) r\, dr \qquad \text{(eqn 2.18)}$$

Now, assuming that $\underset{\sim}{f}(r) = \underset{\sim}{f}(-r)$, then

$$2\underset{\sim}{g}(\gamma) = \int_{-\infty}^\infty \underset{\sim}{f}(r) H_0^{(1)}(\gamma r) r\, dr \qquad \text{(eqn 2.19)}$$

Therefore,

$$\underset{\sim}{p}(R) = -\int_{-\infty}^{\infty} \frac{\gamma H_0^{(1)}(\gamma r)}{\beta} e^{i\beta z_r} \sin(\beta z_s)\, d\gamma \qquad \text{(eqn 2.20)}$$

For $\gamma r > 2\pi$, the asymptotic approximation of the Hankel function for large argument can be used:

$$H_0^{(1)}(\gamma r) \approx \sqrt{\frac{2}{\pi \gamma r}}\; e^{i(\gamma r - \frac{\pi}{4})} \qquad \text{(eqn 2.21)}$$

assuming $|r\, \underset{\sim}{f}(r)|$ goes to zero faster than (ln r),

$$\underset{\sim}{p}(R) \approx -\sqrt{\frac{2}{\pi r}}\; e^{-i\frac{\pi}{4}} \int_{-\infty}^{\infty} \left[\frac{\sqrt{\gamma}}{\beta} e^{i\beta z_r} \sin(\beta z_s)\right] e^{i\gamma r}\, d\gamma \qquad \text{(eqn 2.22)}$$

Let the terms inside the brackets in equation 2.22 be defined as $\underset{\sim}{g}(\gamma)$, then

$$\underset{\sim}{p}(R) = -\sqrt{\frac{2}{\pi r}}\; e^{-i\frac{\pi}{4}} \int_{-\infty}^{\infty} \underset{\sim}{g}(\gamma)\, e^{i\gamma r}\, d\gamma$$

and

$$\int_{-\infty}^{\infty} g(\gamma) e^{i\gamma r}\, d\gamma = -\sqrt{\frac{\pi r}{2}} \sqrt{r}\; \underset{\sim}{p}(R) \qquad \text{(eqn 2.23)}$$

or, using equation 2.12,

$$\underset{\sim}{g}(\gamma) = -\left[e^{i\frac{\pi}{4}}\right] \sqrt{\frac{\pi}{2}}\, \frac{1}{2\pi} \int_{-\infty}^{\infty} \sqrt{r}\; \underset{\sim}{p}(R)\, e^{-i\gamma r}\, dr \qquad \text{(eqn 2.24)}$$

Note that equation 2.24 has the form of the Fourier transform of the pressure function if we define

$$\underset{\sim}{f}(r) \equiv \sqrt{r}\; \underset{\sim}{p}(R) \qquad \text{(eqn 2.25)}$$

so that $\sqrt{r}\, p(R)$ and $g(\gamma)$ are Fourier Transform pairs. This equation can be easily evaluated [Ref. 8],

$$g(\gamma) = -\left[e^{i\frac{\pi}{4}}\right]\frac{1}{\sqrt{2\pi}}\left[\frac{\sqrt{\gamma}}{\beta}\, e^{i\beta z_r} \sin(\beta z_s)\right] \qquad \text{(eqn 2.26)}$$

for $Z_r > Z_s$. And the magnitude of $g(\gamma)$ is

$$\left|g(\gamma)\right| = \frac{\sqrt{\gamma}}{\beta} \sin(\beta z_s) \qquad \text{(eqn 2.27)}$$

For the case where $Z_s > Z_r$, it can be shown that

$$g(\gamma) = -\frac{e^{i\frac{\pi}{4}}}{\sqrt{2\pi}}\left[\frac{\sqrt{\gamma}}{\beta}\, e^{i\beta z_s} \sin(\beta z_r)\right] \qquad \text{(eqn 2.28)}$$

and the magnitude of $g(\gamma)$ is

$$\left|g(\gamma)\right| = \frac{\sqrt{\gamma}}{\beta} \sin(\beta z_r) \qquad \text{(eqn 2.29)}$$

A close look at the magnitude of the pressure spectrum function in equation 2.27 reveals that nodes occur for values of

$$\beta Z_s = n\pi \quad , \; n = 0,1,2,3,\ldots \qquad \text{(eqn 2.30)}$$

If the magnitude of the pressure spectrum is plotted as a function of the vertical wavenumber then the spacing between nodes $\Delta\beta$ is uniform and the depth of the source can be derived from the relationship given by

$$Z_s = \frac{\pi}{\Delta\beta} \qquad \text{(eqn 2.31)}$$

In the event the source is deeper than the receiver, looking at equation 2.29, we can see that nodes now occur for values of

$$\beta Z_r = n\pi \quad , n = 0,1,2,3,\ldots \qquad \text{(eqn 2.32)}$$

Plotting equation 2.29 as a function of the vertical wavenumber, the spacing between nodes will now reveal the receiver depth based on

$$Z_r = \frac{\pi}{\Delta\beta} \qquad \text{(eqn 2.33)}$$

Notice in equations 2.31 and 2.33 the exchange of source and receiver depths. By placing the receiver at a shallower depth than the source, no new information (namely the source depth) is to be found.

In summary, there is a way to calculate the complex pressure amplitude as a function of range using the complex pressure spectrum. Conversely, if the complex pressure $\underset{\sim}{p}(r)$ has been measured at the receiver, then the complex pressure spectrum $\underset{\sim}{p}(k)$ can be derived by making use of the relationship between the Fourier-Bessel Transform Pairs (see equation 2.12), and the depth of the source can be found from the magnitude of that spectrum (see equation 2.31).

The foregoing is the mathematics involved in deriving the theoretical pressure spectrum. One purpose of this thesis was to compare the theoretical value of the pressure spectrum as derived with the Fourier-Bessel Transform with the pressure spectrum obtained by use of the computerized Discrete Fourier Transform (DFT), otherwise known as the Fast Fourier Transform, or FFT. At this point, it will be helpful to review what happens in the FFT.

Starting with the Fourier-Bessel transform pair shown in equation 2.12, $\underset{\sim}{f}(r)$ and $\underset{\sim}{g}(\gamma)$ can be re-written in terms of a discrete sum as is done in the DFT:

$$FFT^{-1}\left\{ \underset{\sim}{g}(\gamma) \right\} = \sum_{n=0}^{N-1} \underset{\sim}{g}(n\Delta\gamma)\, e^{i\frac{2\pi mn}{N}} = \underset{\sim}{f}(m\Delta r) \qquad \text{(eqn 2.34)}$$

where $N = 1,2,3,\ldots,$ up to some large positive integer, and represents the number of transform points, and

$$\gamma r = (n\Delta\gamma)(m\Delta r) = \frac{2\pi mn}{N} \qquad \text{(eqn 2.35)}$$

based on the relationship between Δr and $\Delta\gamma$ as described in sampling theory [Ref. 2: p. 2],

$$\Delta\gamma\Delta r = \frac{2\pi}{N}$$

or

$$\Delta r = \frac{2\pi}{N\Delta r} \qquad \text{(eqn 2.36)}$$

By convention, the sign of the exponential function in equation 2.34 is taken as negative when performing the "forward" transform,

$$FFT\left\{ \underset{\sim}{f}(m\Delta r) \right\} = \underset{\sim}{g}(n\Delta\gamma) \qquad \text{(eqn 2.37)}$$

and is taken as positive when performing the "inverse" transform,

$$FFT^{-1}\left\{g(n\Delta\gamma)\right\} = f(m\Delta r) \qquad \text{(eqn 2.38)}$$

Then, $$\int_{-\infty}^{\infty} g(\gamma)\, e^{i\gamma r}\, d\gamma \approx \left[\sum_{n=1}^{N-1} g(n\Delta\gamma)\, e^{i\frac{2\pi mn}{N}}\right]\Delta\gamma$$

where

$$g(n\Delta\gamma) = \frac{\sqrt{\gamma}}{\beta}\, e^{i\beta z_r} \sin(\beta z_s)$$

Therefore

$$p(m\Delta r) = -\sqrt{\frac{2}{\pi r}}\, e^{-i\frac{\pi}{4}}\left[\Delta\gamma\, FFT^{-1}\left\{g(n\Delta\gamma)\right\}\right]$$

and

$$\left|g(n\Delta\gamma)\right| = \frac{\sqrt{\gamma}}{\beta} \sin(\beta z_s) \qquad \text{(eqn 2.39)}$$

D. THE EFFECTS OF SURFACE ROUGHNESS

Surface roughness [Ref. 5: p.409] reduces the Lloyds Mirror effect. The rougher the surface, the greater the effect for angles increasingly closer to grazing incidence. If M represents the surface roughness factor, then equation 2.3 can be re-written as

$$P(R) = \frac{e^{ikR}}{R} - e^{-M^2}\frac{e^{ikR}}{R}$$

where

$$M \equiv \frac{4H \sin\phi}{\lambda} \qquad \text{(eqn 2.40)}$$

ϕ is the grazing angle of incidence, H is the average height of the surface gravity waves, and λ is the wavelength of the narrowband continuous wave acoustic signal. When M is less than 1, the surface is said to be smooth; when M is greater than 1, the surface is said to be rough.

Looking at Figure 2.1, we can see that the overall effect of increasing surface roughness is to reduce the contribution of the surface reflection or "image" to the interference pattern at the receiver. In other words, as H increases, the energy detected by the receiver is increasingly only the energy coming directly from the source. When the effect of surface roughness is a maximum such that the contribution to the pressure field of the "image" is completely suppressed, then

$$g_s(\gamma) = \int_0^\infty \frac{e^{ikR_1}}{R_1} J_0(\gamma r) r\,dr$$

$$= \frac{e^{i\beta|z_s - z_r|}}{i\beta} \qquad \text{(eqn 2.41)}$$

and the magnitude of the spectrum is

$$|g(\gamma)| = \frac{1}{\beta} \qquad \text{(eqn 2.42)}$$

E. THE EFFECT OF ADDING NOISE

In an effort to simulate a realistic ocean environment, a normally distributed narrowband noise field based on a Rician distribution [Ref. 6: p. 189] was adapted. The resulting acoustic pressure field can be expressed as

$$\underset{\sim}{P}_N(R) = \underset{\sim}{P}(R) + \underset{\sim}{n} \qquad \text{(eqn 2.43)}$$

where $\underset{\sim}{n}$ is a normally-distributed random function with a mean of zero, a standard deviation of one and possesses both amplitude and phase. The noise operates independently on both the amplitude and phase components of the pressure field. Since $\underset{\sim}{n}$ is independent of range and wavenumber, it is treated as a constant by the Fourier Transform.

A fourth intention of this thesis was to discover the degree to which noise degrades the wavenumber spectrum compared with the corresponding degradation of the range domain. To produce the random noise fields used in this research, the routine listed as "GGNML" in the IMSL library [Ref. 9] was called upon twice to generate independent, pseudo-random functions which interact separately and simultaneously with both the amplitude and phase components of $\underset{\sim}{P}(R)$. While not an elaborate scheme, owing to time and resource constraints, it was felt that this modest simulacrum of narrowband noise would give a fairly accurate, first cut "feel" for the effects of noise on the wavenumber spectrum. The reader should be aware, however, that no direct consideration of coherency along the range path was taken into account by this method.

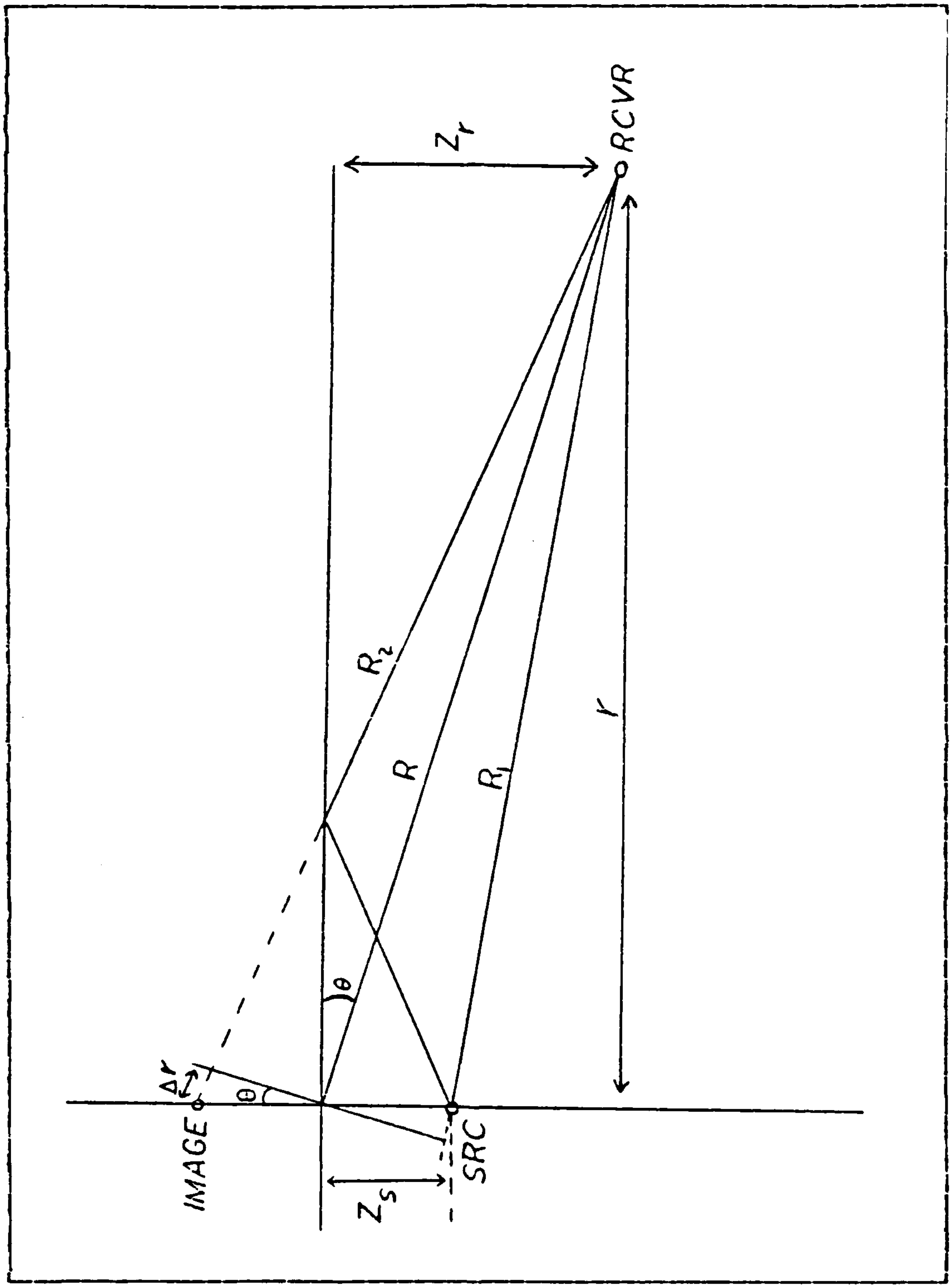

Figure 2.1 The Geometry of the Lloyds Mirror Effect

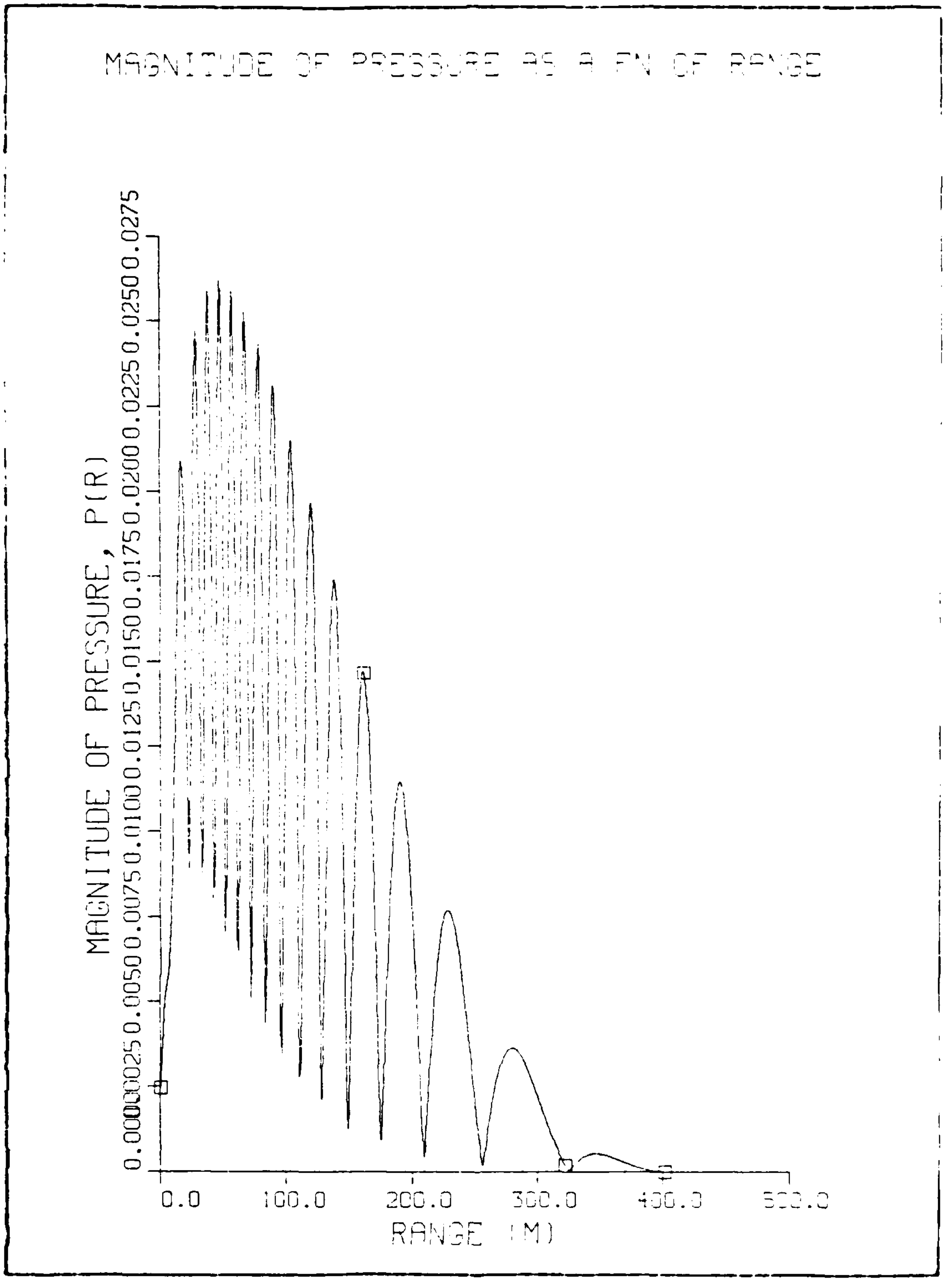

Figure 2.2 A Classic $|P(R)|$ vs. R Curve

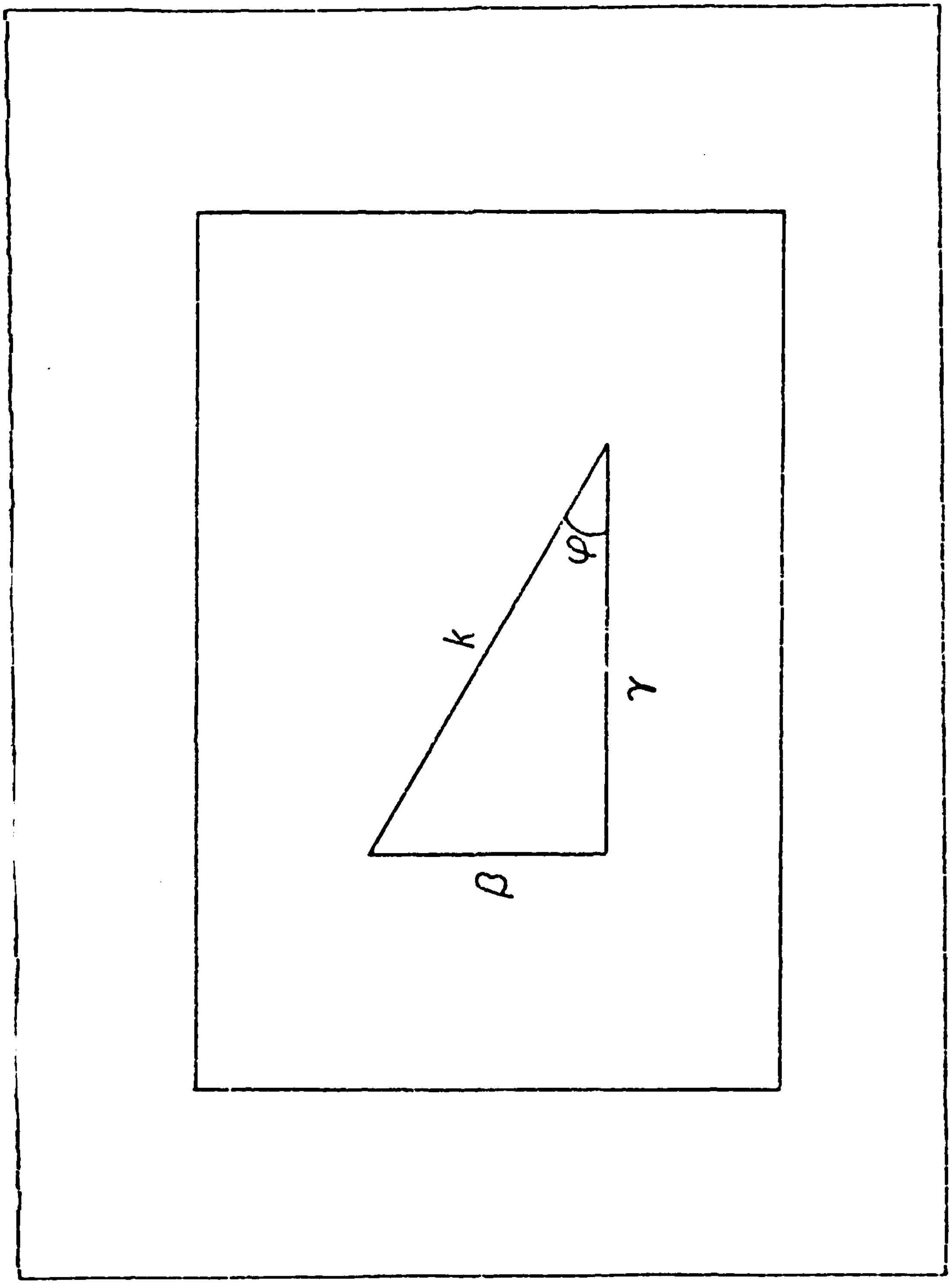

Figure 2.3 The Relationship Between K, γ and β

III. RESULTS AND CONCLUSIONS

A. THE FFT ALGORITHM

The research for this thesis was conducted entirely with computer algorithms to model the Lloyds Mirror, the Fast Fourier Transform, the range windows, waves, and the narrow-band noise. This was necessary since the Lloyds Mirror is an idealized representation of a situation that occurs only rarely in nature, and at that is limited to isospeed surface ducts. Also, time and money constraints were such that the use of computer models was an absolute necessity. For these reasons and because the FFT is the heart of the Wavenumber Technique, finding a reliable, easy-to-use computer algorithm to perform the FFT on the complex pressure function was deemed very important.

Initially, the IMSL library routines, FFT2C and FFTCC [Ref. 9: p. 232], were used to generate the pressure spectra. Although the author was unable to ascertain just how Stamey performed the FFT on his data, it is highly probable that he used an IMSL library routine. While in his thesis, Blanchard stated that he used the FFTCC routine. The magnitude of a typical spectrum generated by the routine FFT2C is shown in Figure 3.1.

The same scenario used to generate Figure 3.1 was used to produce the spectrum shown in Figure 3.2, but the routine FFTCC was utilized. As can be seen, the resulting graphs of the pressure spectrum magnitude are practically identical. Indeed, the set-up of the pressure fields for insertion into each routine differ only in that FFT2C requires a data set consisting of an integral power of two number of points, whereas FFTCC will handle any number of points. And, when

the Cooley-Tukey FFT listed in Appendix I was used to transform the same pressure field as was utilized to produce Figures 3.1 and 3.2, Figure 3.3 was the result. This algorithm differs somewhat from the IMSL routines by the manner in which the pressure field data is treated. Both FFT2C and FFTCC are designed to handle a complex array. The Cooley-Tukey FFT, on the other hand, is designed to transform real data; but the pressure field is complex. To get around this apparent conundrum, the pressure data is defined as either real or imaginary by its placement in the array. As can be seen, the resultant graph of the spectrum magnitude is almost indistinguishable from that produced by either IMSL routine. In conclusion, it does not matter which FFT routine is used to generate the pressure spectrum, as long as the pressure field in the range domain is "fitted" into the array in a manner suitable to the particular algorithm used.

TABLE I

Critical Values Used in the Research

K (m^{-1})	N	r (m)	(m^{-1})
3.0	1024	0.524	1.172×10^{-2}
2.0	1024	0.785	7.816×10^{-3}
1.0	1024	1.571	3.906×10^{-3}

It is important to note four things about the FFT at this point.

1. Since the FFT is given only a finite sample of a function while the theoretical Fourier Transform

looks at the complete function, the computer algorithm is designed to overcome this necessary shortcoming by assuming the submitted finite sample repeats its pattern an infinite number of times. This can present problems. If the right hand side of one pattern does not flow smoothly into the left hand side of the next repetition, as is shown in Figure 3.4, then high frequency oscillations known as the Gibbs Phenomenon can be introduced into the spectrum. (See Figure 3.5) This is a very real danger where accustic pressure fields are concerned. For example: if the sample size does not include the entire pattern (i.e., the pressure magnitude has not been completely attenuated prior to the endpoints of the sample), this unwanted "jitter" in the spectrum can result. To avoid this situation, not only was a pressure field symmetric about the origin (the source) used, but also a Hanning Window was constructed to reduce both the amplitude and the phase components of the pressure field to zero at the endpoints, thus avoiding the Gibbs Phenomenon. Figure 3.6 shows the same pressure field depicted in Figure 3.4 combined with a Hanning Window. Its spectrum is shown in Figure 3.7. The Gibbs Phenomenon is absent. The form of the window is given below. The reader's attention is directed to Appendix I for a view of the manner in which it is combined with the pressure field.

The Hanning Window:

$$W = 0.5\left[1 + \cos\left(\frac{(I-1)\pi}{NPTS}\right)\right] \qquad \text{(eqn 3.1)}$$

where "NPTS" is the number of data points,
and I = 1,2,3,...,NPTS.

The Hanning Window does not affect the acoustic pressure field in any other way; the interference pattern in the range domain characteristic of the Lloyds Mirror for an Acoustic Doublet remains the same except for its amplitude near the end points. As shall be shown later in this chapter, it is the pattern of the entire pressure field, not simply the amplitude of the pattern, on which the W.T. performs its legerdemain.

2. Because the vertical wavenumber beta is real and has physical meaning for values of the horizontal wavenumber less than k, only those values of the magnitude of the acoustic pressure spectrum corresponding to $\gamma < k$ were retained.

3. In the Wavenumber Technique, the relationship between the horizontal range step size Δr and the horizontal wavenumber step size $\Delta\gamma$ is extremely important. Recalling equation 2.36,

$$\Delta\gamma\,\Delta r = \frac{2\pi}{N} \qquad \text{(eqn 3.2)}$$

for a given "N," the term on the right hand side, $2\pi/N$, is a constant. Consequently,

$$\Delta r \propto (\Delta\gamma)^{-1} \qquad \text{(eqn 3.3)}$$

Simultaneously, in accordance with sampling theory, in order to prevent aliasing in the pressure spectrum, there is an upper limit on the size of Δr:

$$\Delta r \le \frac{\lambda}{2} \qquad \text{(eqn 3.4)}$$

Normally, Δr is chosen such that it is much less than half a wavelength; specifically, $\Delta r < \lambda/5$ or $\lambda/6$, thus a good sample of the range domain is ensured. However, from equation 2.36, the smaller Δr becomes, the larger $\Delta\gamma$ becomes and the coarser the sample sizes of the spectrum become. Also, to ensure adequate samples in the spectrum, examination of equations 2.25 and 2.36 and [Ref. 10] reveals that

$$\Delta\gamma \le \frac{1}{2k}\left(\frac{\pi}{z}\right)^2 \qquad \text{(eqn 3.5)}$$

where Z is the deeper of the two depths, whether source or receiver. So there is a delicate balance to maintain between the sizes of Δr and $\Delta\gamma$. In the spirit of compromise, the investigator chose to use a range step size equal to a quarter of a wavelength where

$$\lambda \equiv \frac{2\pi}{k} \qquad \text{(eqn 3.6)}$$

For most cases investigated, values for k , N , Δr and $\Delta\gamma$ are summarized in Table I. As can be seen, using these values and equation 3.5, for a "Z" value of 25 wavelengths, the maximum size $\Delta\gamma$ can assume and still ensure an adequate sample size is $\Delta\gamma$ = 0.0004 /m. Clearly the sizes of $\Delta\gamma$ shown in Table I are too coarse by a factor of approximately 20. Only by increasing N , the number of sample points, can this discrepancy be corrected.

However, as mentioned earlier, computer resources were limited. The effect on the research results is not significant; nevertheless, it is recommended the reader bear this limitation in mind during the succeeding pages.

4. Looking again at Figures 3.1 through 3.3, the FFT is the curve marked by the solid line, while the theoretical Fourier Transform is the curve marked by the dotted line. Notice the large discrepancy between the theoretical values and the actual values in the region corresponding to small vertical wavenumbers. This happens to correspond to a region of the spectrum characterized by more rapid fluctuations in the spectrum. However, the size of beta is constant. Consequently, fewer samples of this region of the spectrum are available as compared with that region corresponding to high beta values. Since the plotting routine utilized is interpolating between sampled points of the spectrum, the graph at this end is less smooth and results in a marked difference between the curves. Where the curves are determined by more points and are smoother, the discrepancy between theory and computerized reality is much less noticeable.

B. SOURCE DEPTH DETERMINATION

Theory predicts that, for a source shallower than the receiver, when the magnitude of the pressure spectrum is plotted as a function of the vertical wavenumber, the resultant nodal spacing can be used to determine source depth by either consulting a chart (see Figure 3.8) or by performing a simple calculation (see equation 2.31). To test this prediction, several scenarios were designed. Figures 3.9

through 3.11 are typical of the many cases run. In each, source depth is less than receiver depth. For each case, careful measurement of the $\Delta\beta$ spacing coupled with use of equation 2.31 yielded the (already known) source depth with less than a two per cent error, which can be attributed to human error in the measurement of $\Delta\beta$.

TABLE II

Results of Source Depth Determination Runs

Figure Nr.	ZS (m)	ZR (M)	(Meas'd)	Z(Calc'd)
3.9	21.998	47.124	0.14 m^{-1}	22.4 m
3.10	31.416	47.124	0.10 "	31.4 "
3.11	15.708	47.124	0.20 "	15.7 "
3.12	47.124	21.998	0.14 "	22.4 "
3.13	47.124	31.416	0.10 "	31.4 "
3.14	47.124	15.708	0.20 "	15.7 "

To test what happens when the receiver depth is shallower than the source depth, the cases depicted in Figures 3.12 through 3.14 were run. The scenario is the same as for Figures 3.9 through 3.11; only the source and receiver depths have been exchanged. As can be seen, the $\Delta\beta$ spacing corresponds with the receiver depth. This is again as predicted by theory. Table II summarizes the findings of Figures 3.9 through 3.14.

The scenarios shown in Figures 3.9 through 3.14 all start with a pressure field measured horizontally from the source; i.e., the exact range to the source is known. What if the range to the source is not known, or only minimal information concerning the range is known? In this case, only a portion of the pressure field starting at some initial range R_0 can be sampled. What is the effect on the spectrum?

To answer these questions, a range window was constructed and placed at varying initial ranges from the source. As Figure 2.2 illustrates, as range from the source increases, the nodes of the Lloyds Mirror interference pattern in the range domain become more widely spaced. Given fewer nodes to sample, will the spectrum be the same? In accordance with theory, the spectrum is independent of range (see equation 2.39) and so should be the same wherever the window is placed.

Figures 3.15 through 3.17 illustrate that the spectrum is not entirely independent of range. The figures utilize the same scenario as was used above, differing only in the range from the source at which the sampling of the pressure field begins. As can be seen, beginning at the right hand side which corresponds to high vertical wavenumber values, or the low horizontal wavenumber values (see equation 2.8), a "washing out" of the spectrum occurs, increasing as the range window is moved further from the source. Again, the theoretical curve is marked by the dotted line.

When the magnitude of the pressure spectrum is plotted as a function of the vertical wavenumber, the useful portion of the resulting graph is the last two-thirds of the beta range. For K = 2.0/m, this is the range $0.67/m < \beta < 2.0/m$. This phenomenon is explained more fully in Section III A 4. With this caveat in mind and based upon multiple source, receiver, range window

combinations run through the model, the following criterion was established: the nodal spacing of the spectral plots was no longer determinable once the initial range R_0 was increased to approximately three times the source depth. In other words, minimum knowledge of the range from receiver to source must be available to ensure adequate sampling of the acoustic pressure field in the range domain. This, in turn, will produce a pressure spectrum of such a quality that source depth determination can be made.

What causes this not entirely unexpected result? As the range window is moved further from the source, for $Z_s \neq Z_r$, those samples of the pressure field corresponding to low gamma values are lost to the spectrum first. Low gamma values correspond to waves arriving at high angles with respect to the horizontal. At greater receiver ranges, R more closely approximates r and the arrival angles become closer to the horizontal (see Figure 2.1).

As the window is moved further from the source and fewer nodes of the interference pattern are encountered, if a wider window were used, could this "washing out" effect in the spectrum be minimized or even eliminated? In the author's opinion, it would be minimized; because of the reasoning in the preceding paragraph, it probably would not be eliminated. However, a wider window would require more sample points; because of equation 2.36, one cannot merely make Δr larger. Time and the computer resources available to this investigator were limited, and the test cases run were already using the maximum available array sizes, thus precluding a quantitative illustration of this hypothesis. Succeeding research into the W.T. might include ways to test this point.

In conclusion, the Wavenumber Technique has the potential for being a valuable operational tool in determining the depth of an acoustic source provided the receiver is at

a greater depth than the source. It is strongly reccmmended that further research into use of the W.T. in a realistic ocean environment be done.

C. THE EFFECT OF SURFACE ROUGHNESS

This and the succeeding section were purely qualitative portions of the research. Therefore, in the figures the spectra were plotted as functions of the horizontal wavenumber for ease of discussion except where a particular point about the vertical wavenumber was being illustrated, and the theoretical curve was omitted.

As described in Chapter II, the effect of surface roughness is to suppress the contribution of the image to the dipole interference pattern. Moreover, by increasing M, the effect is to suppress the image's contribution to the pressure field in the range domain and reduce the pressure spectrum to the contribution of the direct path wave only (see equation 2.41); the resultant magnitude of the spectrum is inversely proportional to the vertical wavenumber (see equation 2.42). As Figures 3.18 through 3.21 illustrate, this is exactly what happens in the FFT. In Figure 3.21, an inverse beta curve has been manually superimposed onto the actual curve to reflect this point.

Looking at the pressure field in the range domain $\underset{\sim}{P}(R)$ the effect of surface roughness is inversely proportional to the wavelength of the signal. For longer wavelengths, the Lloyds Mirror effect is more tolerant of surface roughness than it is for shorter wavelengths. Does the same relationship hold for the pressure spectrum? Comparison of the respective sea states in Figures 3.22 and 3.23 with Figures 3.24 and 3.25 illustrate that it does.

This investigator also looked at the effect of varying the range window in the presence of waves. This is similar

to what was looked at in Section B of this chapter. Results should be similar and for the same reasons. For a given sea state, source and receiver geometry and wavelength, the range window was moved successively further from the source (see Figures 3.26 through 3.29). As can be seen, the "washing out" effect of the spectral nodes begins to effect the lower horizontal wavenumber values first.

D. THE EFFECT OF NOISE

Random noise was simulated in this research. Being independent of range and frequency, it was treated as a constant by both the Fourier Transform and the FFT. The investigator wished to compare qualitatively the effects of equal amounts of noise on the pressure field in the range domain and in the wavenumber domain. To do this, successively larger values of the "noise factor" were used in computing $\underset{\sim}{n}$ (see equation 2.43). Values of the noise factor used in the research were limited to the maximum amplitude of the pressure field $\underset{\sim}{P}(R)$. Since dipole radiation is predicated, as range from the source increases, the maxima of the interference pattern decrease as the inverse square of the range (i.e., R^{-2}). Hence, even small noise factors can have a devastating effect on the pressure field as the receiver is stepped out in range. The destructive effect on the spectrum of successively more intense amounts of noise at varying wavelengths is illustrated in Figures 3.30 through 3.47

Several conclusions concerning the pressure spectra can be drawn from these results:

1. For equal amounts of noise, longer wavelengths are affected less than shorter wavelengths. Compare Figures 3.31 and 3.32 with Figures 3.43 and 3.44, and Figures 3.34 and 3.35 with Figures 3.46 and 3.47.

This was not a surprising result since the same principle holds for the range domain.

2. The spectrum is affected less by noise than is the range domain. Compare Figures 3.30 through 3.35 and Figures 3.36 through 3.47 for an illustration of this point at two different wavelengths and various noise levels. This was a rather welcome surprise.
3. If the magnitude of the pressure spectrum is plotted as a function of beta, the $\Delta\beta$ spacing can still be detected even after the pressure function in the range domain has been "swallowed up" by the noise field. Compare Figures 3.33 through 3.35 and Figures 3.42 through 3.44. This was not surprising in view of 2. above.

E. SUMMATION

All of the foregoing results are based specifically on the Lloyds Mirror for an Acoustic Doublet. This is a highly idealized and artificial environment. Any thought of immediately applying conclusions reached in this paper to a real world situation is premature. However, the results are still significant if only for supporting the statement made by each preceding investigator that the Wavenumber Technique should be examined very closely for a future operational role, especially in view of the current trends in source levels and ambient noise levels.

Certain fundamental conclusions regarding the author's research into the Wavenumber Technique can now be made within the confines of the above restriction:

1. Source depth can be determined quickly and easily from the acoustic pressure spectrum provided

   a) the receiver is deeper than the source,

b) some knowledge of the range from receiver to source is available, and

c) the magnitude of the pressure spectrum is plotted as a function of the vertical wavenumber.

2. Source depth determination in even a noisy environment is possible. While the introduction of increasing amounts of narrow band noise adversely affects both the range domain and the wavenumber domain, the pressure spectrum seems able to withstand the chaotic destruction longer than does the pressure field in the range domain.

3. The ability to determine source depth is adversely affected by the height of surface gravity waves since surface roughness reduces the Lloyds Mirror as the sea state increases.

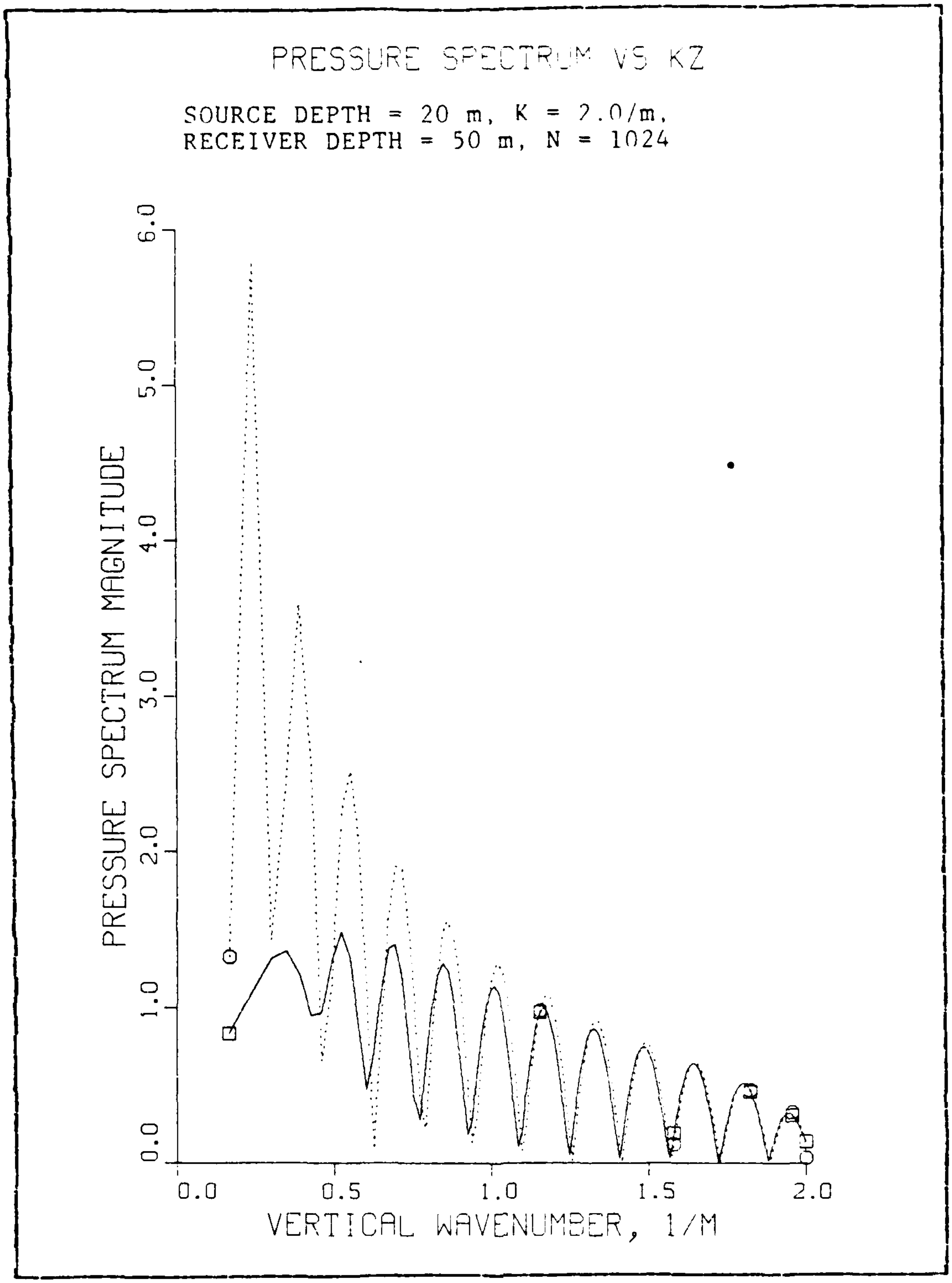

Figure 3.1 Pressure Spectrum Using FFT2C

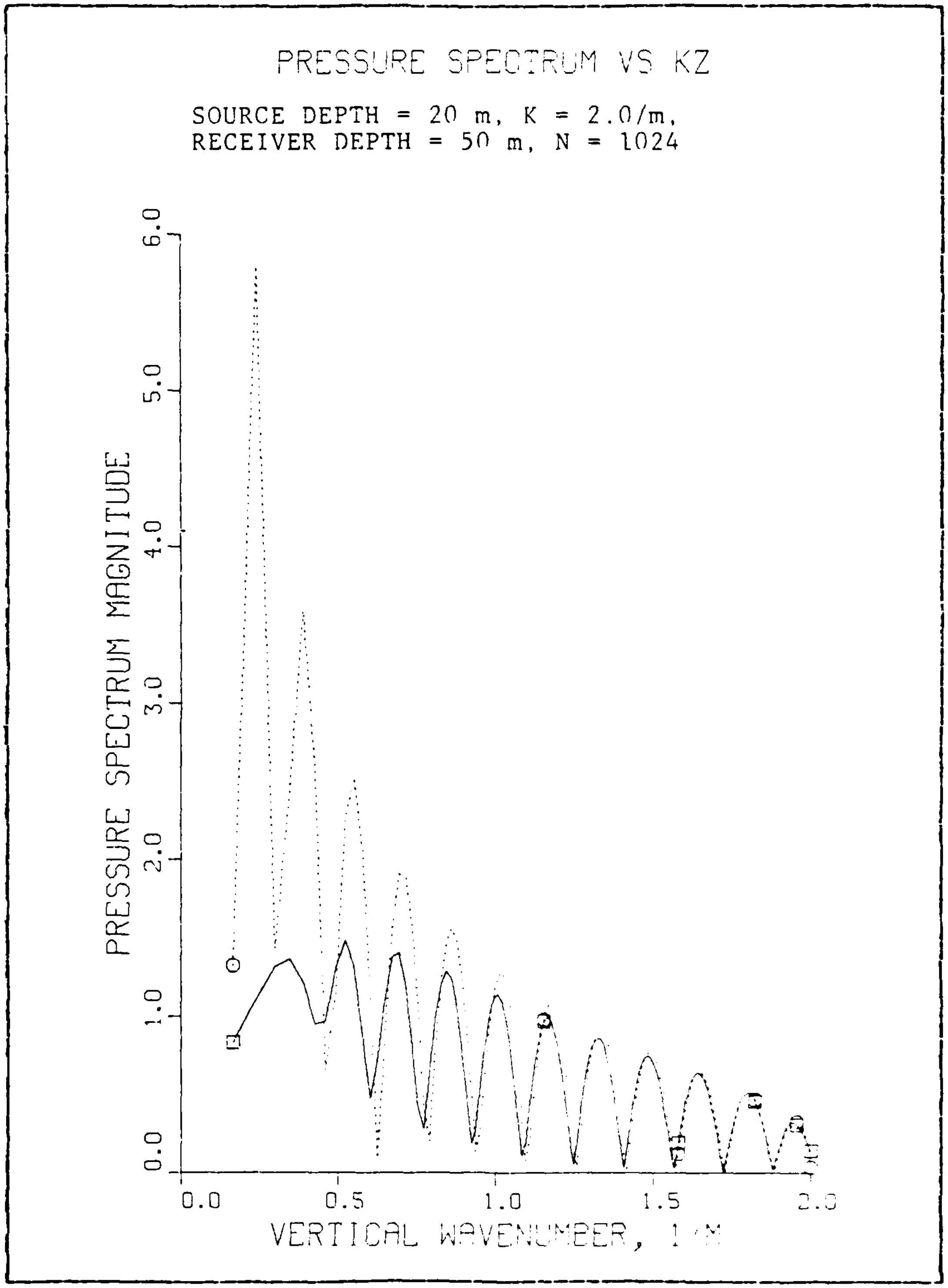

Figure 3.2 Pressure Spectrum Using FFTCC

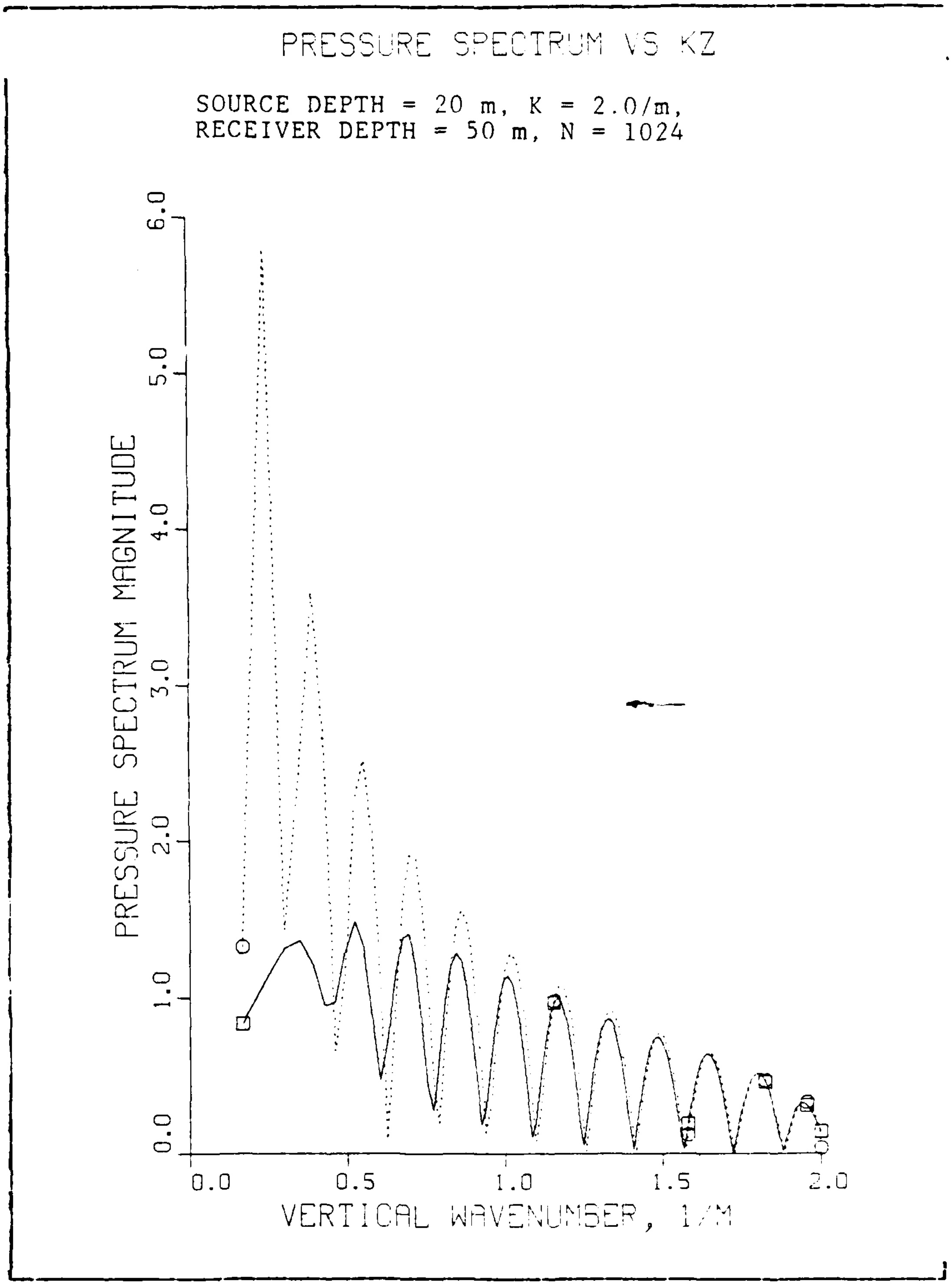

Figure 3.3 Pressure Spectrum Using Cooley-Tukey FFT

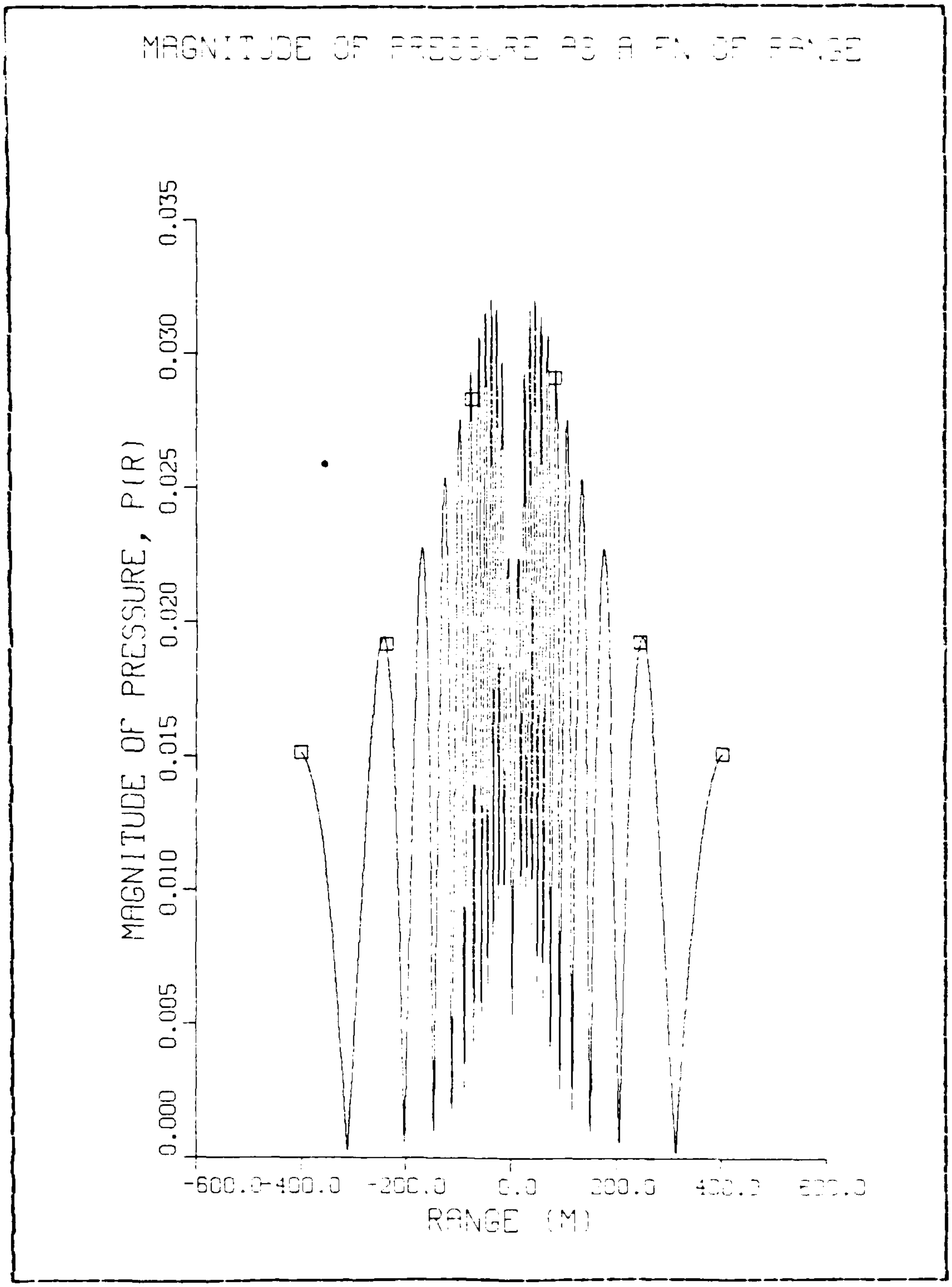

Figure 3.4 Non-smoothed Pressure Field

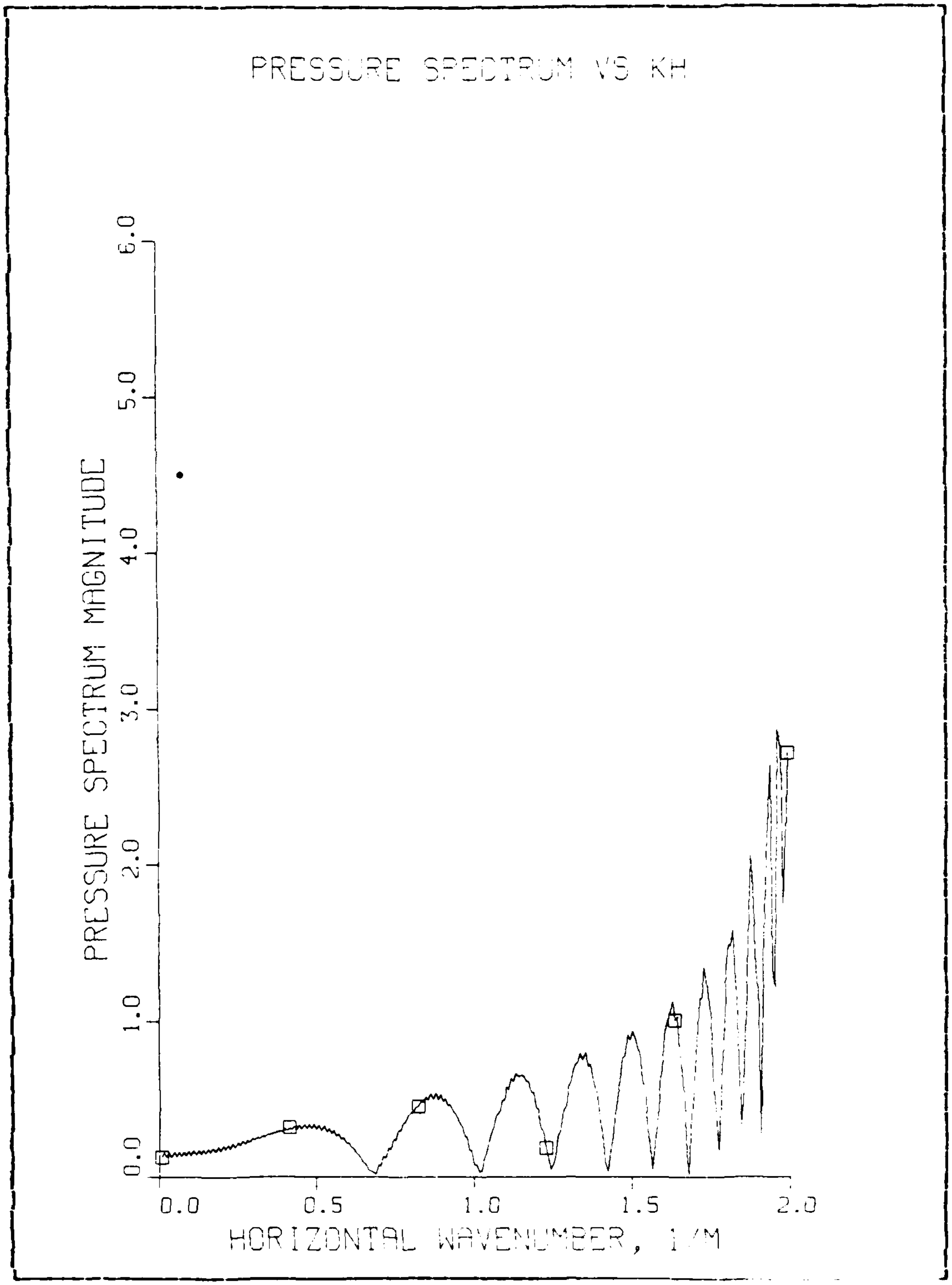

Figure 3.5 Pressure Spectrum Showing Gibbs Phenomenon

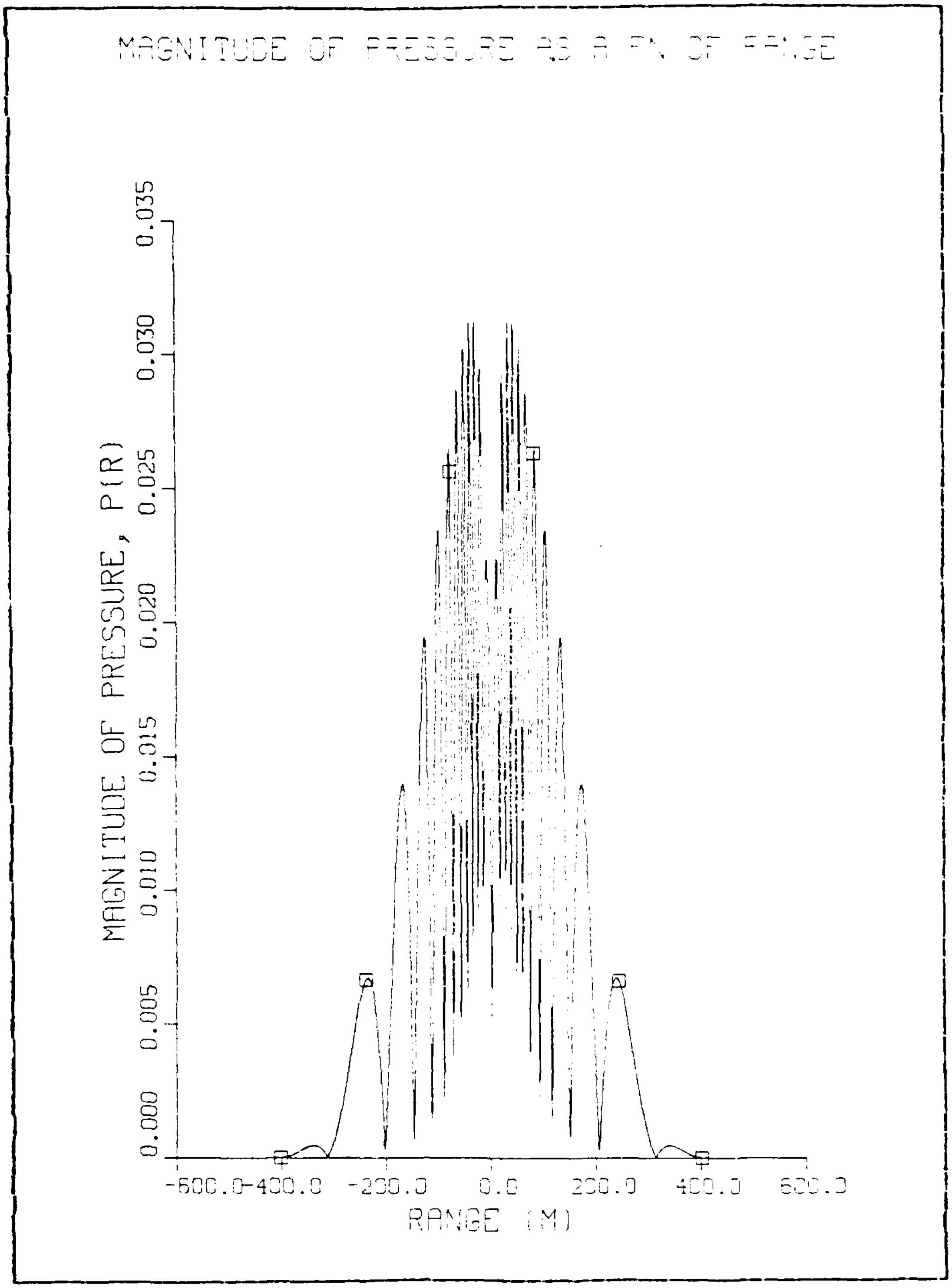

Figure 3.6 Pressure Field Combined With a Hanning Window

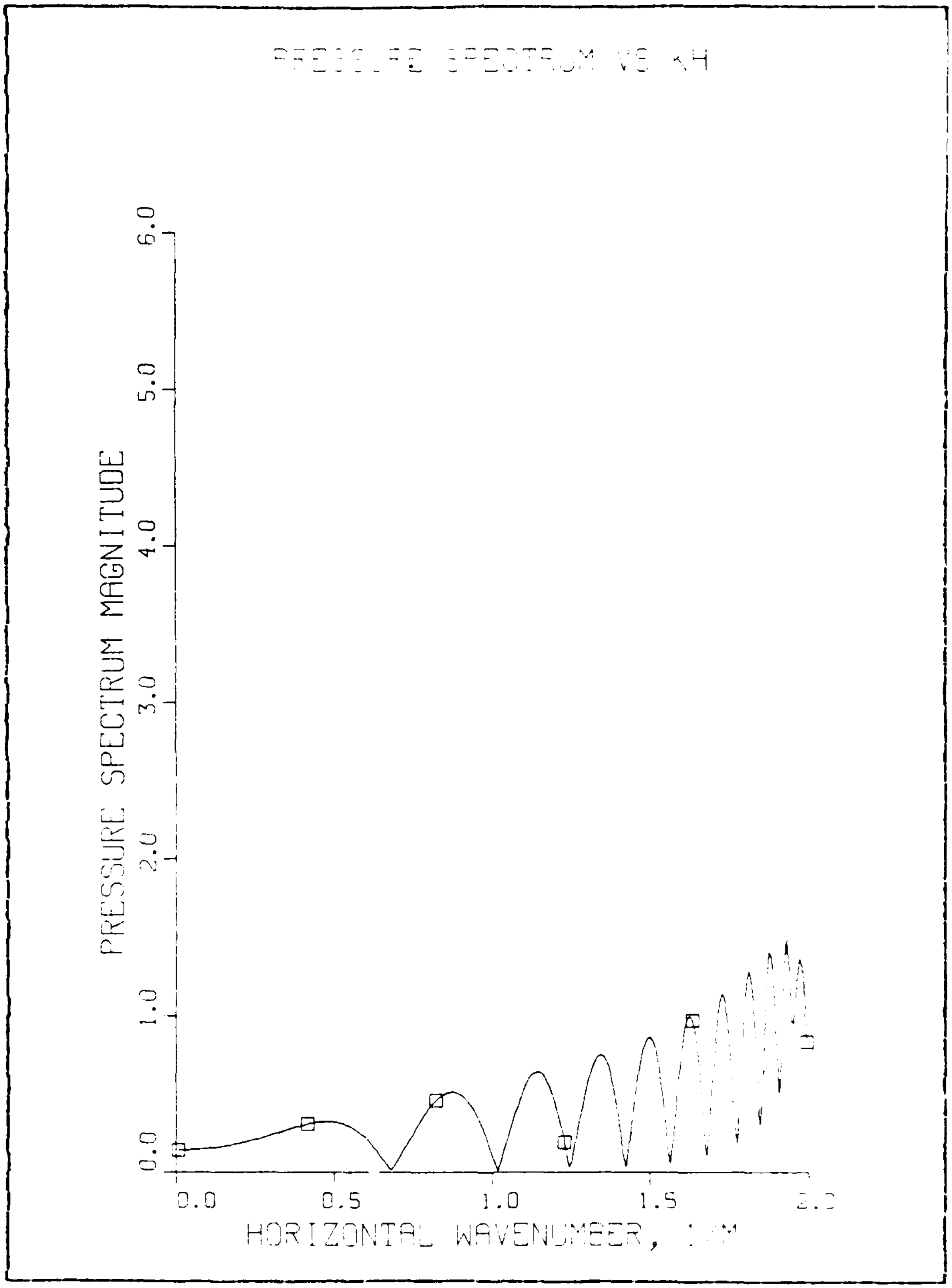

Figure 3.7 Pressure Spectrum Combined With a Hanning Window

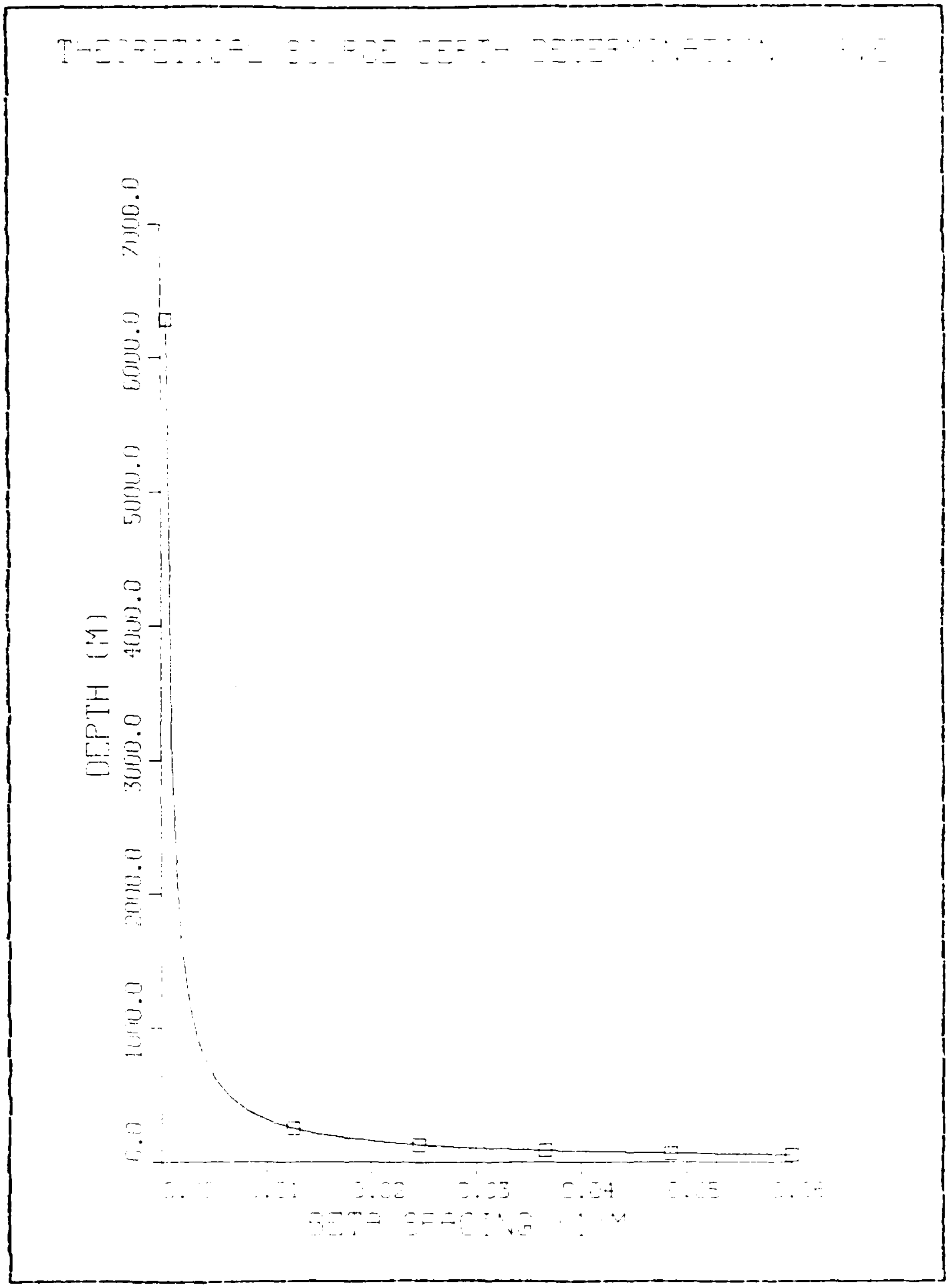

Figure 3.8   Theoretical Source Depth Determination Curve

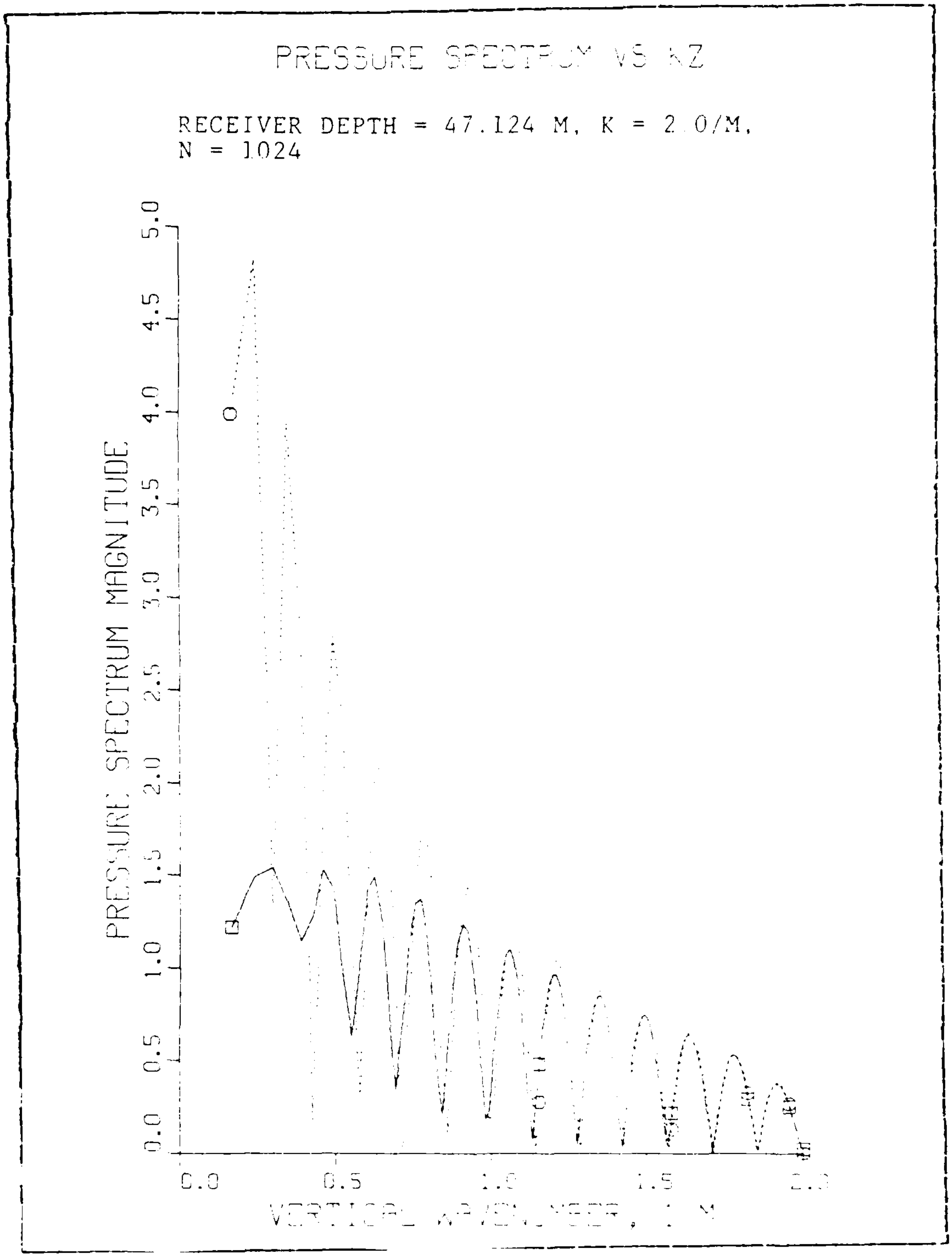

Figure 3.9 Graph of Pressure Spectrum, Source at 22.0 Meters

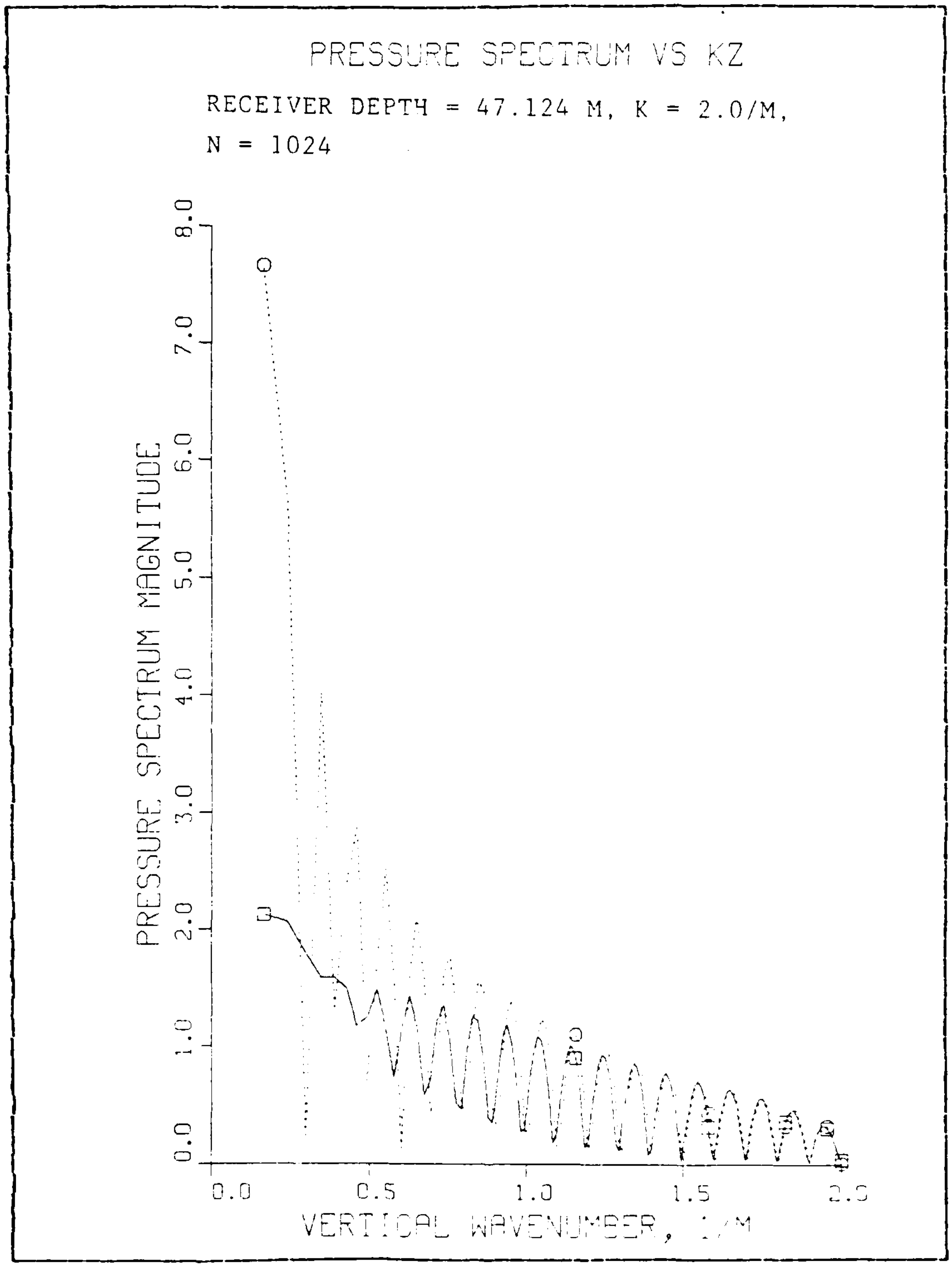

Figure 3.10 Graph of Pressure Spectrum, Source at 31.4 Meters

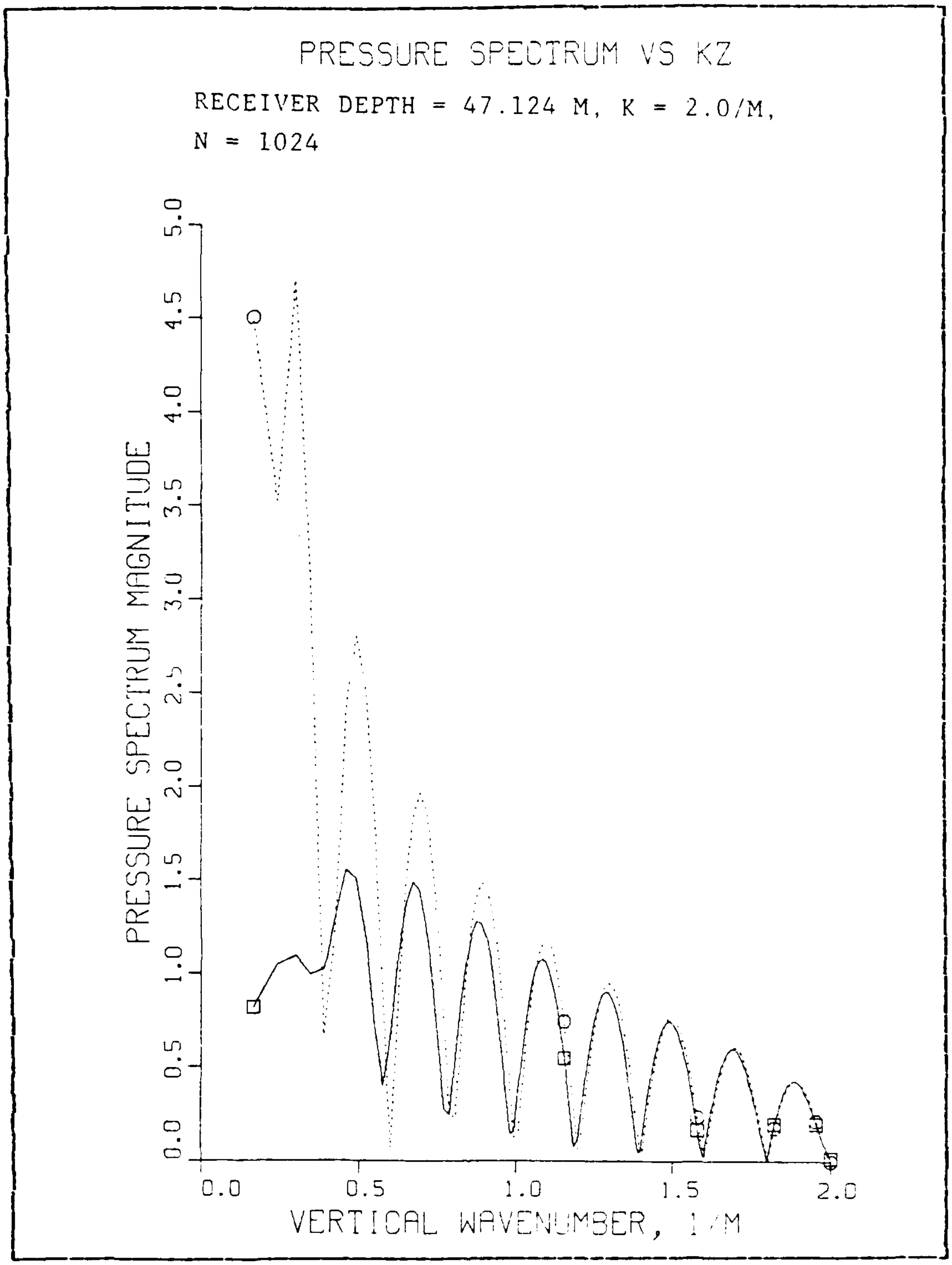

Figure 3.11 Graph of Pressure Spectrum, Source at 15.7 Meters

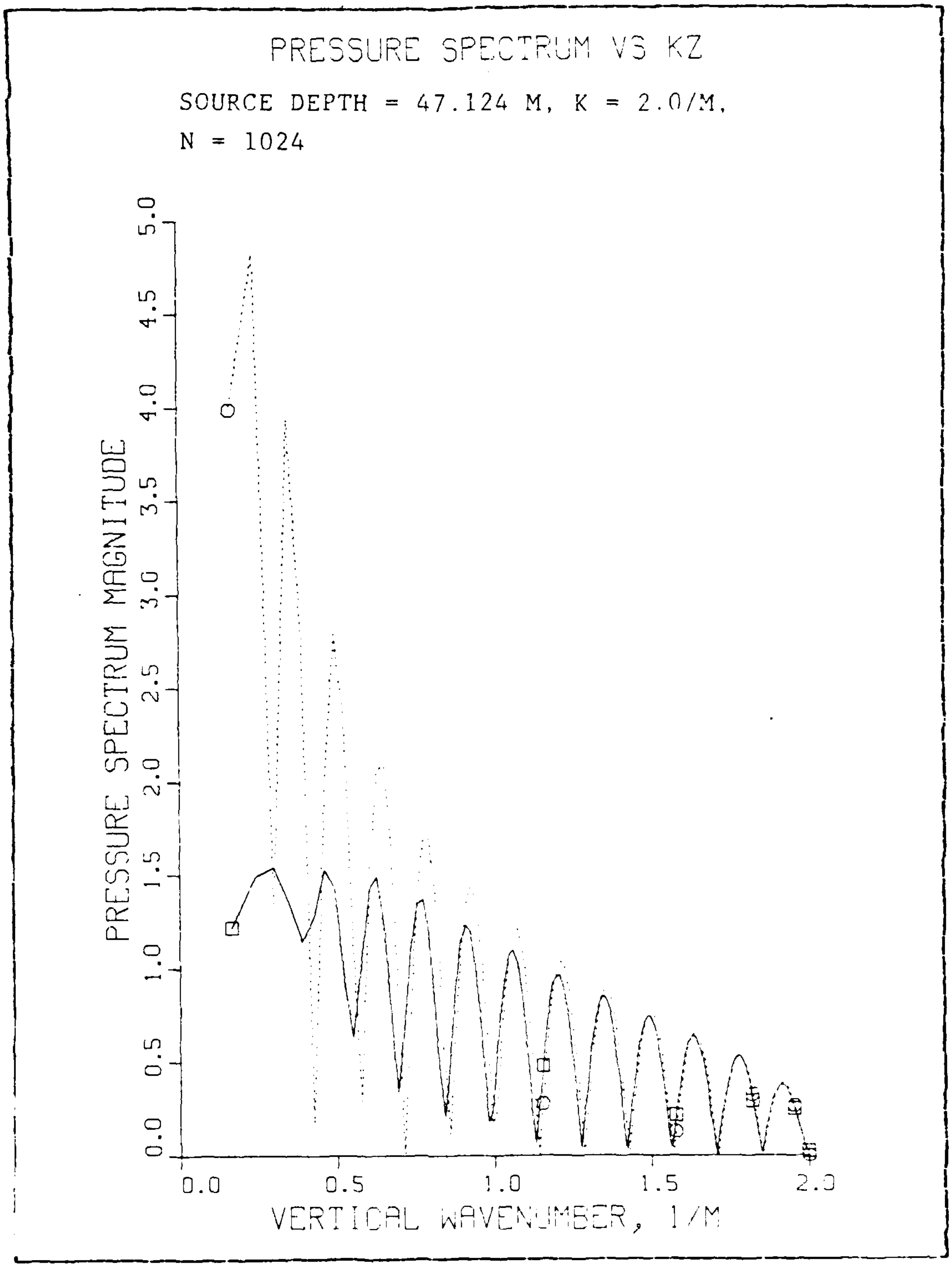

Figure 3.12 Graph of Pressure Spectrum, Receiver at 22.0 Meters

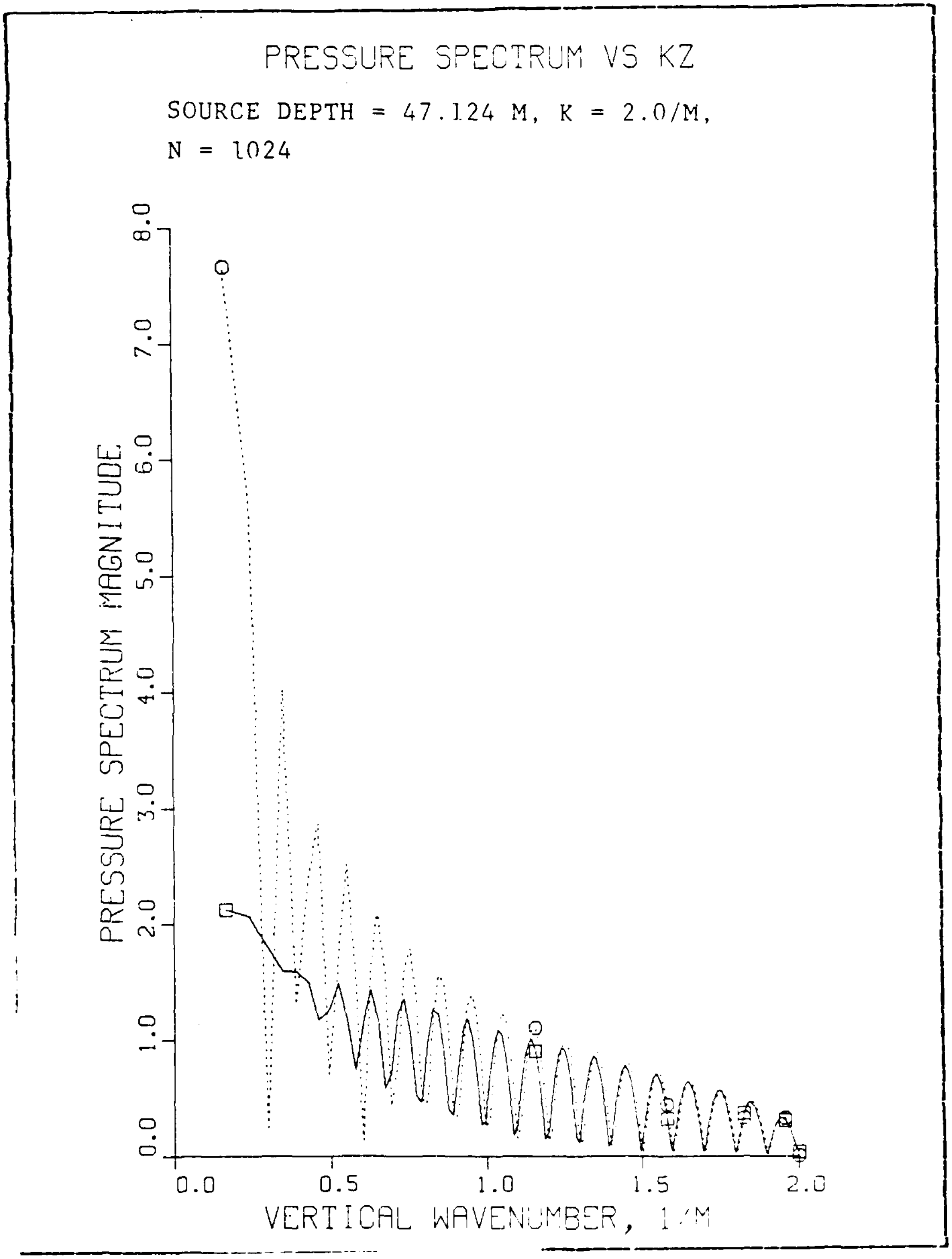

Figure 3.13 Graph of Pressure Spectrum, Receiver at 31.4 Meters

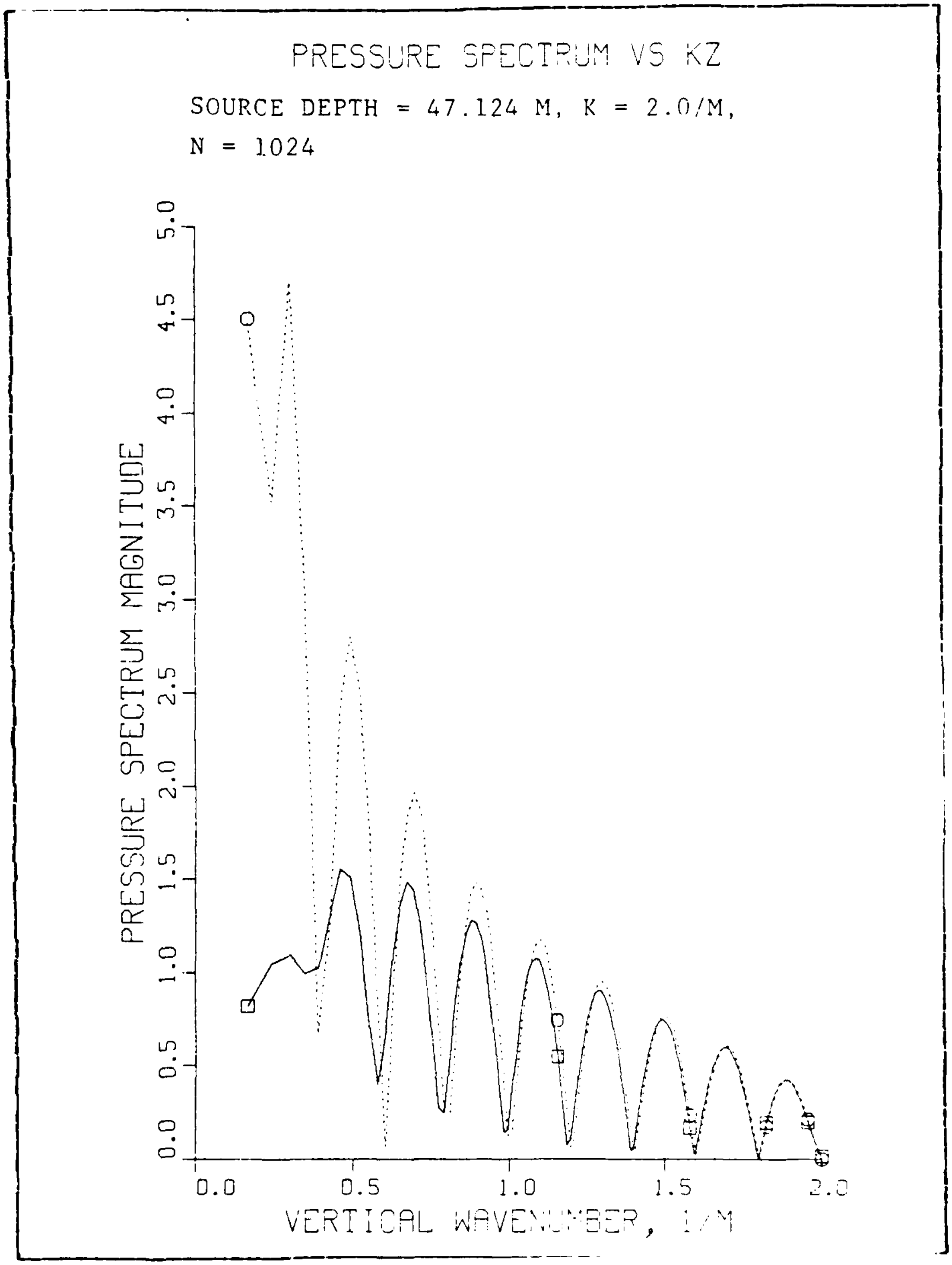

Figure 3.14 Graph of Pressure Spectrum, Receiver at 15.7 Meters

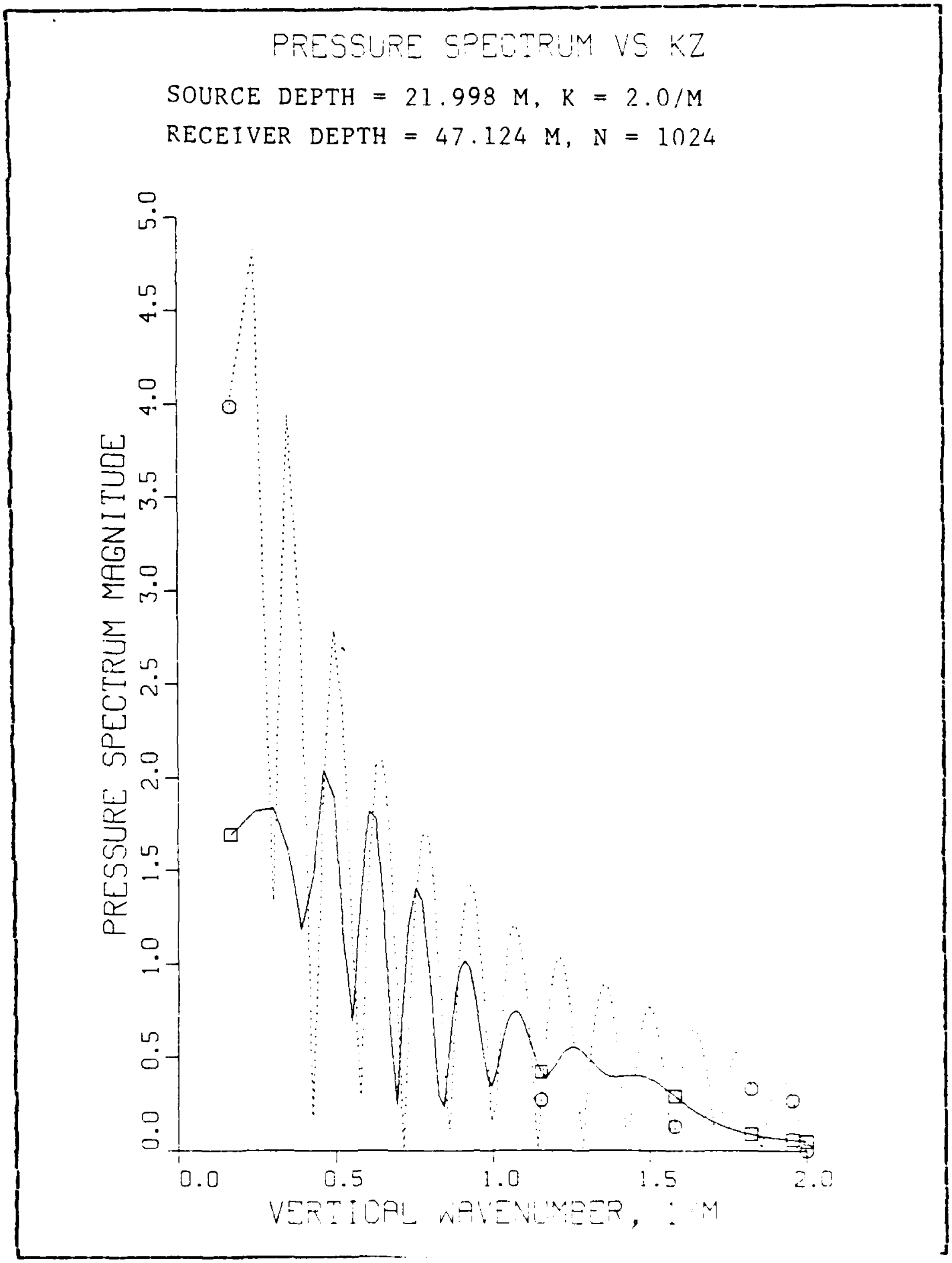

Figure 3.15 Pressure Spectrum, Range Window Set at 47.1 Meters

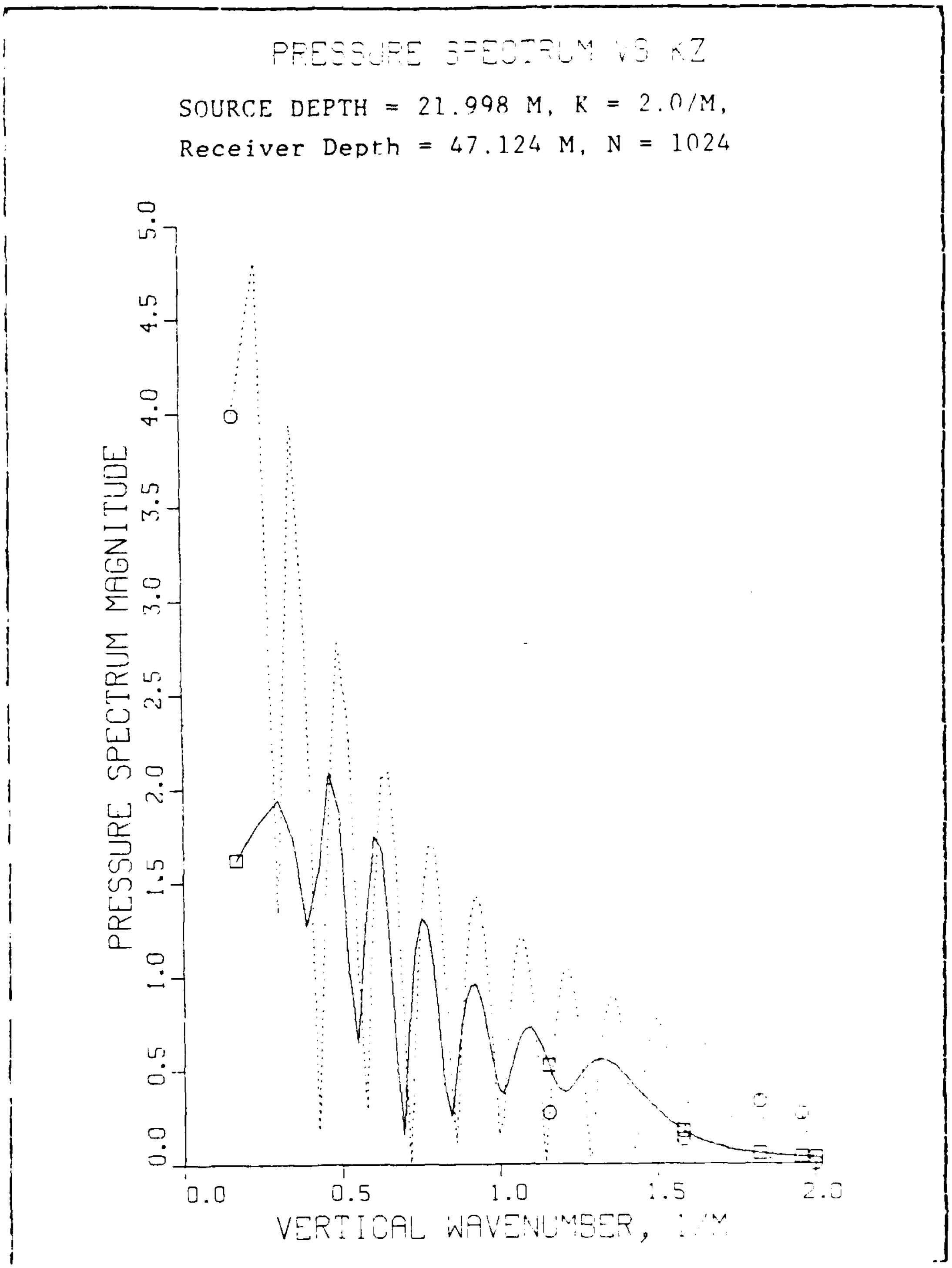

Figure 3.16 Pressure Spectrum, Range Window Set at 50.3 Meters

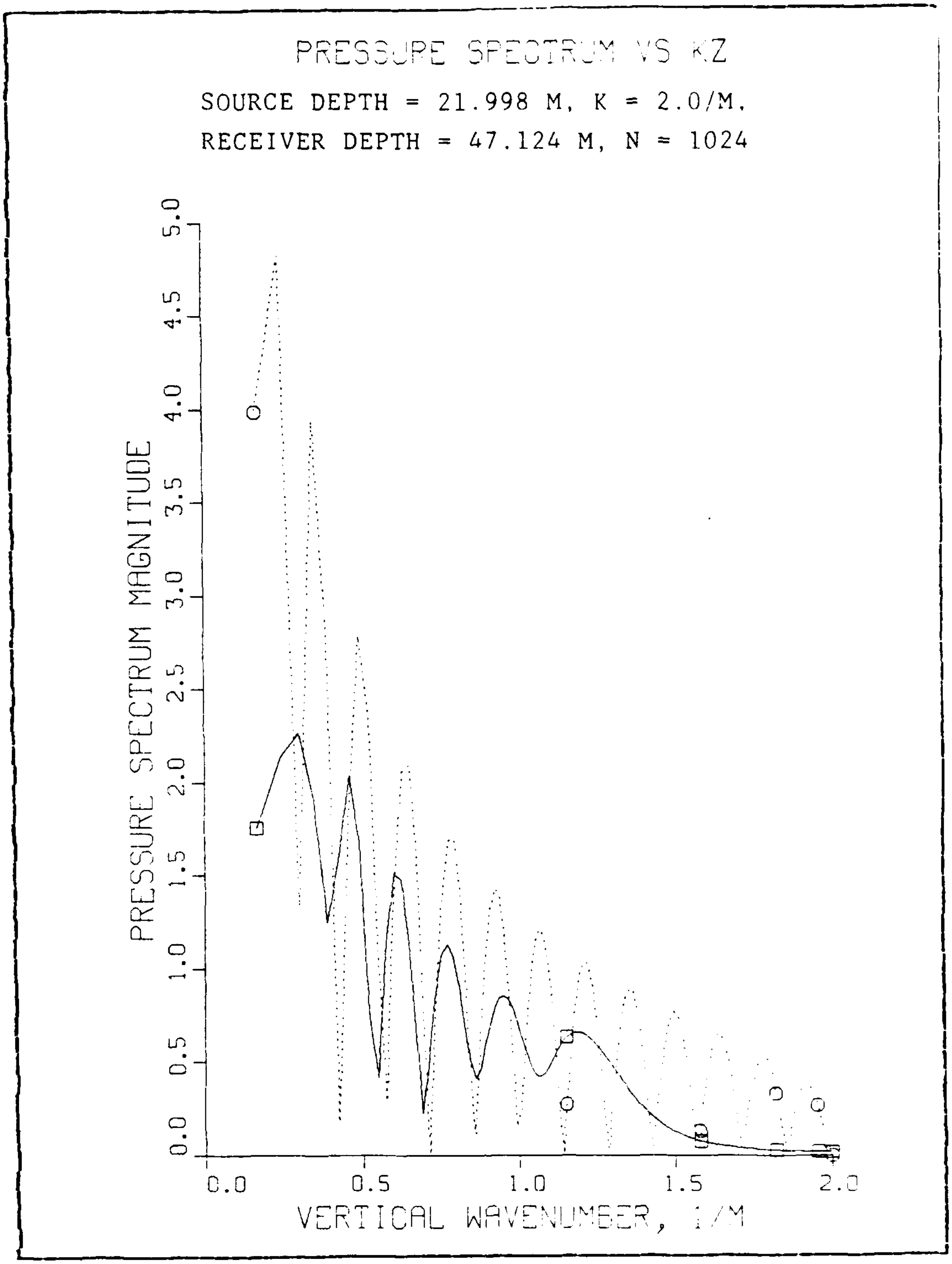

Figure 3.17 Pressure Spectrum, Range Window Set at 62.8 Meters

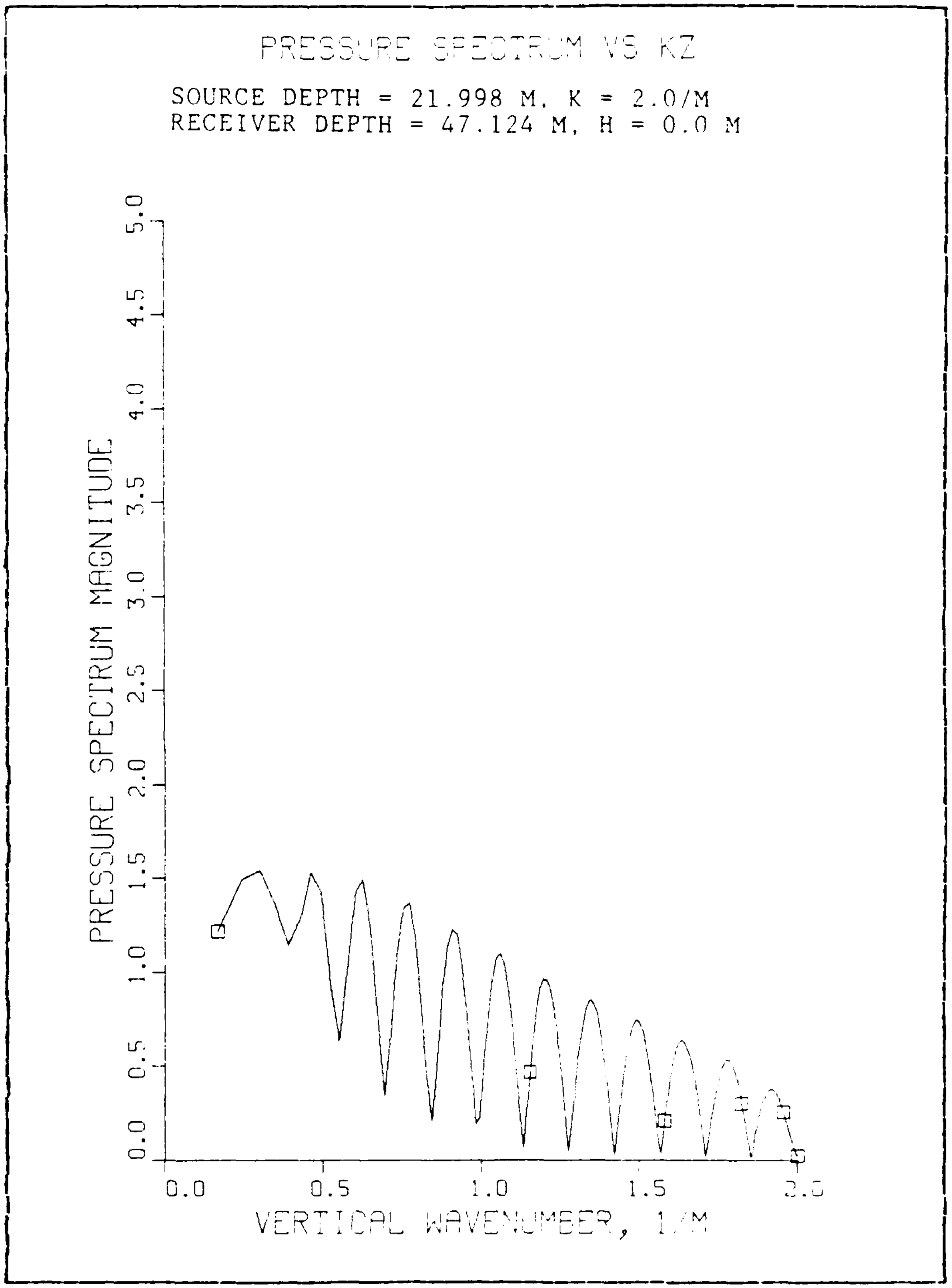

Figure 3.18 Pressure Spectrum, Sea State 0

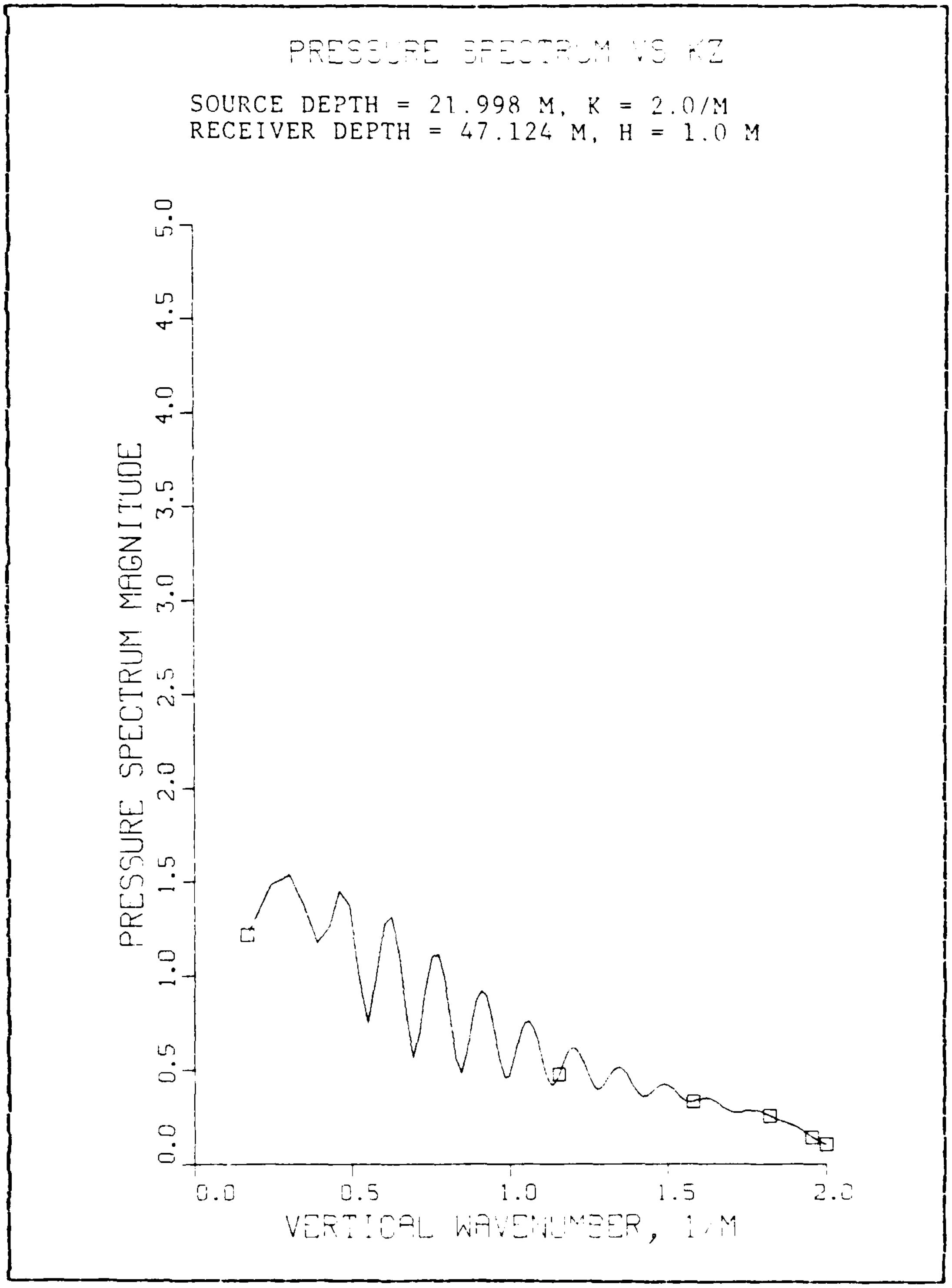

Figure 3.19 Pressure Spectrum, Sea State 2

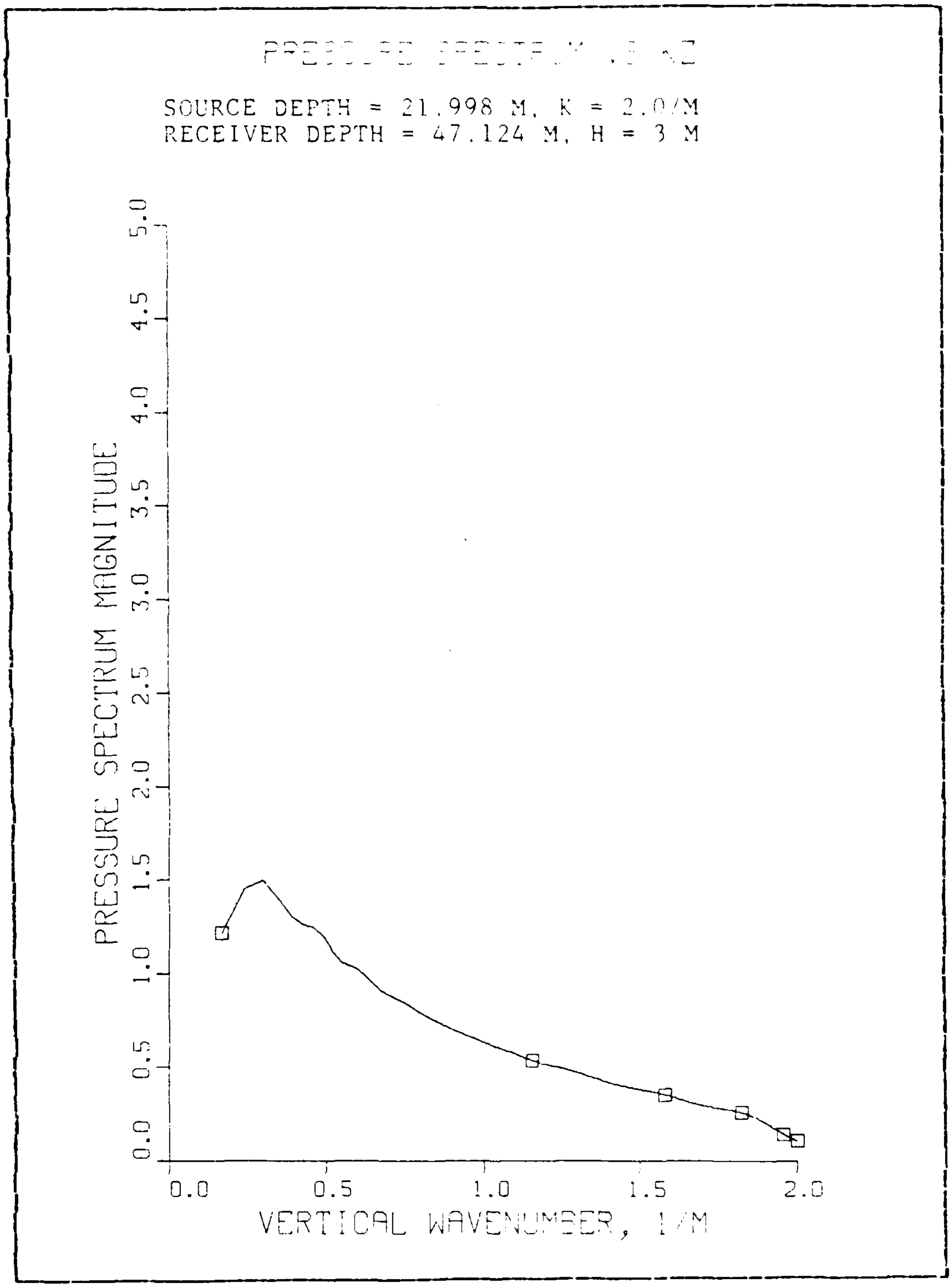

Figure 3.20 Pressure Spectrum, Sea State 3

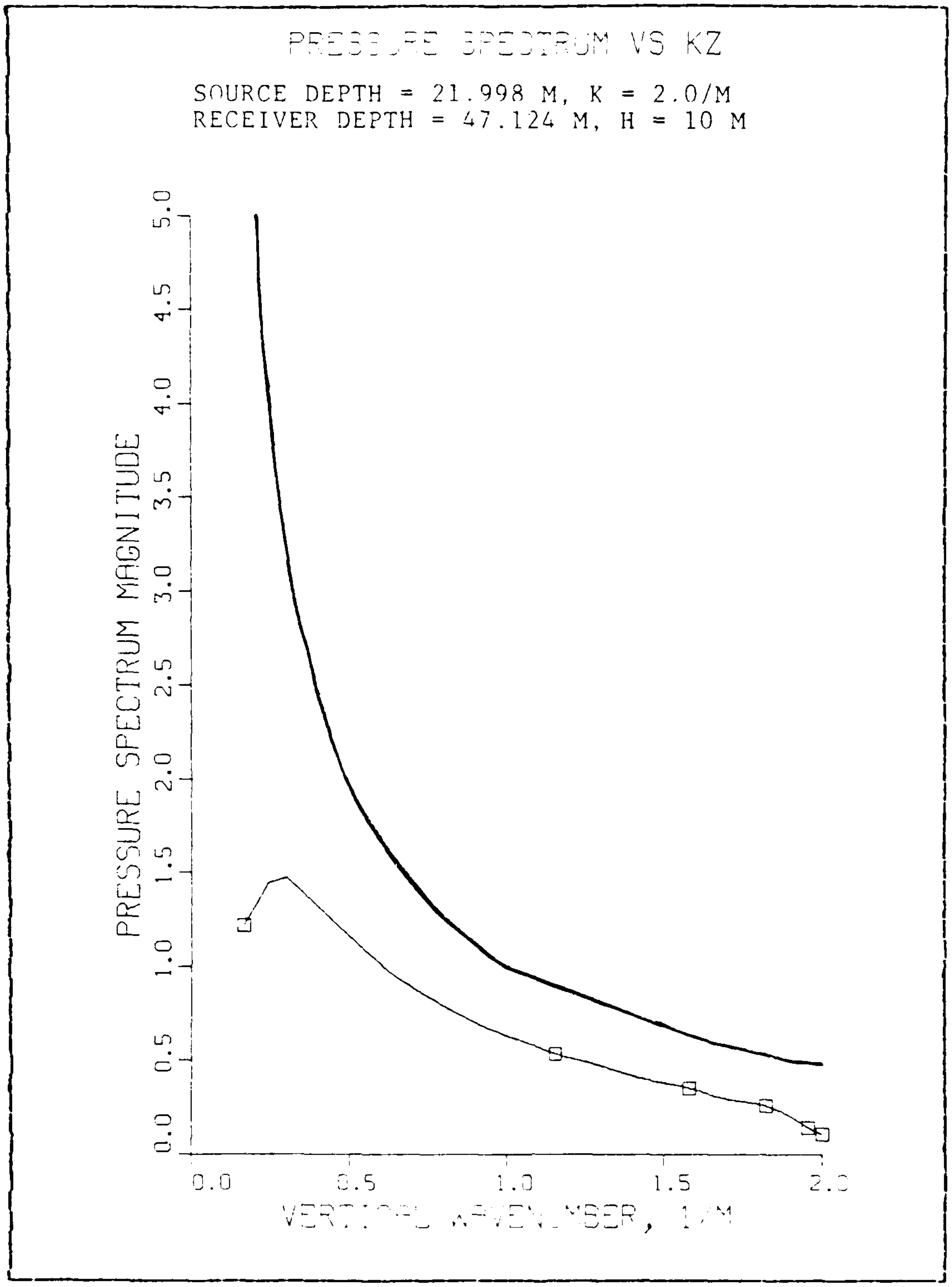

Figure 3.21 Pressure Spectrum, Sea State 5

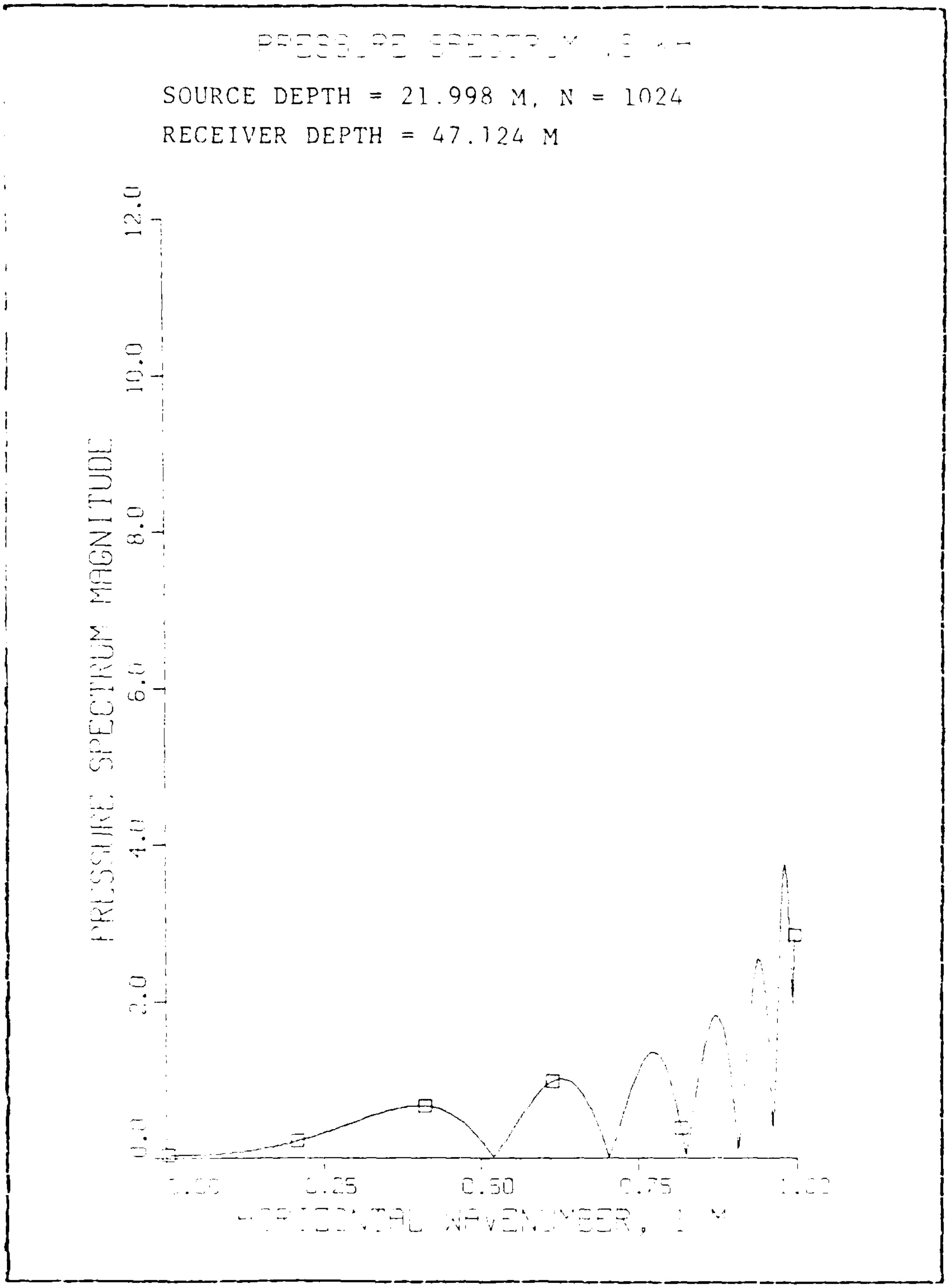

Figure 3.22 Pressure Spectrum, Sea State 0, K = 1.0

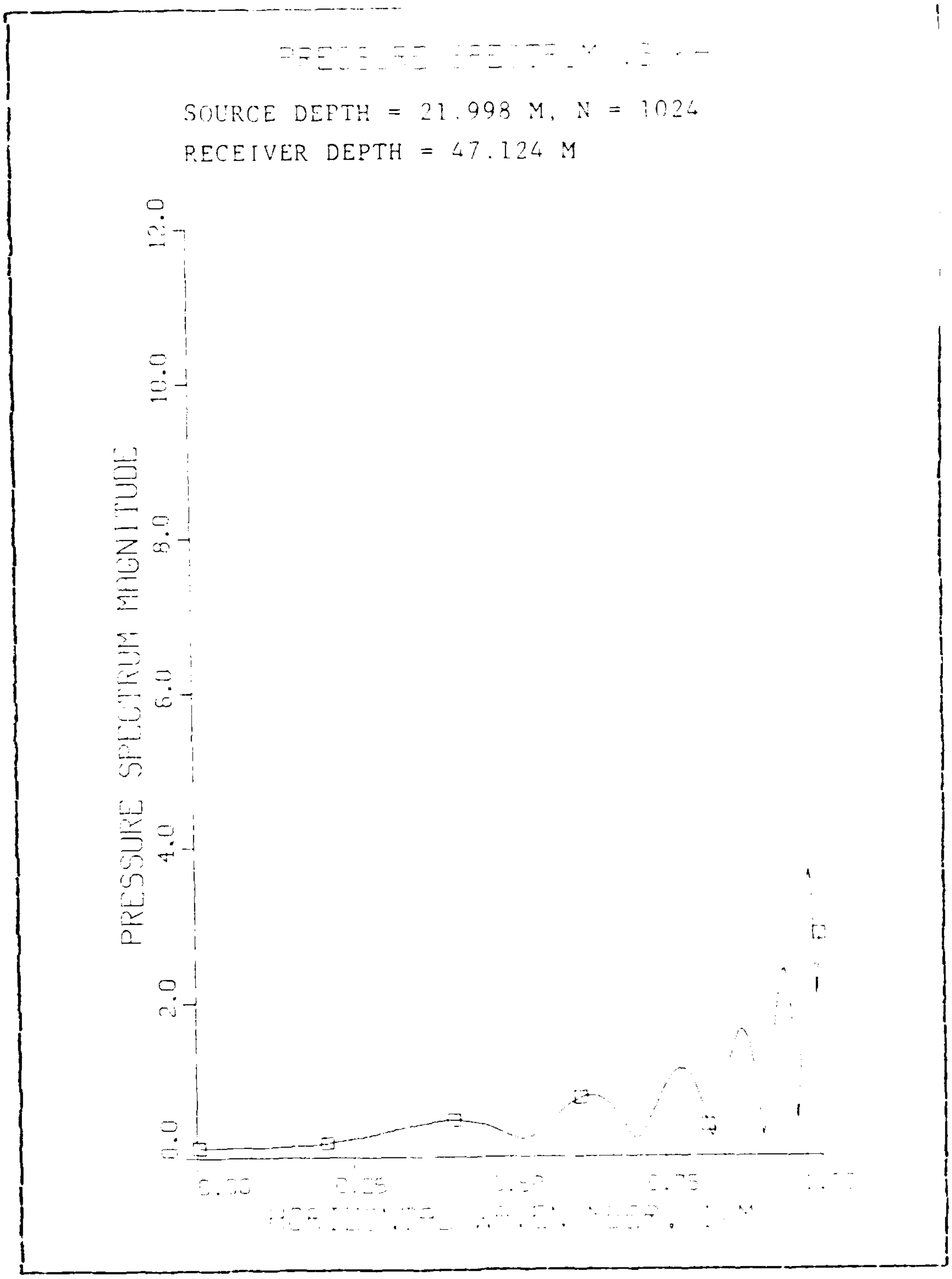

Figure 3.23 Pressure Spectrum, Sea State 3, K = 1.0

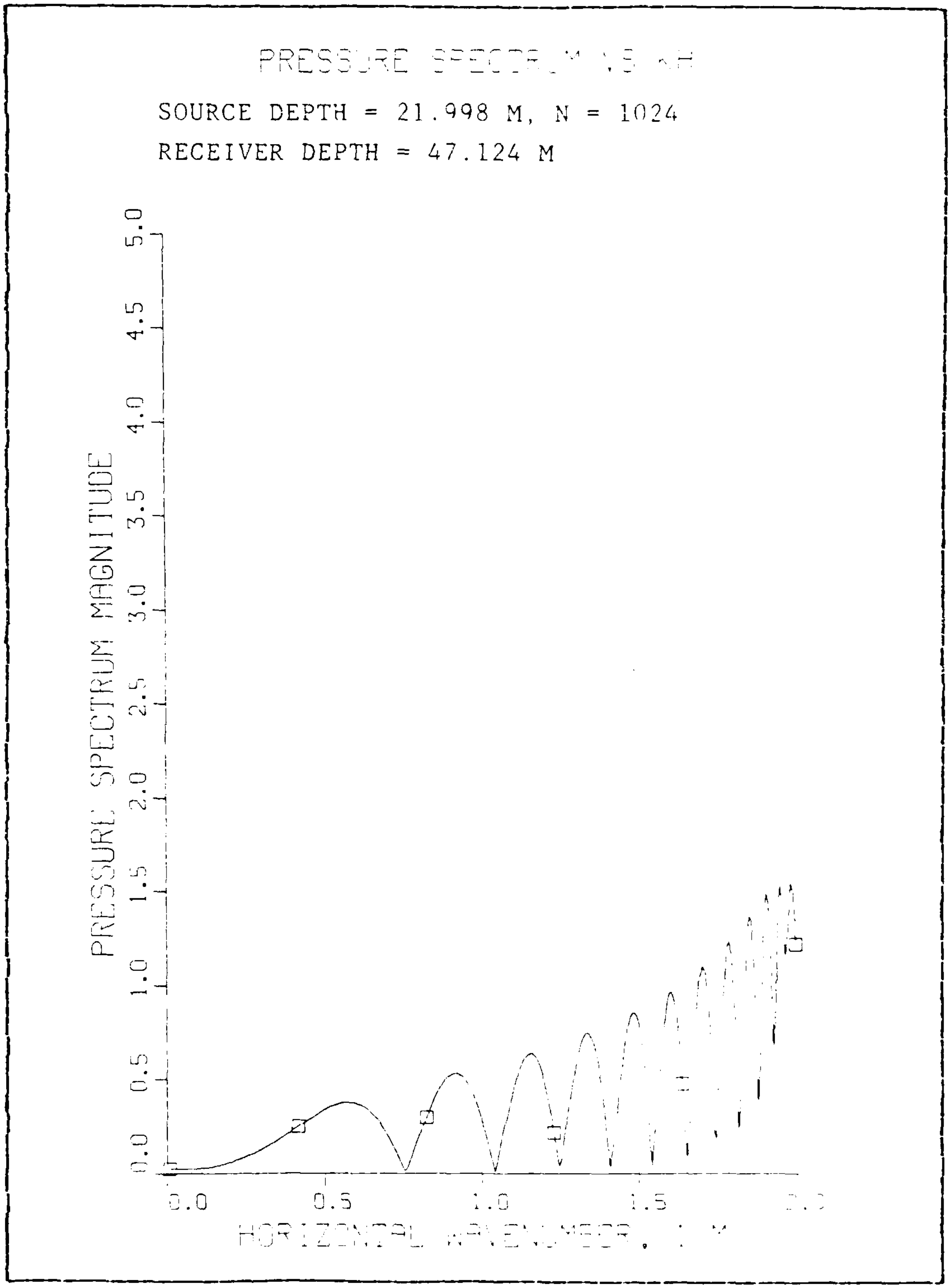

Figure 3.24 Pressure Spectrum, Sea State 0, K = 2.0

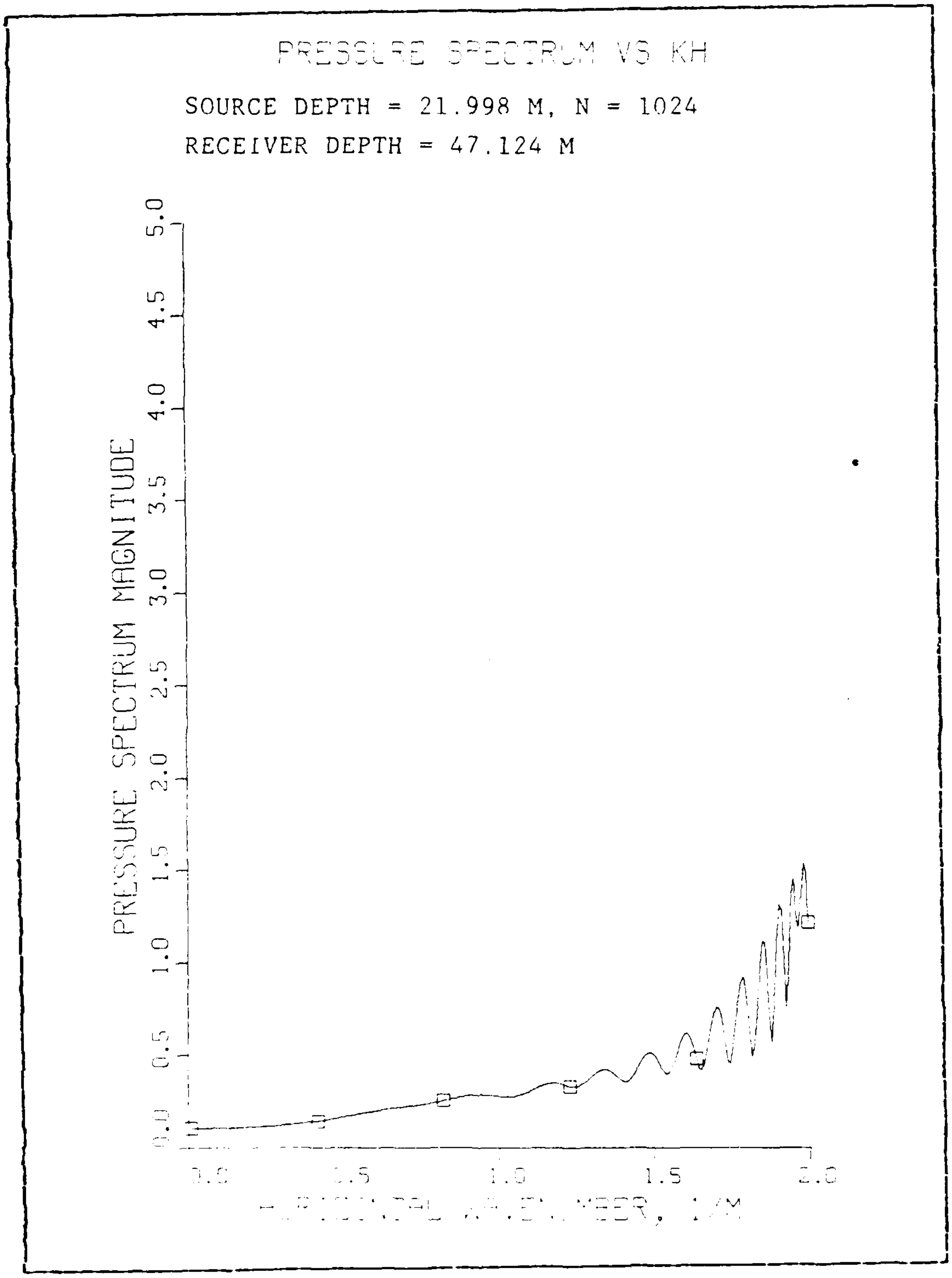

Figure 3.25 Pressure Spectrum, Sea State 3, K = 2.0

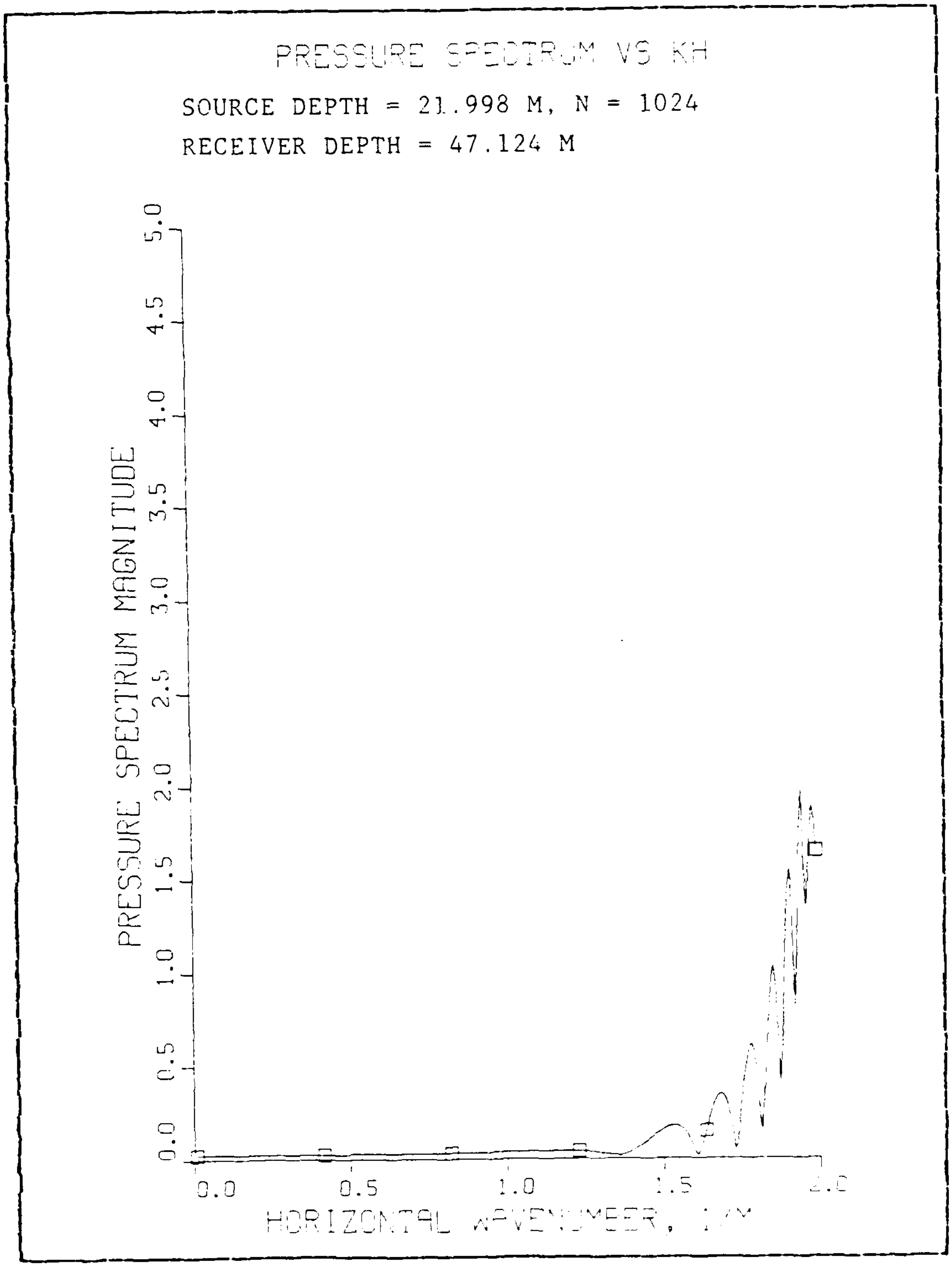

Figure 3.26 Pressure Spectrum, SS 2, Range Window Set at 50 Meters

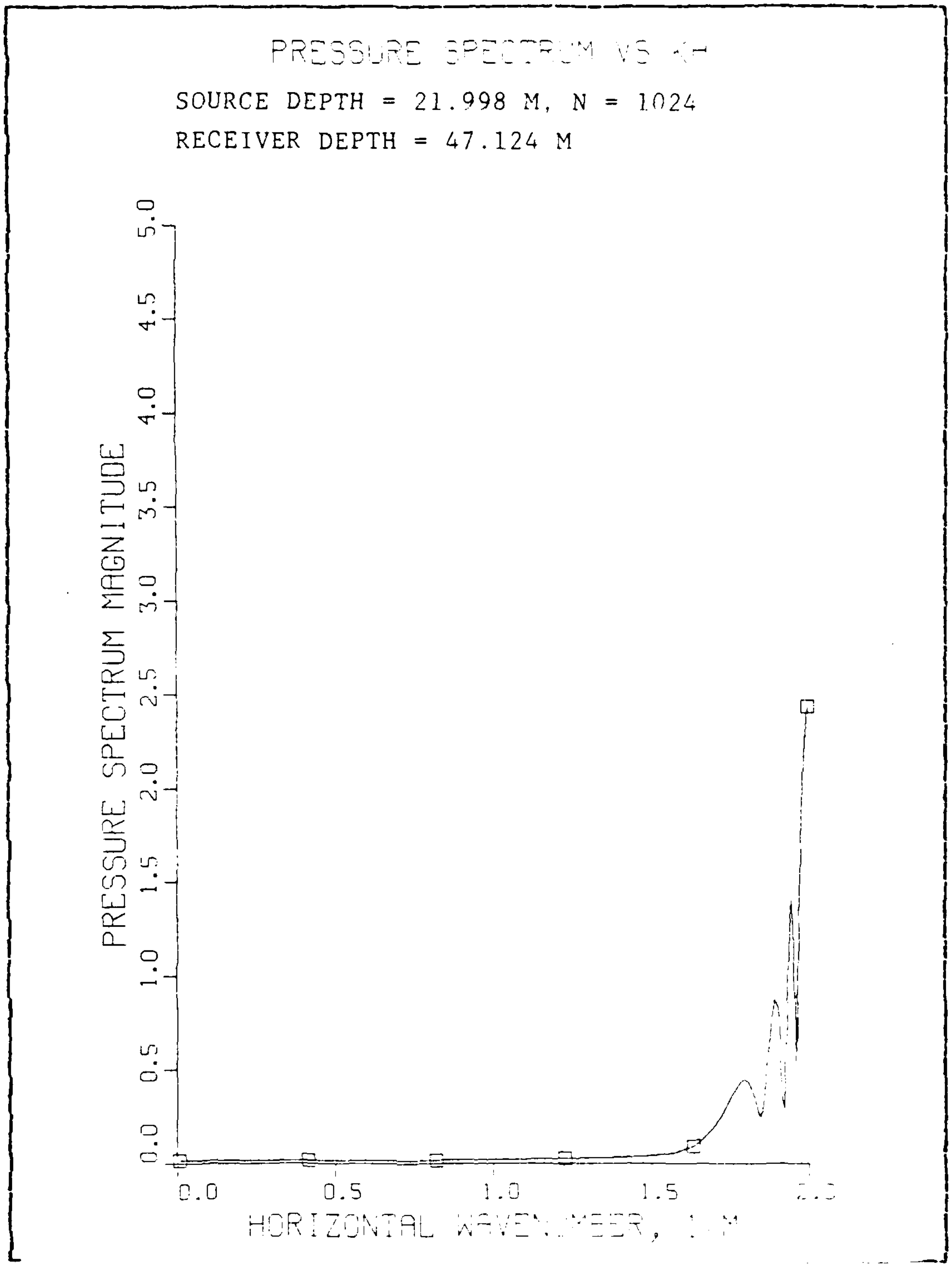

Figure 3.27 Pressure Spectrum,
SS 2, Range Window Set at 100 Meters

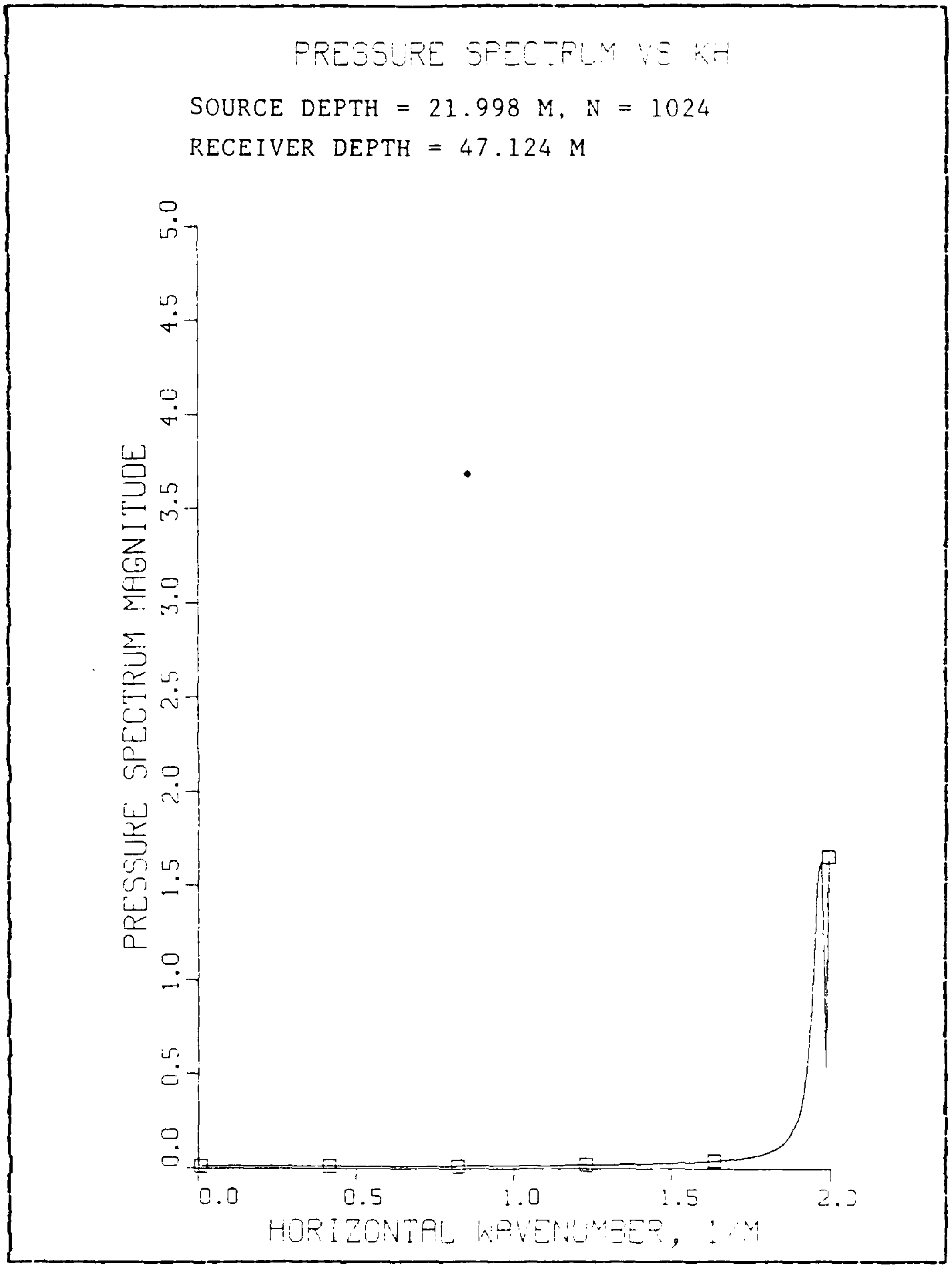

Figure 3.28 Pressure Spectrum, SS 2, Range Window Set at 200 Meters

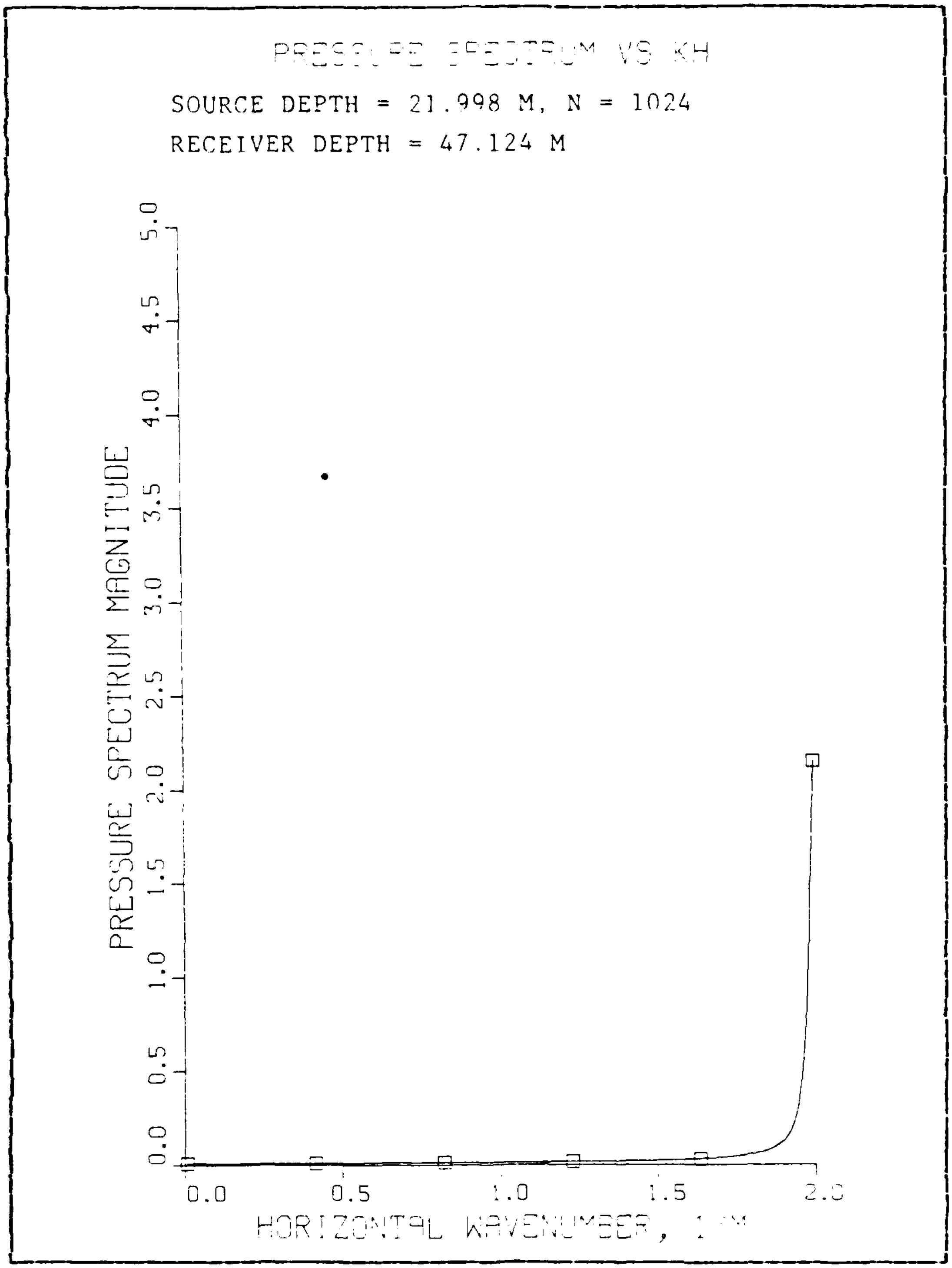

Figure 3.29 Pressure Spectrum, SS 2, Range Window Set at 300 Meters

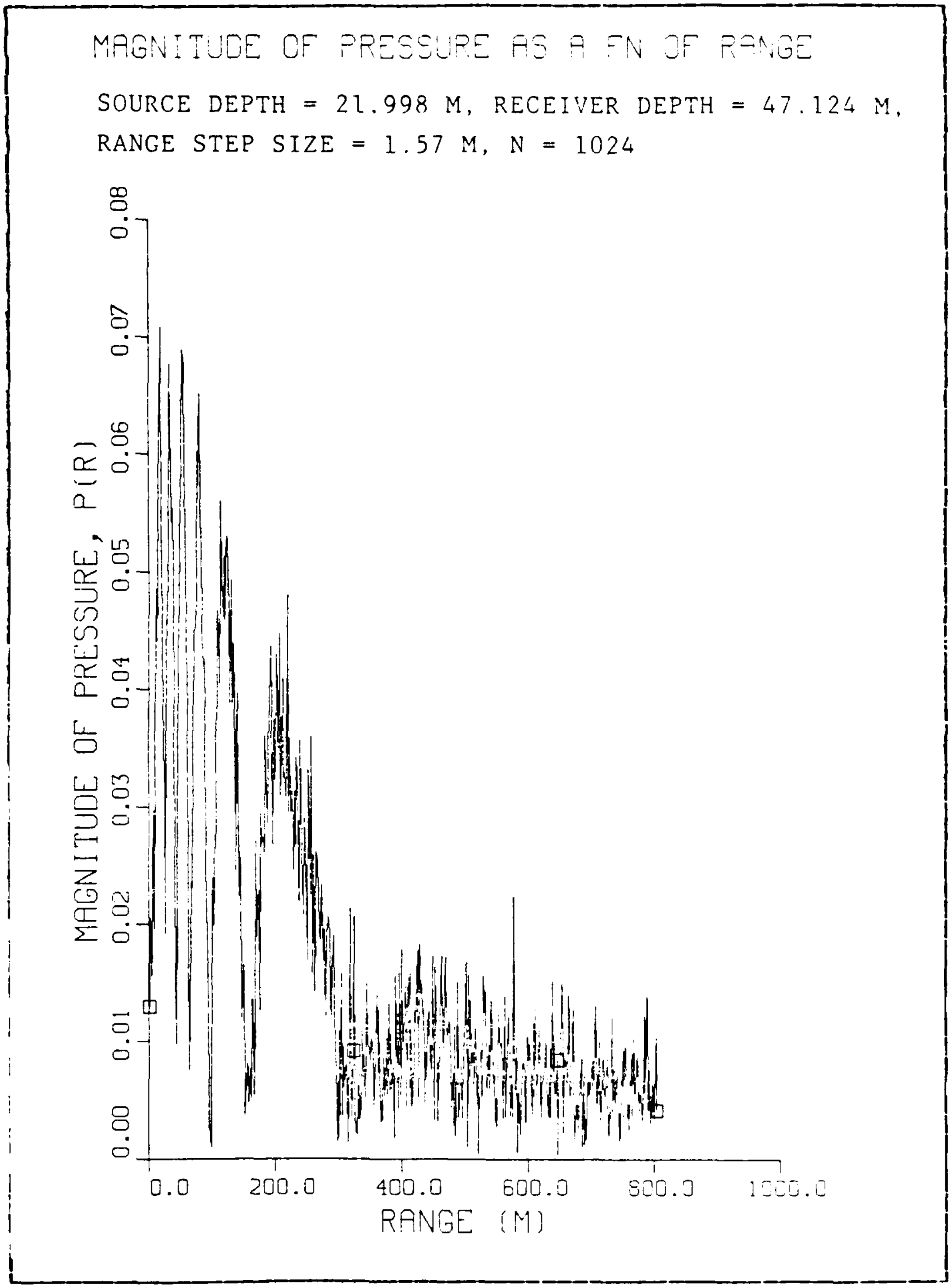

Figure 3.30 Pressure Field, K = 1.0, μ = 0.005

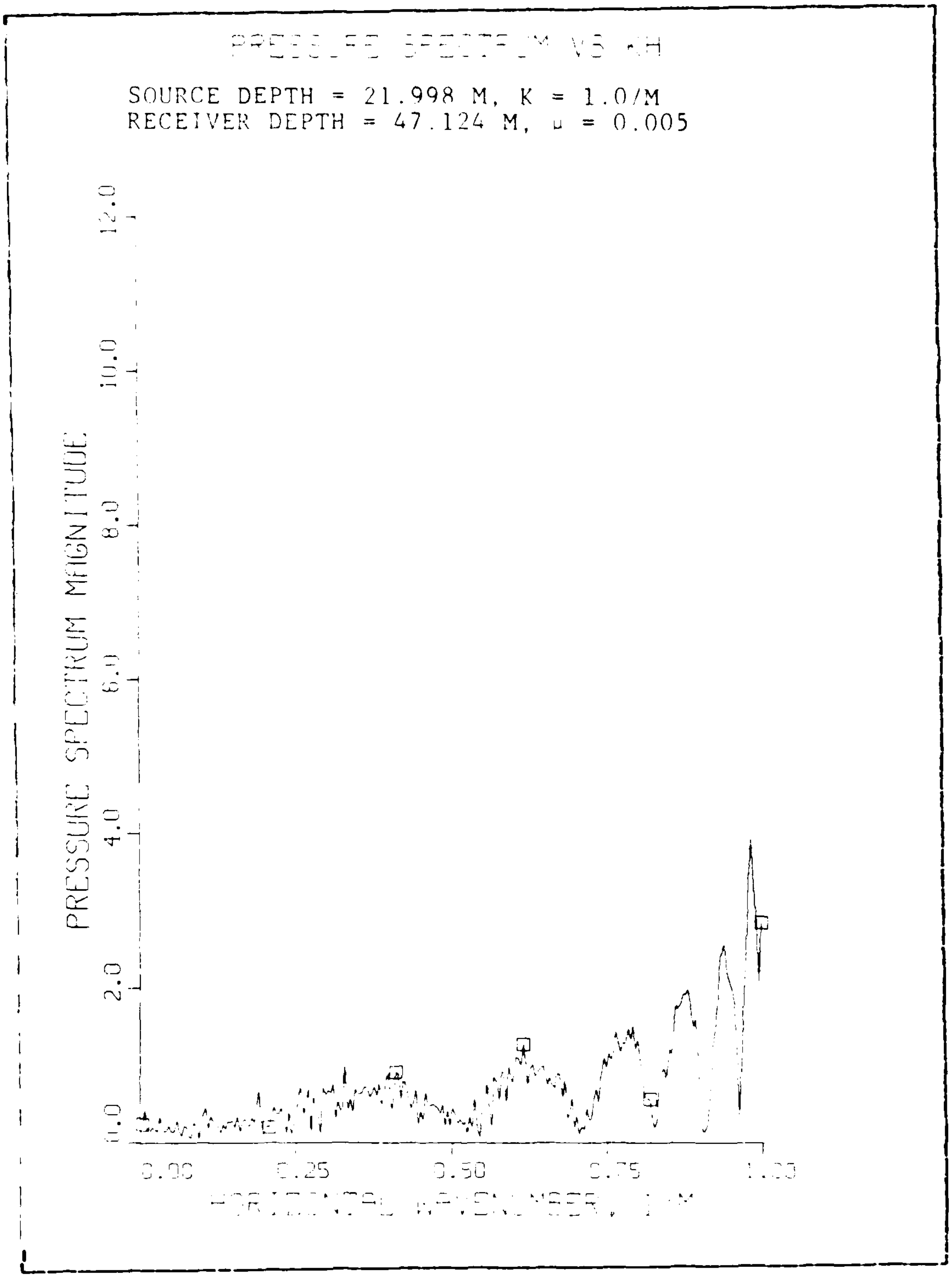

Figure 3.31 Pressure Spectrum vs. Gamma

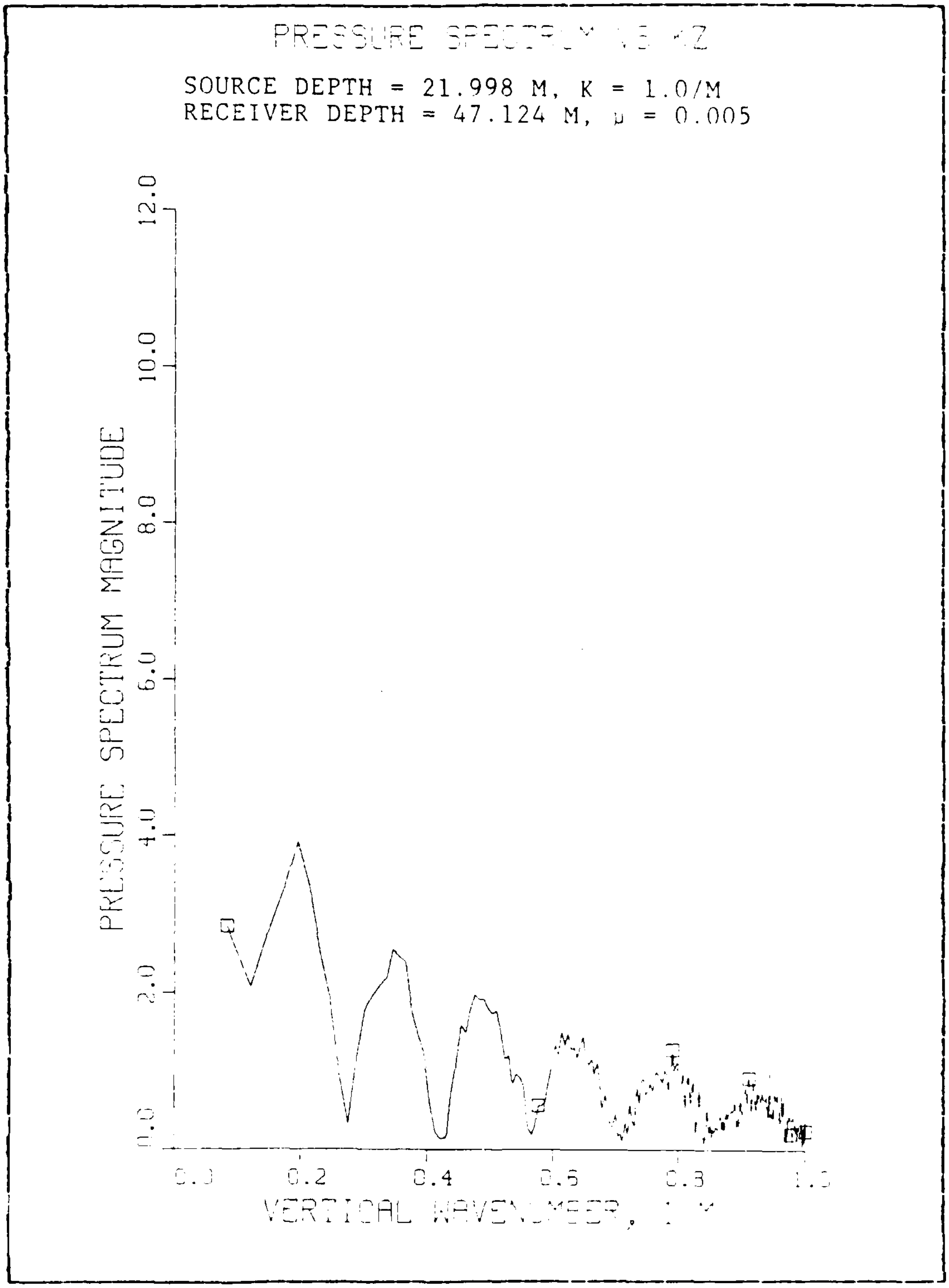

Figure 3.32 Pressure Spectrum vs. Beta

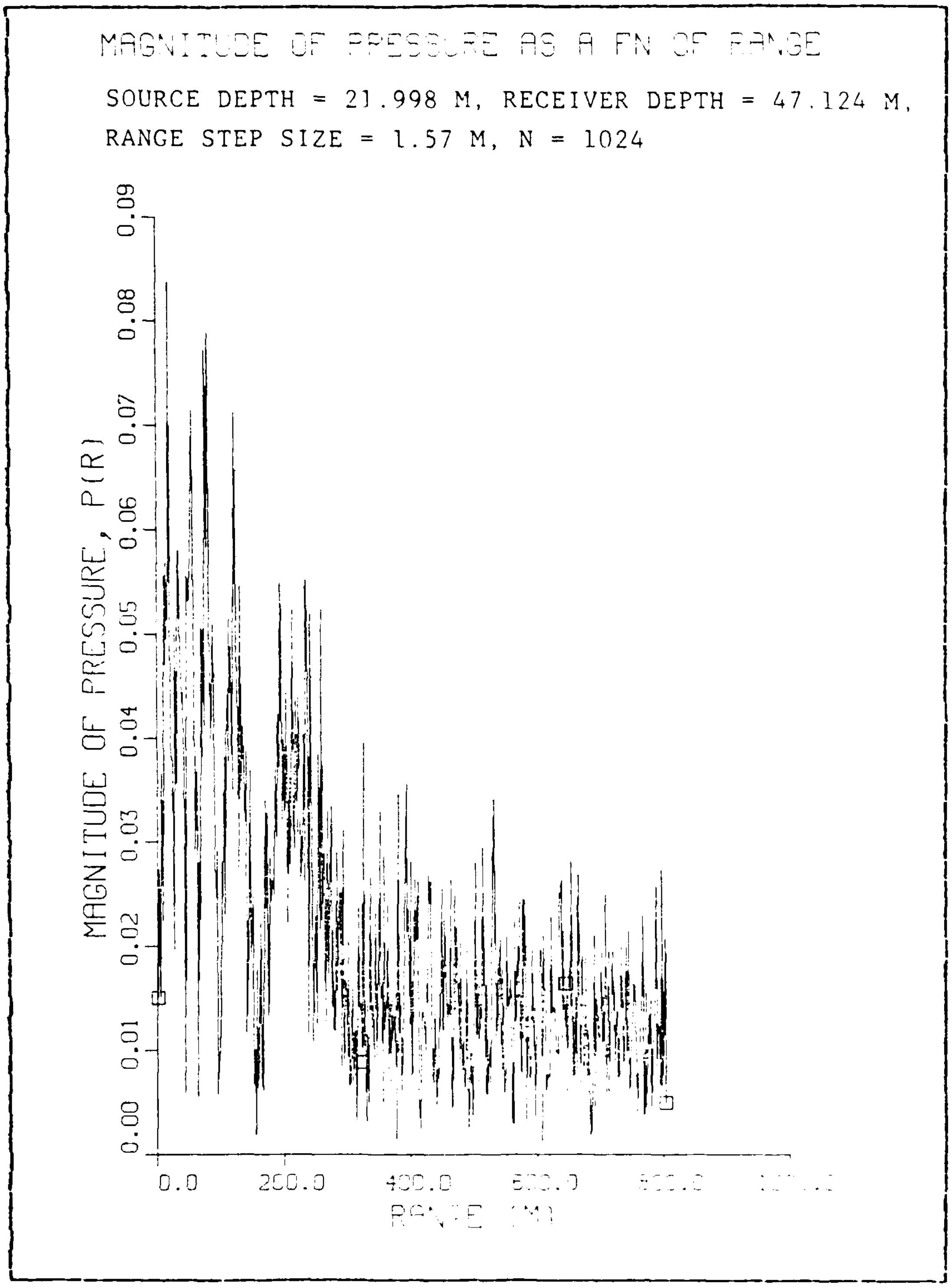

Figure 3.33 Pressure Field, K = 1.0, μ = 0.01

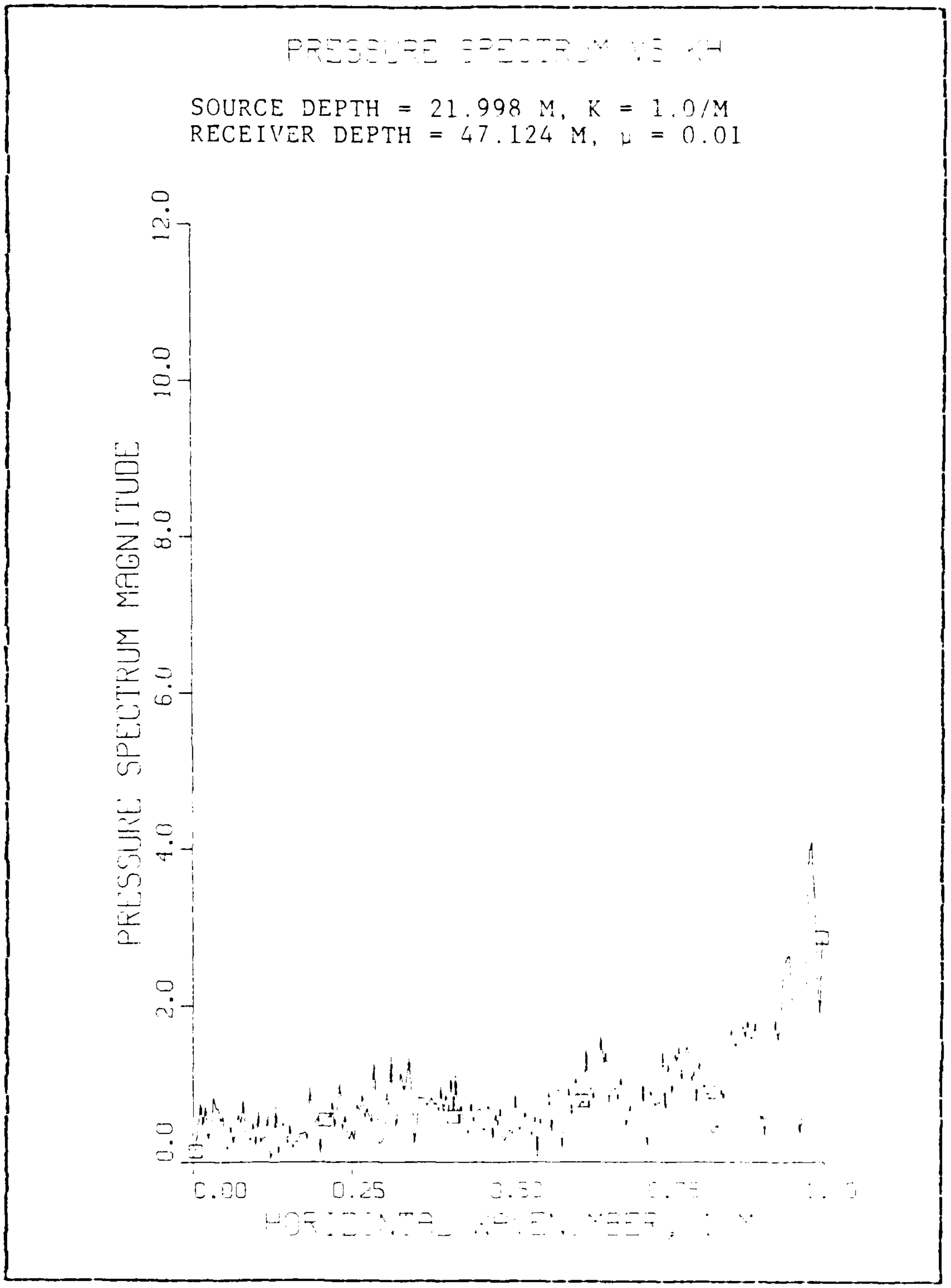

Figure 3.34 Pressure Spectrum vs. Gamma

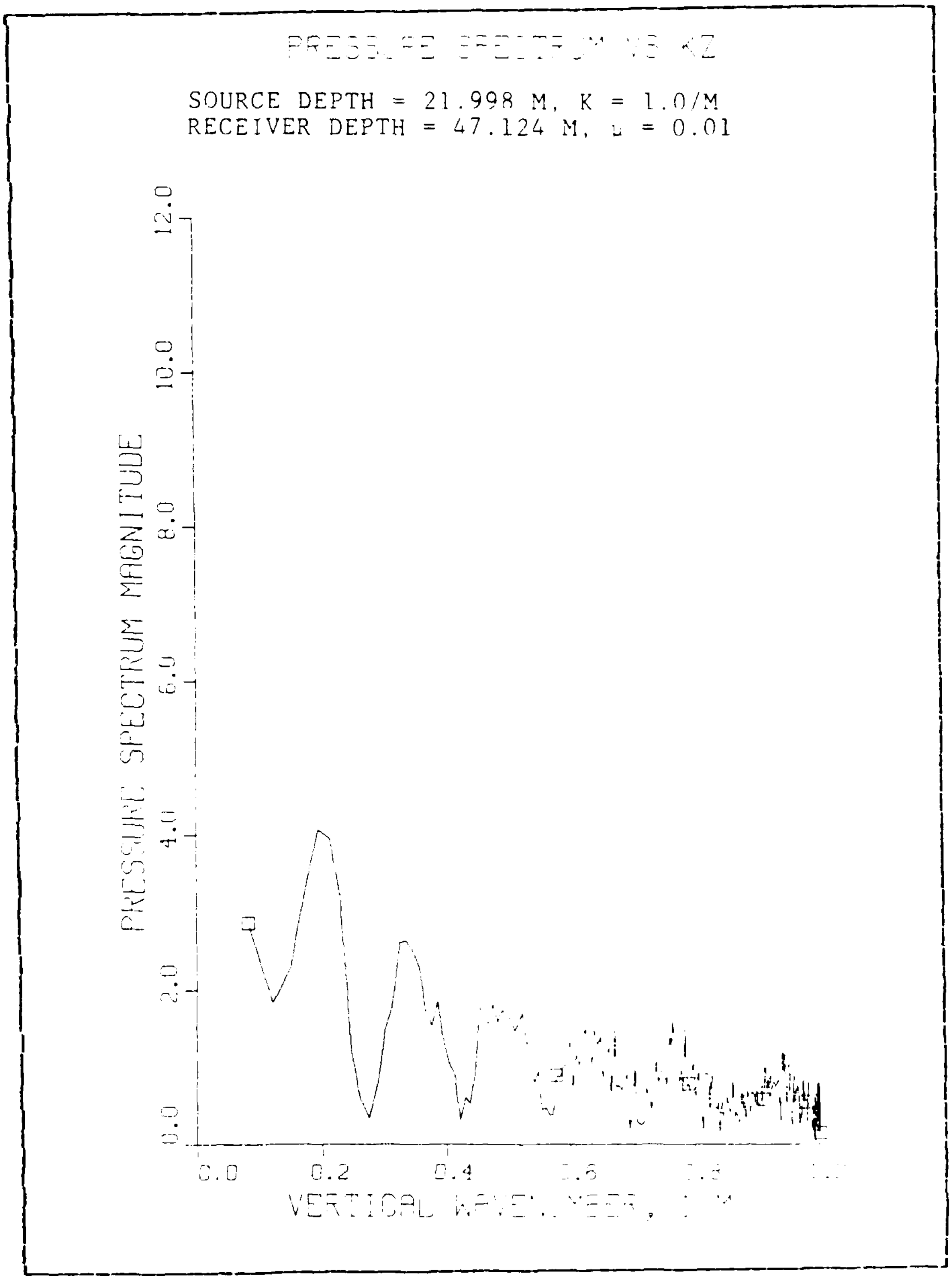

Figure 3.35 Pressure Spectrum vs. Beta

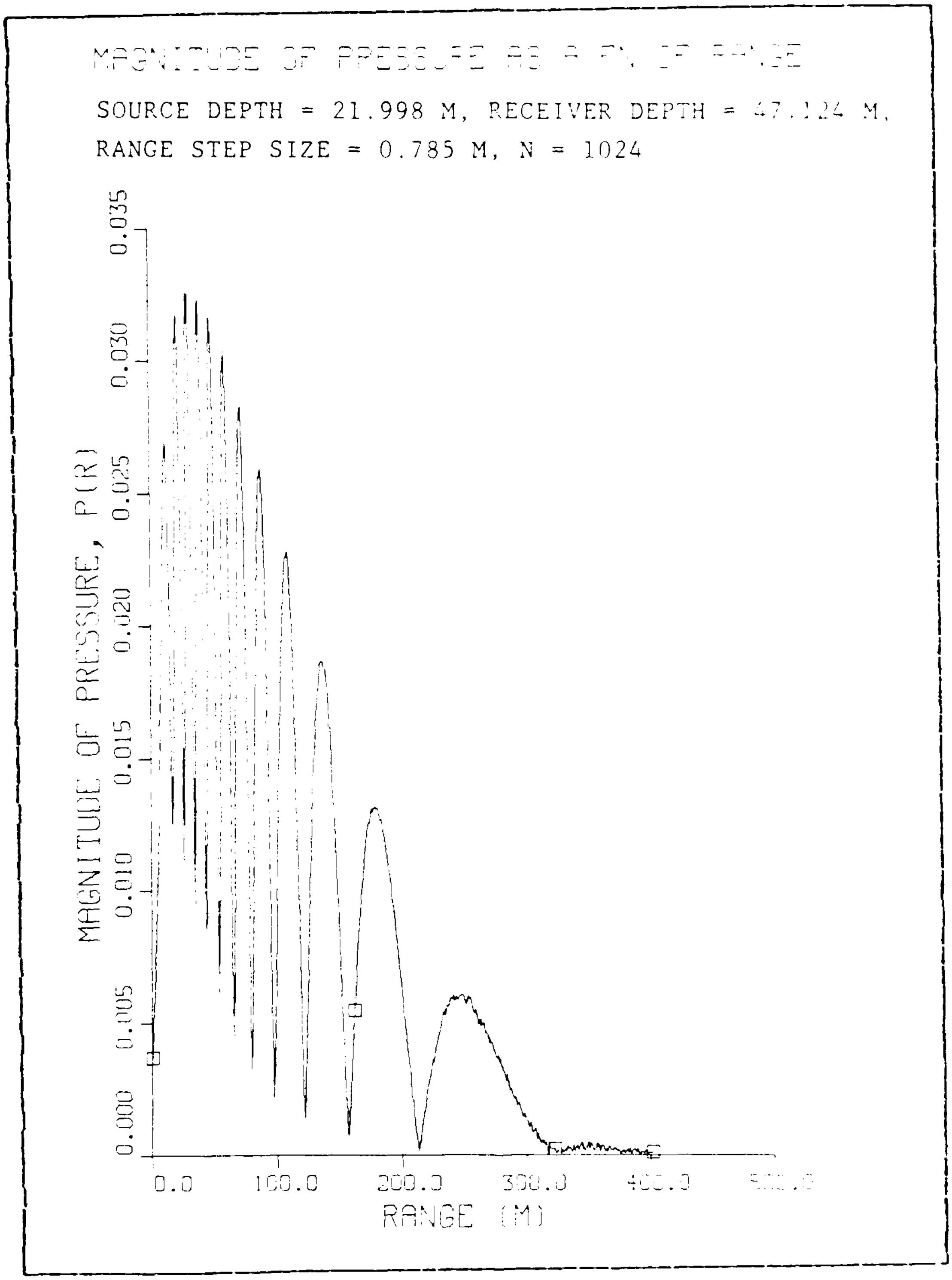

Figure 3.36 Pressure Field, K = 2.0, μ = 0.0001

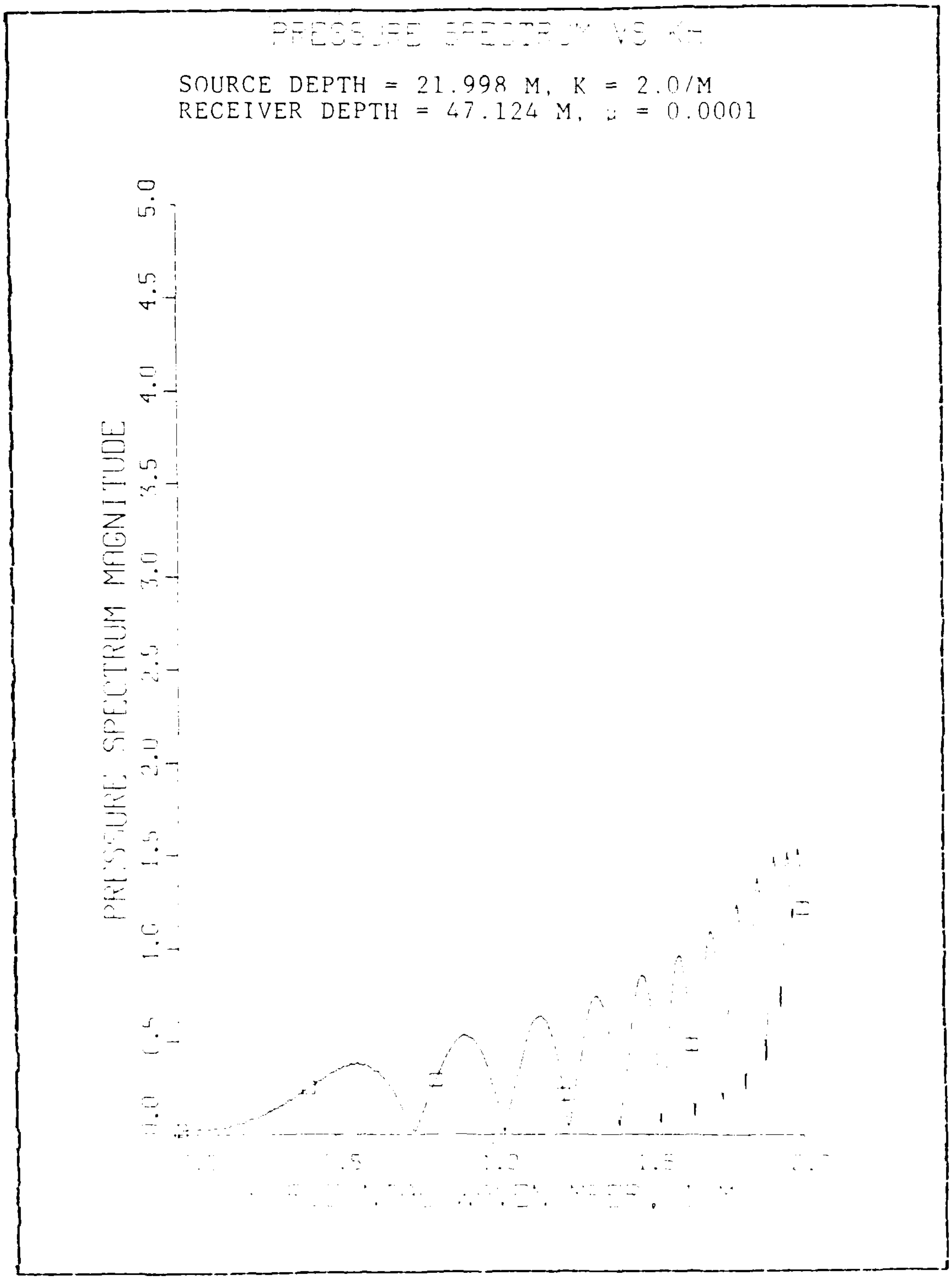

Figure 3.37 Pressure Spectrum vs. Gamma

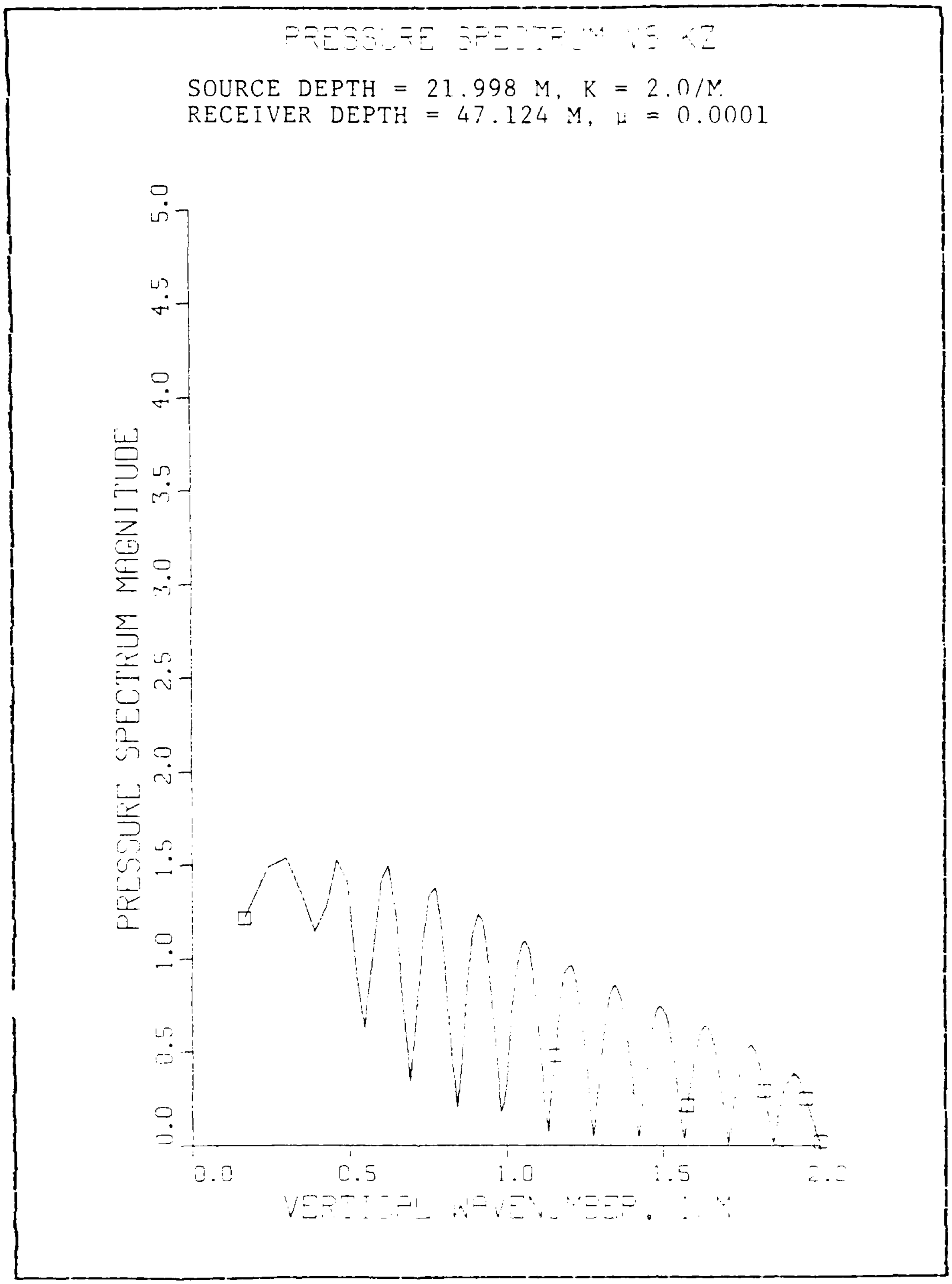

Figure 3.38 Pressure Spectrum vs. Beta

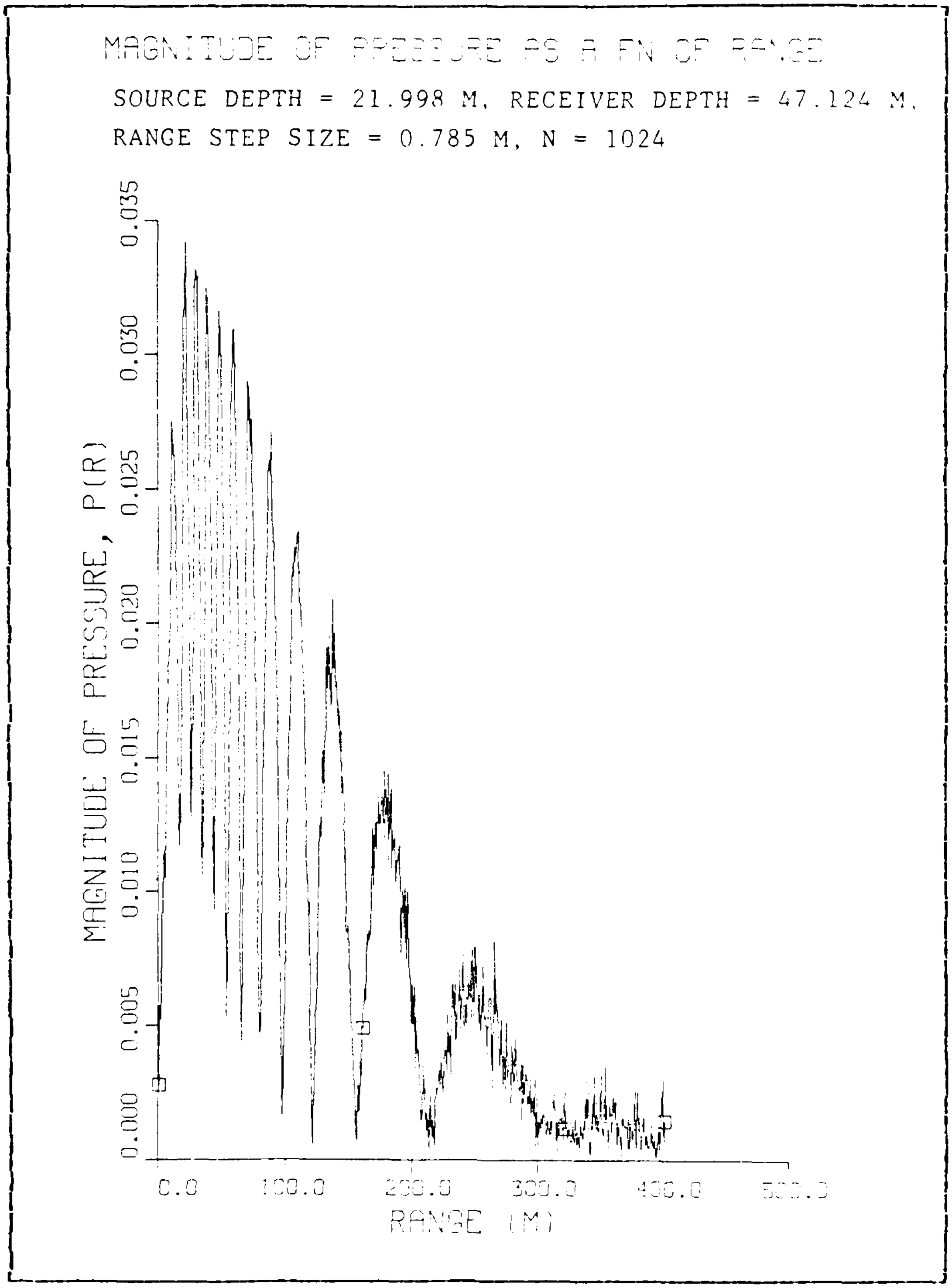

Figure 3.39 Pressure Field, K = 2.0, μ = 0.001

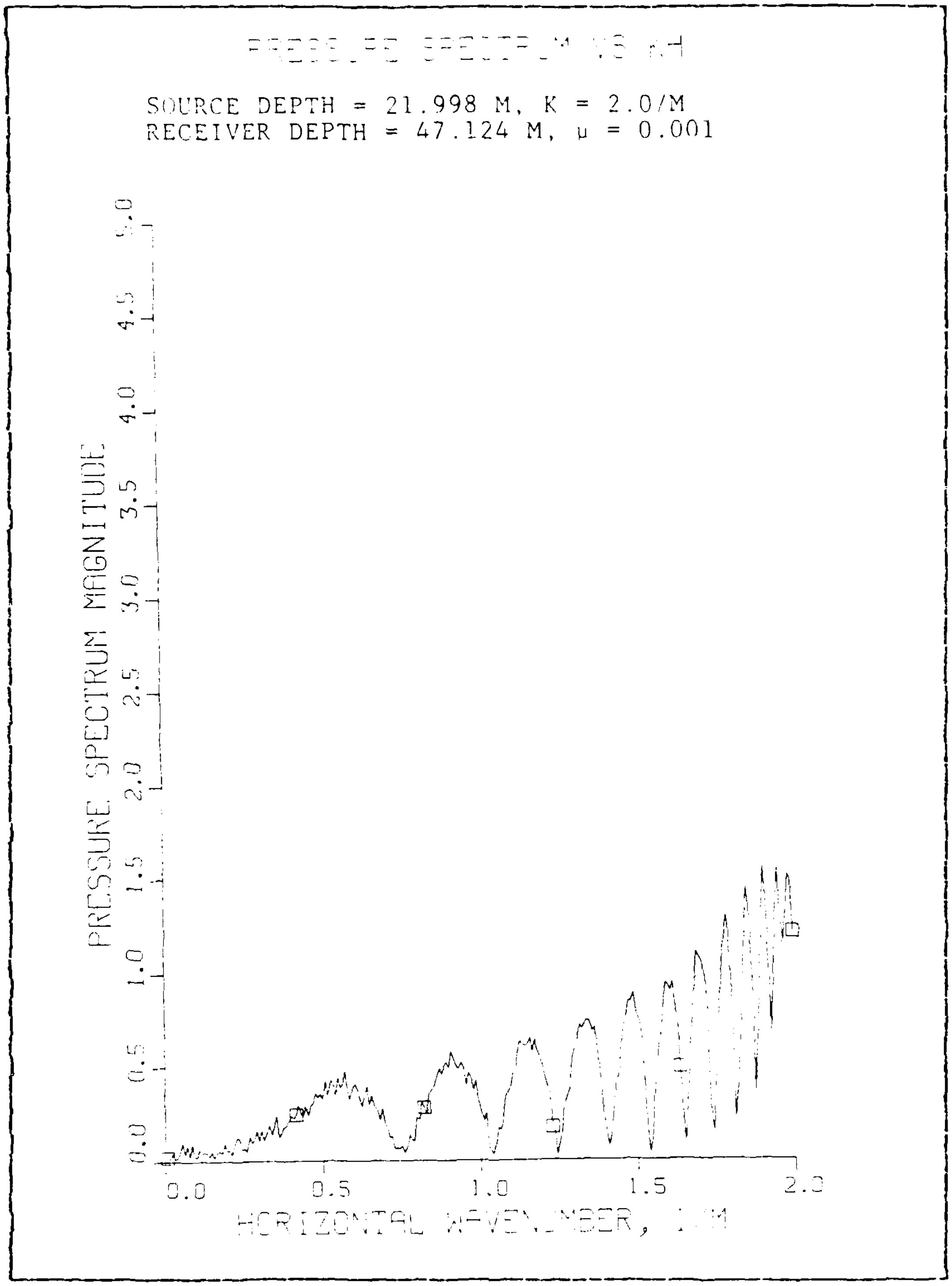

Figure 3.40 Pressure Spectrum vs. Gamma

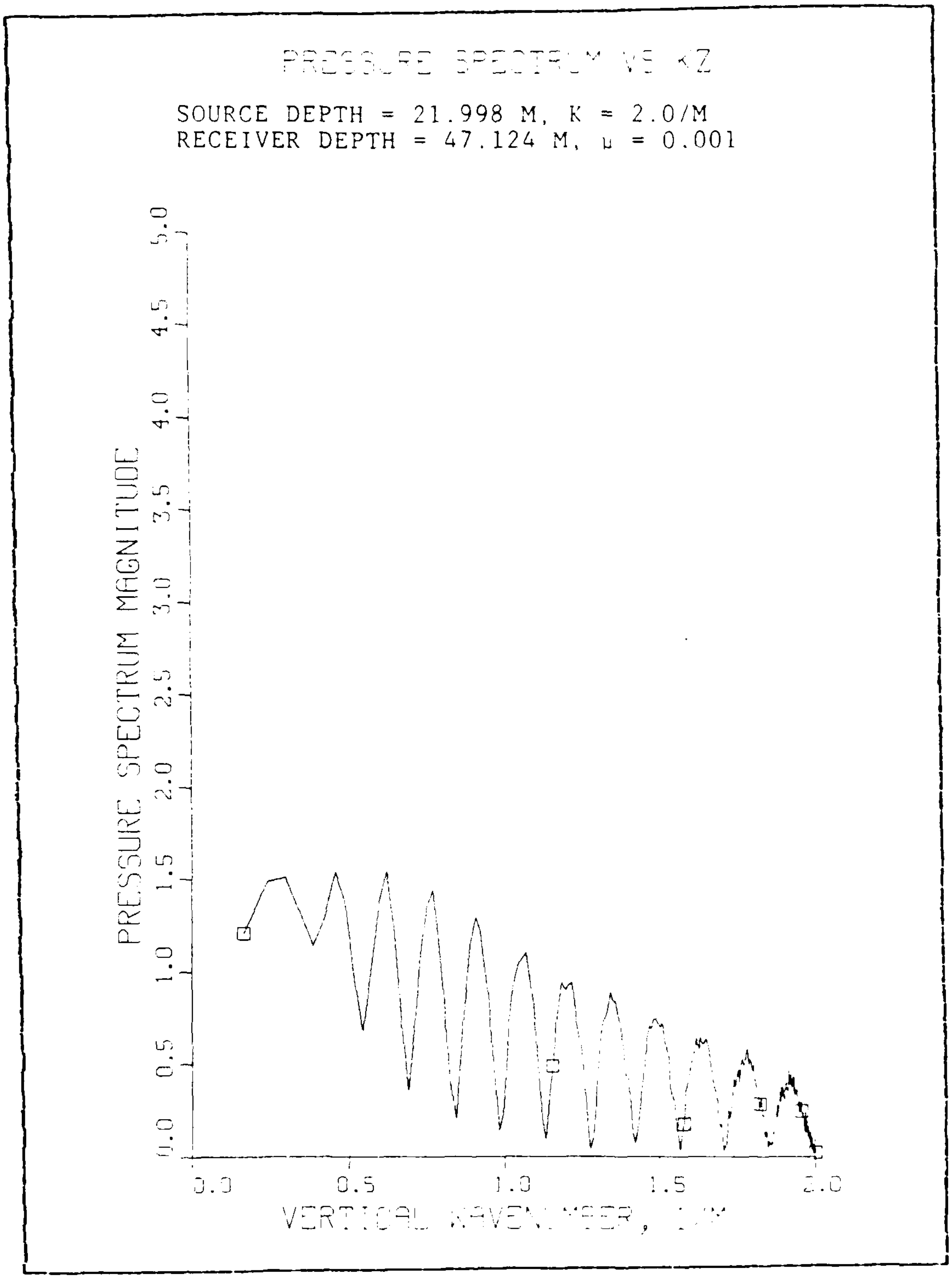

Figure 3.41 Pressure Spectrum vs. Beta

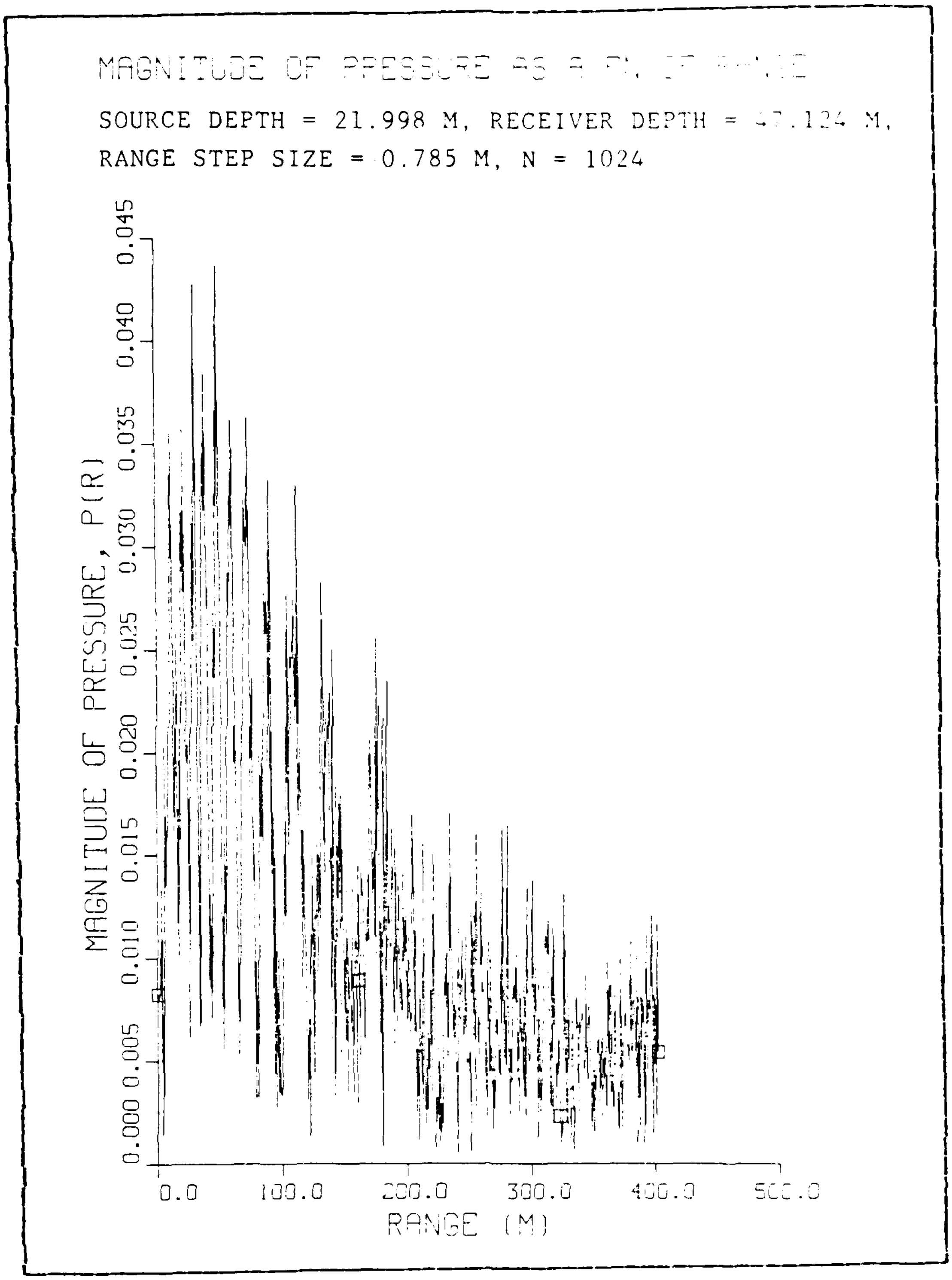

Figure 3.42 Pressure Field, K = 2.0, μ = 0.005

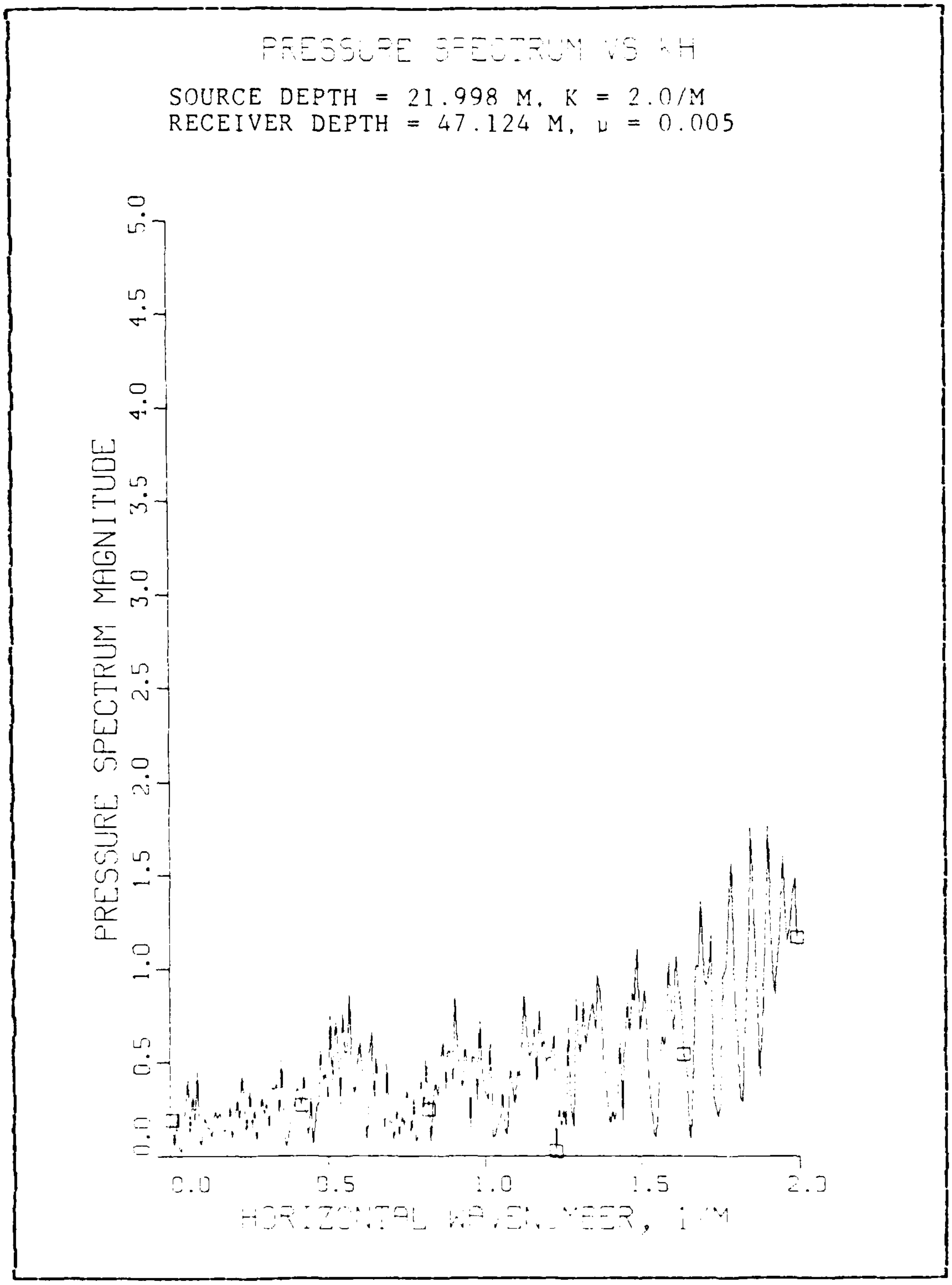

Figure 3.43 Pressure Spectrum vs. Gamma

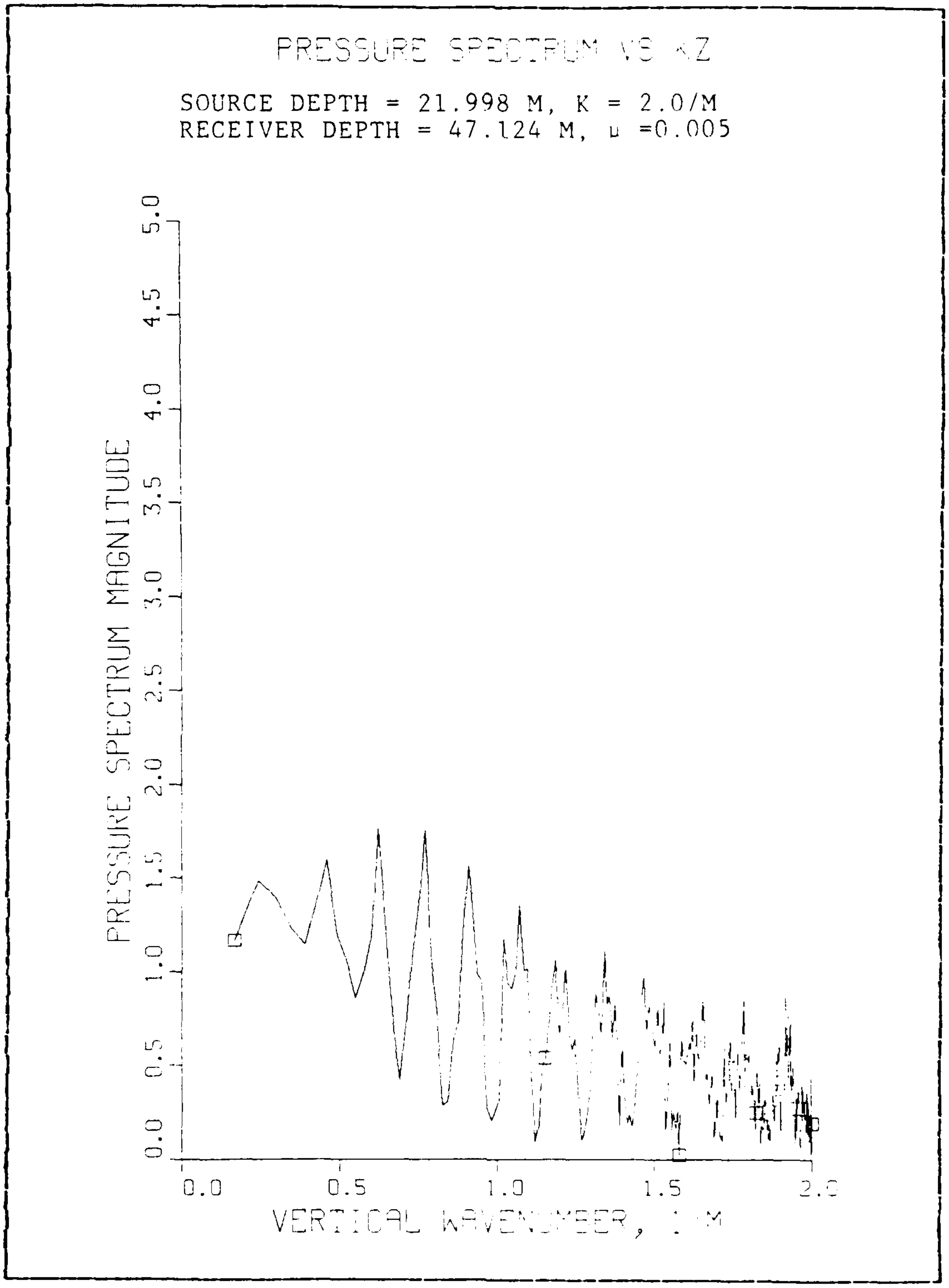

Figure 3.44 Pressure Spectrum vs. Beta

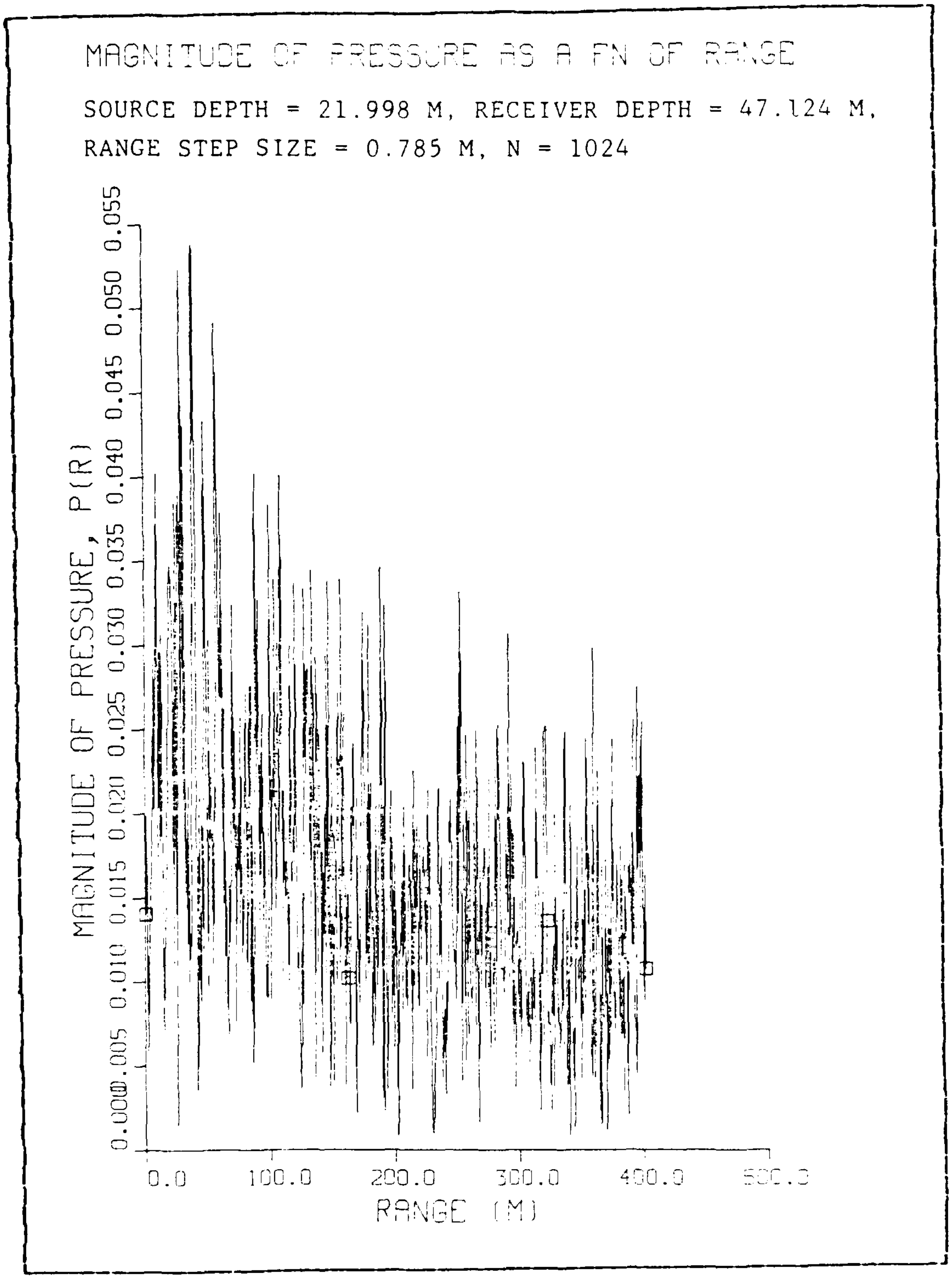

Figure 3.45 Pressure Field, K = 2.0, μ = 0.01

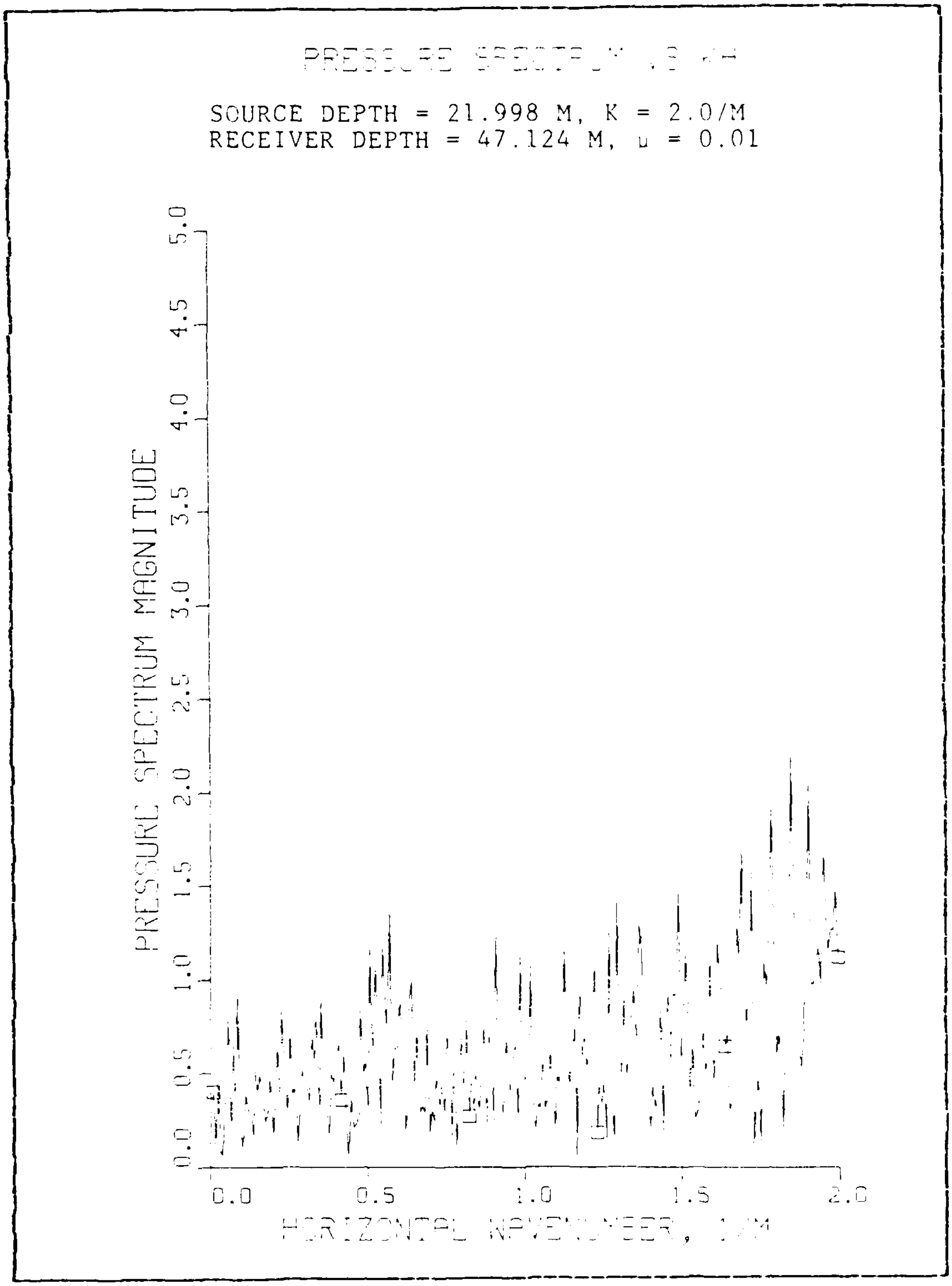

Figure 3.46 Pressure Spectrum vs. Gamma

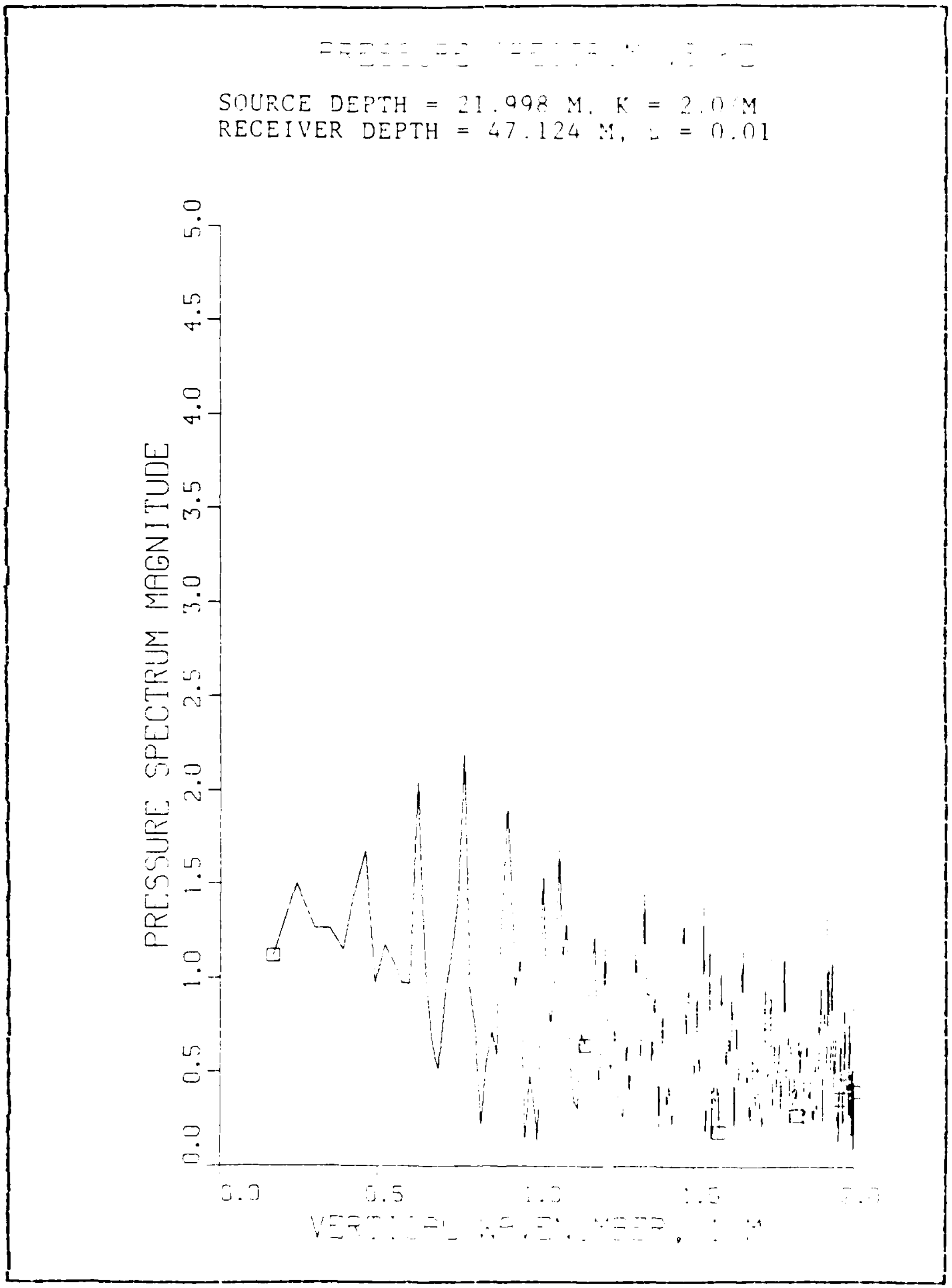

Figure 3.47 Pressure Spectrum vs. Beta

APPENDIX A: LLOYDS MIRROR PRESSURE FIELD SOURCE CODE

```
C ******************************************************************
C
C     THIS PROGRAM WILL PLOT THE |P(R)| VS R CURVE STARTING AT THE ORIGIN
C     (I.E., THE SOURCE).
C
C     THIS PROGRAM ALSO PLOTS THE SPECTRUM VS THE HORIZONTAL WAVENUMBER.
C                          ALSO THE  SPECTRUM VS THE VERTICAL WAVENUMBER.
C
C     IT USES THE COOLEY-TUKEY FFT.
C
C
C ******************************************************************
       DIMENSION DATA(8192),S(4096),CKM(4096),GM(4096),BE(4096),T(4096),
      1U(4096),ANOIZ(4096),AINOIZ(4096),DADA(8192)
       DOUBLE PRECISION DSEED1,DSEED2
       REAL LAMBDA
       DATA Y/'Y'/,DN/'N'/
       PIE = 4.0 * ATAN(1.0)
       EPS = 1.00E-6
C
C    THE USER SELECTABLE VARIABLES ARE ENTERED
C
       WRITE(6,2)
2      FORMAT(1X,'ENTER THE SOURCE DEPTH IN METERS.')
       READ(5,*)ZS
       ZS = ZS
       WRITE(6,4)
4      FORMAT(1X,'ENTER THE RECEIVER DEPTH IN METERS.')
       READ(5,*)ZR
       ZR = ZR
       WRITE(6,5)
5      FORMAT(1X,'ENTER THE VALUE OF K, THE WAVENUMBER.')
       READ(5,*)AK
       AK = AK
       WRITE(6,3)
3      FORMAT(/,1X,'ENTER THE AVERAGE SURFACE WAVEHEIGHT, IN REAL METERS.
      1')
       READ(5,*)AICH
       AICH = AICH
       WRITE(6,6)
6      FORMAT(/,1X,'ENTER THE VALUE OF R(NAUGHT), RO.')
       READ(5,*)RO
       RO = RO
       WRITE(6,7)
7      FORMAT(1X,'ENTER N, THE NUMBER OF TRANSFORM POINTS.')
       READ(5,*)IMAX
       IMAX = IMAX
```

```
      IF(ZR.GE.ZS) GO TO 360                                            TESO0490
      ZX = ZR                                                           TESO0500
      GO TO 370                                                         TESO0510
360   ZX = ZS                                                           TESO0520
370   WRITE(6,123) ZX                                                   TESO0530
123   FORMAT(/,1X,'THE SHALLOWER DEPTH =   ',F8.2)                      TESO0540
C                                                                       TESO0550
      REALN = FLOAT(IMAX)                                               TESO0560
      REALM = ALOG10(REALN)/ALOG10(2.0) + 0.9                           TESO0570
      I22 = INT(REALM)                                                  TESO0580
      JMAX = IMAX/2                                                     TESO0590
      IMAX4 = IMAX/4                                                    TESO0600
      KMAX = IMAX/2 + 1                                                 TESO0610
      LMAX = IMAX - 1                                                   TESO0620
      MMAX = IMAX + 3                                                   TESO0630
      NMAX = IMAX + 4                                                   TESO0640
      IMAX2 = IMAX * 2                                                  TESO0650
      IMAX3 = IMAX2 + 2                                                 TESO0660
      FLIMAX = FLOAT(IMAX)                                              TESO0670
      FJMAX = FLOAT(JMAX)                                               TESO0680
      IMAX8 = INT(FLIMAX/8.0)                                           TESO0690
C                                                                       TESO0700
      WRITE(6,8) FLIMAX,FJMAX,IMAX,IMAX8,JMAX,KMAX,LMAX,MMAX,NMAX       TESO0710
8     FORMAT(1X,2(2X,F7.2),7(2X,I4))                                    TESO0720
11    WRITE(6,9) ZS,ZR,AK,AICH                                          TESO0730
9     FORMAT(1X,'THE SELECTED PARAMETERS ARE:',/,10X,'SOURCE DEPTH IN METESO0740
     1TERS:    ',F8.2,/,10X,'RCVR DEPTH IN METERS:   ',F8.2,/,10X,'VALUE OFTESO0750
     2 THE WAVENUMBER  :',F8.5,/,10X,'THE WAVEHEIGHT IS:   ',F8.2,/,/,5X,TESO0760
     3'DO YOU DESIRE TO MAKE ANY CHANGES? (YES/NO)')                    TESO0770
      READ(5,121) ANS                                                   TESO0780
121   FORMAT(A1)                                                        TESO0790
      IF(ANS.EQ.ON) GO TO 122                                           TESO0800
      IF(ANS.NE.Y) GO TO 11                                             TESO0810
      GO TO 1                                                           TESO0820
122   LAMBDA = 2.0 * PIE/AK                                             TESO0830
      WRITE(6,14) LAMBDA                                                TESO0840
14    FORMAT(1X,'THE WAVELENGTH IN METERS IS:   ',F12.4,/,5X,'THE RANGE ITESO0850
     1NCREMENT MUST BE LESS THAN -LAMBDA/(2*PIE)- TO PREVENT ALIASING.  TESO0860
     2ENTER THE RANGE INCREMENT.')                                      TESO0870
      READ(5,*) DR                                                      TESO0880
      DX = DR                                                           TESO0890
      RMAX = R0 + DX * JMAX                                             TESO0900
      RMIN = (-1.0) * RMAX                                              TESO0910
      FAC = (-1.0) * DX/(2.0 * SQRT(2.0 * PIE))                         TESO0920
15    WRITE(6,16) RMIN,RMAX,DX,FAC                                      TESO0930
16    FORMAT(1X,'RANGE SELECTIONS ARE:   ',/,10X,'MINIMUM RANGE IN METERSTESO0940
     1:   ',F10.2,/,10X,'MAXIMUM RANGE IN METERS:   ',F10.2,/,10X,'RANGE  TESO0950
     2 INCREMENT IN METERS:   ',F10.7,/,10X,'FACTOR TERM IS:   ',F10.7,/,/TESO0960
```

```
     3,5X,'DO YOU DESIRE TO MAKE ANY CHANGES? (YES/NO)')
      READ(5,121)BANS
      IF(BANS.EQ.ON)GO TO 211
      IF(BANS.NE.Y)GO TO 15
      GO TO 1

211   WRITE(6,212)
212   FORMAT(1X,'THIS WILL BE THE SURFACE REFLECTION CASE. DO YOU WANT T
     1O QUIT? (YES/NO)')
      READ(5,121)GANS
      IF(GANS.EQ.ON)GO TO 320
      IF(GANS.NE.Y)GO TO 211
      GO TO 451
C ***********************************************************************
C   NOW WE GENERATE THE COMPLEX PRESSURE FIELD
C ***********************************************************************
C
320   WRITE(6,354)
354   FORMAT(4X,'I',8X,'GRE',10X,'GIM',10X,'WINDOW FACTOR',/)
      DO 17 I = 1,IMAX
      FLY = FLOAT(I)
      W = 0.5 * (1.0 + COS((FLY-1.0)*PIE/IJMAX))
C     W = 1.0
      R = R0 + FLY * DR
      RSQ = SQRT(R)
      R1 = SQRT(R**2 + (ZZ-ZS)**2)
      R2 = SQRT(R**2 + (ZZ+ZS)**2)
      AINC = ATAN2((ZZ+ZS),R)
      SRAY = 2.0 * PIE * AICH * SIN(AINC)/LAMBDA
      SSRAY = -(SRAY**2)
      XIJ = EXP(SSRAY)
      GRE = (COS(AK*R1)/R1 - XIJ * COS(AK*R2)/R2) * RSQ * FAC
      GIM = (SIN(AK*R1)/R1 - XIJ * SIN(AK*R2)/R2) * RSQ * FAC
      DATA(IMAX + 2*I) = GRE * W
      DATA(IMAX - 2*I) = GRE * W
      DATA(IMAX + 2*I) = GIM * W
      DATA(IMAX - 2*I) = GIM * W
C     WRITE(6,100)I,GRE,GIM,W
C100  FORMAT(2X,I5,3(5X,F10.7))
17    CONTINUE
C ***********************************************************************
C
C     THIS SECTION OF THE PROGRAM ADDS A NORMALLY-DISTRIBUTED RANDOM
C     ERROR FACTOR TO THE FIELD. IT CALLS UPON THE IMSL ROUTINE
C     "GGNML" TWICE TO GENERATE THE MAGNITUDE AND PHASE RANDOM FACTORS,
C     A AND B. THIS ROUTINE SEEKS TO DUPLICATE THE RICIAN DISTRIBUTION
```

```
C     DESCRIBED BY BRICK ON PAGE 189 OF HIS "PRINCIPLES ...", 3RD ED.
C
C ****************************************************************
C
1100  WRITE(6,1110)
1110  FORMAT(/,2X,'DO YOU DESIRE TO ADD NOISE? (YES/NO)')
      READ(5,121) RANS
      IF(RANS.EQ.ON)GO TO 27
      IF(RANS.NE.Y)GO TO 1100
      GO TO 1120
C
1120  WRITE(6,1112)
1112  FORMAT(/,2X,'WHAT IS THE NOISE FACTOR? (A POSITIVE REAL NUMBER <=
     1 0.01)')
      READ(5,*) XNU
      XNU = XNU
      WRITE(6,1113)
1113  FORMAT(/,2X,'WHAT IS DSEED1?')
      READ(5,*)DSEED1
      DSEED1 = DSEED1
      WRITE(6,1116)
1116  FORMAT(/,2X,'WHAT IS DSEED2?')
      READ(5,*)DSEED2
      DSEED2 = DSEED2
      CALL GGNML(DSEED1,IMAX,T)
      CALL GGNML(DSEED2,IMAX,U)
      WRITE(6,1114)T(IMAX),U(IMAX)
1114  FORMAT(/,2X,'FINAL RANDOM NUMBERS, T AND U, ARE ',2(2X,F10.8))
C
      DO 28 I = 1,IMAX
      RNOIZ(I) = T(I) * XNU
      AINOIZ(I) = U(I) * XNU
28    CONTINUE
C
      DO 29 I = 1,IMAX
      DATA(2*I-1) = DATA(2*I-1) + RNOIZ(I)
      DATA(2*I) = DATA(2*I) + AINOIZ(I)
29    CONTINUE
C
C ****************************************************************
C     THIS PART OF THE PROGRAM ISOLATES THAT PART OF THE P(R) CURVE
C     CORRESPONDING TO THE RANGE STARTING AT THE SOURCE AND MOVING
C     IN A POSITIVE DIRECTION.
C     THIS METHOD ENABLES ONE TO PLOT ONLY ONE-HALF THE |P(R)| VS R
C     CURVE, AS IS DONE CONVENTIONALLY.
C ****************************************************************
27    DO 37 I = 1,IMAX
      DATA(2*I-1) = DATA(IMAX + (2*I-1))
```

AD-A156 463 USE OF THE WAVENUMBER TECHNIQUE WITH THE LLOYDS MIRROR FOR AN ACOUSTIC DOUBLET(U) NAVAL POSTGRADUATE SCHOOL MONTEREY CA P B KING MAR 85 2/2

UNCLASSIFIED F/G 17/1 NL

END

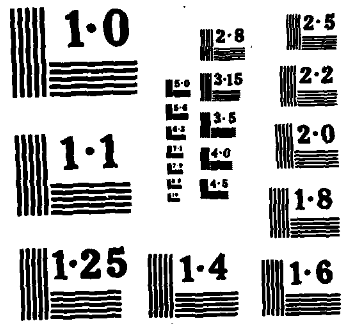

NATIONAL BUREAU OF STANDARDS
MICROCOPY RESOLUTION TEST CHART

```
      DADA(2*I) = DATA(IMAX + (2*I))                                    TES01930
37    CONTINUE                                                          TES01940
C                                                                       TES01950
C39    CALL PRPLOT(DADA,DR,IMAX,JMAX,RO)                                TES01960
C                                                                       TES01970
C                                                                       TES01980
C                                                                       TES01990
      CALL FOUR2(DATA,IMAX,-1,1)                                        TES02000
C                                                                       TES02010
C      WRITE(6,352)                                                     TES02020
C352   FORMAT(/,5X,'I',4X,'SPEC DATA REAL',3X,'SPEC DATA IMAG',/)       TES02030
C                                                                       TES02040
C      DO 18 I = 1,IMAX                                                 TES02050
C      WRITE(6,353) I,DATA(2*I - 1),DATA(2*I)                           TES02060
C18    CONTINUE                                                         TES02070
C353   FORMAT(2X,I4,2(4X,F10.7))                                        TES02080
C                                                                       TES02090
      DG = 2.0 * PIE/(FLIMAX * DR)                                      TES02100
      WRITE(6,300) DG                                                   TES02110
300   FORMAT(/,2X,'DG =  ',F12.8,/)                                     TES02120
C                                                                       TES02130
      WRITE(6,201)                                                      TES02140
201   FORMAT(/,5X,'I',6X,'CKM',10X,'Q',10X,'KZ',/)                      TES02150
C                                                                       TES02160
      DO 50 I=1,IMAX4                                                   TES02170
      FLY = FLOAT(I)                                                    TES02180
      GM(I) = FLY * DG                                                  TES02190
      IF(GM(I).GE.AK) GO TO 400                                         TES02200
      GO TO 420                                                         TES02210
C                                                                       TES02220
420   CONTINUE                                                          TES02230
C                                                                       TES02240
C ******************************************************************** TES02250
C     IF GM(I) < AK, THEN BE(I) IS REAL, AND Q REDUCES TO A FORM OF     TES02260
C     THE SIN(X)/X FUNCTION, APPROXIMATELY. ACTUAL FORM IS GIVEN BELOW. TES02270
C ******************************************************************** TES02280
C                                                                       TES02290
      BE(I) = SQRT(AK**2 - GM(I)**2) + EPS                              TES02300
      Q(I) = ABS(SIN(BE(I)*ZX)*SQRT(GM(I))/BE(I))                       TES02310
      GO TO 450                                                         TES02320
C                                                                       TES02330
C                                                                       TES02340
400   CONTINUE                                                          TES02350
C                                                                       TES02360
C ******************************************************************** TES02370
C     IF GM(I) >= AK, THEN BE(I) = SQRT OF A NEGATIVE NUMBER, AND THE   TES02380
C     THEORETICAL FUNCTION, P(K), REDUCES TO THE HYPERBOLIC SIN (SINH). TES02390
C ******************************************************************** TES02400
```

```
      BER = SQRT(GM(I)**2 - AK**2)
      QQ = EXP(-BER * (ZP - ZS)) - EXP(-BER * (ZR + ZS))
      QQ = ABS(CC * SQRT(GM(I))/(2.0 * BER))
      GO TO 50
C
450   CONTINUE
C
      CKRE = DATA(2*I - 1)
      CKIM = DATA(2*I)
      CKM(I) = SQRT(CKRE**2 + CKIM**2)
50    CONTINUE
C
      IMAX5 = IMAX4 - 1
C
      CALL WIHPLT(IMAX5,GM,CKM,Q,AK,BE)
C
      CALL WTVPLT(IMAX5,CKM,Q,AK,BE)
431   CALL DONEPL
      STOP
      END
C
C
      SUBROUTINE FOUR2(DATA,N,ISIGN,IFORM)
C     COOLEY-TUKEY FAST FOURIER TRANSFORM IN USASI BASIC FORTRAN.
C     MULTI-DIMENSIONAL TRANSFORM, EACH DIMENSION A POWER OF TWO,
C     COMPLEX OR REAL DATA.
C     TRANSFORM(K1,K2,...) = SUM(DATA(J1,J2,...)*EXP(ISIGN*2*PI*SQRT(-1)
C     *((J1-1)*(K1-1)/N(1)+(J2-1)*(K2-1)/N(2)+...))), SUMMED FOR ALL
C     J1 AND K1 FROM 1 TO N(1), J2 AND K2 FROM 1 TO N(2),
C     ETC. FOR ALL NDIM SUBSCRIPTS.  NDIM MUST BE POSITIVE AND
C     EACH N(IDIM) MUST BE A POWER OF TWO.  ISIGN IS +1 OR -1.
C     LET NTOT = N(1)*N(2)*...*N(NDIM).  THEN A -1 TRANSFORM
C     FOLLOWED BY A +1 ONE (OR VICE VERSA) RETURNS NTOT
C     TIMES THE ORIGINAL DATA.  IFORM = 1, 0 OR -1, AS DATA IS
C     COMPLEX, REAL OR THE FIRST HALF OF A COMPLEX ARRAY.  TRANSFORM
C     VALUES ARE RETURNED TO ARRAY DATA.  THEY ARE COMPLEX, REAL OR
C     THE FIRST HALF OF A COMPLEX ARRAY, AS IFORM = 1, -1 OR 0.
C     THE TRANSFORM OF A REAL ARRAY (IFORM = 0) DIMENSIONED N(1) BY N(2)
C     BY ... WILL BE RETURNED IN THE SAME ARRAY, NOW CONSIDERED TO
C     BE COMPLEX OF DIMENSIONS N(1)/2+1 BY N(2) BY ....  NOTE THAT IF
C     IFORM = 0 OR -1, N(1) MUST BE EVEN, AND ENOUGH ROOM MUST BE
C     RESERVED.  THE MISSING VALUES MAY BE OBTAINED BY COMPLEX CONJUGA-
C     TION.  THE REVERSE TRANSFORMATION, OF A HALF COMPLEX ARRAY DIMEN-
C     SIONED N(1)/2+1 BY N(2) BY ..., IS ACCOMPLISHED BY SETTING IFORM
C     TO -1.  IN THE N ARRAY, N(1) MUST BE THE TRUE N(1), NOT N(1)/2+1.
C     THE TRANSFORM WILL BE REAL AND RETURNED TO THE INPUT ARRAY.
C     RUNNING TIME IS PROPORTIONAL TO NTOT*LOG2(NTOT), RATHER THAN
C     THE NAIVE NTOT**2.  FURTHERMORE, LESS ERROR IS BUILT UP.
```

```
C     WRITTEN BY NORMAN BRENNER OF MIT LINCOLN LABORATORY, JANUARY 1969.
C     SEE-- IEEE AUDIO TRANSACTIONS (JUNE 1967), SPECIAL ISSUE ON FFT.
      DIMENSION DATA(1), N(1)
      NDIM = 1
      NTOT=1
      DO 10 IDIM=1,NDIM
   10 NTOT=NTOT*N(IDIM)
      IF (IFORM) 70,20,20
   20 NREM=NTOT
      DO 60 IDIM=1,NDIM
      NREM=NREM/N(IDIM)
      NPREV=NTOT/(N(IDIM)*NREM)
      NCURR=N(IDIM)
      IF (IDIM-1+IFORM) 30,30,40
   30 NCURR=NCURR/2
   40 CALL BITRV (DATA,NPREV,NCURR,NREM)
      CALL COOL2 (DATA,NPREV,NCURR,NREM,ISIGN)
      IF (IDIM-1+IFORM) 50,50,60
   50 CALL FIXRL (DATA,N(1),NREM,ISIGN,IFORM)
      NTOT=(NTOT/N(1))*(N(1)/2+1)
   60 CONTINUE
      RETURN
   70 NTOT=(NTOT/N(1))*(N(1)/2+1)
      NREM=1
      DO 100 JDIM=1,NDIM
      IDIM=NDIM+1-JDIM
      NCURR=N(IDIM)
      IF (IDIM-1) 80,80,90
   80 NCURR=NCURR/2
      CALL FIXRL (DATA,N(1),NREM,ISIGN,IFORM)
      NTOT=NTOT/(N(1)/2+1)*N(1)
   90 NPREV=NTOT/(N(IDIM)*NREM)
      CALL BITRV (DATA,NPREV,NCURR,NREM)
      CALL COOL2 (DATA,NPREV,NCURR,NREM,ISIGN)
  100 NREM=NREM*N(IDIM)
      RETURN
      END

      SUBROUTINE BITRV (DATA,NPREV,N,NREM)
C     SHUFFLE THE DATA BY BIT REVERSAL.
C     DIMENSION DATA(NPREV,N,NREM)
C     COMPLEX DATA
C     EXCHANGE DATA(J1,J4REV,J5) WITH DATA(J1,J4,J5) FOR ALL J1 FROM 1
C     TO NPREV, ALL J4 FROM 1 TO N (WHICH MUST BE A POWER OF TWO), AND
C     ALL J5 FROM 1 TO NREM.  J4REV-1 IS THE BIT REVERSAL OF J4-1.  E.G.
C     SUPPOSE N = 32.  THEN FOR J4-1 = 10011, J4REV-1 = 11001, ETC.
      DIMENSION DATA(1)
      IP0=2
```

```
      IP1=IP0*NPREV
      IP4=IP1*N
      IP5=IP4*NREM
      I4REV=1
C     I4REV = 1+(J4REV-1)*IP1
      DO 60 I4=1,IP4,IP1
C     I4 = 1+(J4-1)*IP1
      IF (I4-I4REV) 10,30,30
10    I1MAX=I4+IP1-IP0
      DO 20 I1=I4,I1MAX,IP0
C     I1 = 1+(J1-1)*IP0+(J4-1)*IP1
      DO 20 I5=I1,IP5,IP4
C     I5 = 1+(J1-1)*IP0+(J4-1)*IP1+(J5-1)*IP4
      I5REV=I4REV+I5-I4
C     I5REV = 1+(J1-1)*IP0+(J4REV-1)*IP1+(J5-1)*IP4
      TEMPR=DATA(I5)
      TEMPI=DATA(I5+1)
      DATA(I5)=DATA(I5REV)
      DATA(I5+1)=DATA(I5REV+1)
      DATA(I5REV)=TEMPR
20    DATA(I5REV+1)=TEMPI
C     ADD ONE WITH DOWNWARD CARRY TO THE HIGH ORDER BIT OF J4REV-1.
30    IP2=IP4/2
40    IF (I4REV-IP2) 60,60,50
50    I4REV=I4REV-IP2
      IP2=IP2/2
      IF (IP2-IP1) 60,40,40
60    I4REV=I4REV+IP2
      RETURN
      END

      SUBROUTINE COOL2 (DATA,NPREV,N,NREM,ISIGN)
C     DISCRETE FOURIER TRANSFORM OF LENGTH N.  IN-PLACE COOLEY-TUKEY
C     ALGORITHM, BIT-REVERSED TO NORMAL ORDER, SANDE-TUKEY PHASE SHIFTS.
C     DIMENSION DATA(NPREV,N,NREM)
C     COMPLEX DATA
C     DATA(J1,K4,J5) = SUM(DATA(J1,J4,J5)*EXP(ISIGN*2*PI*I*(J4-1)*
C     (K4-1)/N)), SUMMED OVER J4 = 1 TO N FOR ALL J1 FROM 1 TO NPREV,
C     K4 FROM 1 TO N AND J5 FROM 1 TO NREM.  N MUST BE A POWER OF TWO.
C     METHOD--LET IPREV TAKE THE VALUES 1, 2 OR 4, 4 OR 8, ..., N/16,
C     N/4, N.  THE CHOICE BETWEEN 2 OR 4, ETC., DEPENDS ON WHETHER N IS
C     A POWER OF FOUR.  DEFINE IFACT = 2 OR 4, THE NEXT FACTOR THAT
C     IPREV MUST TAKE, AND IREM = N/(IFACT*IPREV).  THEN--
C     DIMENSION DATA(NPREV,IPREV,IFACT,IREM,NREM)
C     COMPLEX DATA
C     DATA(J1,J2,K3,J4,J5) = SUM(DATA(J1,J2,J3,J4,J5)*EXP(ISIGN*2*PI*I*
C     (K3-1)*((J3-1)/IFACT+(J2-1)/(IFACT*IPREV)))), SUMMED OVER J3 = 1
C     TO IFACT FOR ALL J1 FROM 1 TO NPREV, J2 FROM 1 TO IPREV, K3 FROM
```

```
C     1 TO IFACT, J4 FROM 1 TO IREM AND J5 FROM 1 TO NREM.  THIS IS    TES03850
C     A PHASE-SHIFTED DISCRETE FOURIER TRANSFORM OF LENGTH IFACT.        TES03860
C     FACTORING N BY FOURS SAVES ABOUT TWENTY FIVE PERCENT OVER FACTOR-  TES03870
C     ING BY TWOS.  DATA MUST BE BIT-REVERSED INITIALLY.                 TES03880
C     IT IS NOT NECESSARY TO REWRITE THIS SUBROUTINE INTO COMPLEX        TES03890
C     NOTATION SO LONG AS THE FORTRAN COMPILER USED STORES REAL AND      TES03900
C     IMAGINARY PARTS IN ADJACENT STORAGE LOCATIONS.  IT MUST ALSO       TES03910
C     STORE ARRAYS WITH THE FIRST SUBSCRIPT INCREASING FASTEST.          TES03920
      DIMENSION DATA(1)                                                  TES03930
      TWOPI=6.2831853072*FLOAT(ISIGN)                                    TES03940
      IP0=2                                                              TES03950
      IP1=IP0*NPREV                                                      TES03960
      IP4=IP1*N                                                          TES03970
      IP5=IP4*NREM                                                       TES03980
      IP2=IP1                                                            TES03990
C     IP2=IP1*IPROD                                                      TES04000
      NPART=N                                                            TES04010
   10 IF (NPART-2) 60,30,20                                              TES04020
   20 NPART=NPART/4                                                      TES04030
      GO TO 10                                                           TES04040
C     DO A FOURIER TRANSFORM OF LENGTH TWO                               TES04050
   30 IF (IP2-IP4) 40,160,160                                            TES04060
   40 IP3=IP2*2                                                          TES04070
C     IP3=IP2*IFACT                                                      TES04080
      DO 50 I1=1,IP1,IP0                                                 TES04090
C     I1 = 1+(J1-1)*IP0                                                  TES04100
      DO 50 I5=I1,IP5,IP3                                                TES04110
C     I5 = 1+(J1-1)*IP0+(J4-1)*IP3+(J5-1)*IP4                            TES04120
      I3A=I5                                                             TES04130
      I3B=I3A+IP2                                                        TES04140
C     I3 = 1+(J1-1)*IP0+(J2-1)*IP1+(J3-1)*IP2+(J4-1)*IP3+(J5-1)*IP4      TES04150
      TEMPR=DATA(I3B)                                                    TES04160
      TEMPI=DATA(I3B+1)                                                  TES04170
      DATA(I3B)=DATA(I3A)-TEMPR                                          TES04180
      DATA(I3B+1)=DATA(I3A+1)-TEMPI                                      TES04190
      DATA(I3A)=DATA(I3A)+TEMPR                                          TES04200
   50 DATA(I3A+1)=DATA(I3A+1)+TEMPI                                      TES04210
      IP2=IP3                                                            TES04220
C     DO A FOURIER TRANSFORM OF LENGTH FOUR (FROM BIT REVERSED ORDER)    TES04230
   60 IF (IP2-IP4) 70,160,160                                            TES04240
   70 IP3=IP2*4                                                          TES04250
C     IP3=IP2*IFACT                                                      TES04260
C     COMPUTE TWOPI THRU WR AND WI IN DOUBLE PRECISION, IF AVAILABLE.    TES04270
      THETA=TWOPI/FLOAT(IP3/IP1)                                         TES04280
      SINTH=SIN(THETA/2.)                                                TES04290
      WSTPR=-2.*SINTH*SINTH                                              TES04300
      WSTPI=SIN(THETA)                                                   TES04310
      WR=1.                                                              TES04320
```

```
      WI=0.                                                            TES04330
      DO 150 I2=1,IP2,IP1                                              TES04340
C     I2 = 1+(J2-1)*IP1                                                TES04350
      IF (I2-1) 90,90,80                                               TES04360
 80   W2R=WR*WR-WI*WI                                                  TES04370
      W2I=2.*WR*WI                                                     TES04380
      W3R=W2R*WR-W2I*WI                                                TES04390
      W3I=W2R*WI+W2I*WR                                                TES04400
 90   I1MAX=I2+IP1-IP0                                                 TES04410
      DO 140 I1=I2,I1MAX,IP0                                           TES04420
C     I1 = 1+(J1-1)*IP0+(J2-1)*IP1                                     TES04430
      DO 140 I5=I1,IP5,IP3                                             TES04440
C     I5 = 1+(J1-1)*IP0+(J2-1)*IP1+(J4-1)*IP3+(J5-1)*IP4               TES04450
      I3A=I5                                                           TES04460
      I3B=I3A+IP2                                                      TES04470
      I3C=I3B+IP2                                                      TES04480
      I3D=I3C+IP2                                                      TES04490
C     I3 = 1+(J1-1)*IP0+(J2-1)*IP1+(J3-1)*IP2+(J4-1)*IP3+(J5-1)*IP4    TES04500
      IF (I2-1) 110,110,100                                            TES04510
C     APPLY THE PHASE SHIFT FACTORS                                    TES04520
 100  TEMPR=DATA(I3B)                                                  TES04530
      DATA(I3B)=W2R*DATA(I3B)-W2I*DATA(I3B+1)                          TES04540
      DATA(I3B+1)=W2R*DATA(I3B+1)+W2I*TEMPR                            TES04550
      TEMPR=DATA(I3C)                                                  TES04560
      DATA(I3C)=WR*DATA(I3C)-WI*DATA(I3C+1)                            TES04570
      DATA(I3C+1)=WR*DATA(I3C+1)+WI*TEMPR                              TES04580
      TEMPR=DATA(I3D)                                                  TES04590
      DATA(I3D)=W3R*DATA(I3D)-W3I*DATA(I3D+1)                          TES04600
      DATA(I3D+1)=W3R*DATA(I3D+1)+W3I*TEMPR                            TES04610
 110  T0R=DATA(I3A)+DATA(I3B)                                          TES04620
      T0I=DATA(I3A+1)+DATA(I3B+1)                                      TES04630
      T1R=DATA(I3A)-DATA(I3B)                                          TES04640
      T1I=DATA(I3A+1)-DATA(I3B+1)                                      TES04650
      T2R=DATA(I3C)+DATA(I3D)                                          TES04660
      T2I=DATA(I3C+1)+DATA(I3D+1)                                      TES04670
      T3R=DATA(I3C)-DATA(I3D)                                          TES04680
      T3I=DATA(I3C+1)-DATA(I3D+1)                                      TES04690
      DATA(I3A)=T0R+T2R                                                TES04700
      DATA(I3A+1)=T0I+T2I                                              TES04710
      DATA(I3C)=T0R-T2R                                                TES04720
      DATA(I3C+1)=T0I-T2I                                              TES04730
      IF (ISIGN) 120,120,130                                           TES04740
 120  T3R=-T3R                                                         TES04750
      T3I=-T3I                                                         TES04760
 130  DATA(I3B)=T1R-T3I                                                TES04770
      DATA(I3B+1)=T1I+T3R                                              TES04780
      DATA(I3D)=T1R+T3I                                                TES04790
 140  DATA(I3D+1)=T1I-T3R                                              TES04800
```

```
      TEMPR=WR                                                          TES04810
      WR=WSTPR*TEMPR-WSTPI*WI+TEMPR                                     TES04820
150   WI=WSTPR*WI+WSTPI*TEMPR+WI                                        TES04830
      IP2=IP3                                                           TES04840
      GO TO 60                                                          TES04850
160   RETURN                                                            TES04860
      END                                                               TES04870
                                                                        TES04880
      SUBROUTINE FIXRL (DATA,N,NREM,ISIGN,IFORM)                        TES04890
C     FOR IFORM = 0, CONVERT THE TRANSFORM OF A DOUBLED-UP REAL ARRAY,  TES04900
C     CONSIDERED COMPLEX, INTO ITS TRUE TRANSFORM.  SUPPLY ONLY THE     TES04910
C     FIRST HALF OF THE COMPLEX TRANSFORM, AS THE SECOND HALF HAS       TES04920
C     CONJUGATE SYMMETRY.  FOR IFORM = -1, CONVERT THE FIRST HALF       TES04930
C     OF THE TRUE TRANSFORM INTO THE TRANSFORM OF A DOUBLED-UP REAL     TES04940
C     ARRAY.  N MUST BE EVEN.                                           TES04950
C     USING COMPLEX NOTATION AND SUBSCRIPTS STARTING AT ZERO, THE       TES04960
C     TRANSFORMATION IS--                                               TES04970
C     DIMENSION DATA(N,NREM)                                            TES04980
C     ZSTP = EXP(ISIGN*2*PI*I/N)                                        TES04990
C     DO 10 I2=0,NREM-1                                                 TES05000
C     DATA(0,I2) = CONJ(DATA(0,I2))*(1+I)                               TES05010
C     DO 10 I1=1,N/4                                                    TES05020
C     Z = (1+(2*IFORM+1)*I*ZSTP**I1)/2                                  TES05030
C     I1CNJ = N/2-I1                                                    TES05040
C     DIF = DATA(I1,I2)-CONJ(DATA(I1CNJ,I2))                            TES05050
C     TEMP = Z*DIF                                                      TES05060
C     DATA(I1,I2) = (DATA(I1,I2)-TEMP)*(1-IFORM)                        TES05070
C  10 DATA(I1CNJ,I2) = (DATA(I1CNJ,I2)+CONJ(TEMP))*(1-IFORM)            TES05080
C     IF I1=I1CNJ, THE CALCULATION FOR THAT VALUE COLLAPSES INTO        TES05090
C     A SIMPLE CONJUGATION OF DATA(I1,I2).                              TES05100
      DIMENSION DATA(1)                                                 TES05110
      TWOPI=6.283185307*FLOAT(ISIGN)                                    TES05120
      IP0=2                                                             TES05130
      IP1=IP0*(N/2)                                                     TES05140
      IP2=IP1*NREM                                                      TES05150
      IF (IFORM) 10,70,70                                               TES05160
C     PACK THE REAL INPUT VALUES (TWO PER COLUMN)                       TES05170
10    J1=IP1+1                                                          TES05180
      DATA(2)=DATA(J1)                                                  TES05190
      IF (NREM-1) 70,70,20                                              TES05200
20    J1=J1+IP0                                                         TES05210
      I2MIN=IP1+1                                                       TES05220
      DO 60 I2=I2MIN,IP2,IP1                                            TES05230
      DATA(I2)=DATA(J1)                                                 TES05240
      J1=J1+IP0                                                         TES05250
      IF (N-2) 50,50,30                                                 TES05260
30    I1MIN=I2+IP0                                                      TES05270
      I1MAX=I2+IP1-IP0                                                  TES05280
```

```
      DO 40 I1=I1MIN,I1MAX,IP0                                          TES05290
      DATA(I1)=DATA(J1)                                                 TES05300
      DATA(I1+1)=DATA(J1+1)                                             TES05310
   40 J1=J1+IP0                                                         TES05320
   50 DATA(I2+1)=DATA(J1)                                               TES05330
   60 J1=J1+IP0                                                         TES05340
   70 DO 80 I2=1,IP2,IP1                                                TES05350
      TEMPR=DATA(I2)                                                    TES05360
      DATA(I2)=DATA(I2)+DATA(I2+1)                                      TES05370
   80 DATA(I2+1)=TEMPR-DATA(I2+1)                                       TES05380
      IF (N-2) 200,200,90                                               TES05390
   90 THETA=TWOPI/FLOAT(N)                                              TES05400
      SINTH=SIN(THETA/2.)                                               TES05410
      ZSTPR=-2.*SINTH*SINTH                                             TES05420
      ZSTPI=SIN(THETA)                                                  TES05430
      ZR=(1.-ZSTPI)/2.                                                  TES05440
      ZI=(1.+ZSTPR)/2.                                                  TES05450
      IF (IFORM) 100,110,110                                            TES05460
  100 ZR=1.-ZR                                                          TES05470
      ZI=-ZI                                                            TES05480
  110 I1MIN=IP0+1                                                       TES05490
      I1MAX=IP0*(N/4)+1                                                 TES05500
      DO 190 I1=I1MIN,I1MAX,IP0                                         TES05510
      DO 180 I2=I1,IP2,IP1                                              TES05520
      I2CNJ=IP0*(N/2+1)-2*I1+I2                                         TES05530
      IF (I2-I2CNJ) 150,120,120                                         TES05540
  120 IF (ISIGN*(2*IFORM+1)) 130,140,140                                TES05550
  130 DATA(I2+1)=-DATA(I2+1)                                            TES05560
  140 IF (IFORM) 170,180,180                                            TES05570
  150 DIFR=DATA(I2)-DATA(I2CNJ)                                         TES05580
      DIFI=DATA(I2+1)+DATA(I2CNJ+1)                                     TES05590
      TEMPR=DIFR*ZR-DIFI*ZI                                             TES05600
      TEMPI=DIFR*ZI+DIFI*ZR                                             TES05610
      DATA(I2)=DATA(I2)-TEMPR                                           TES05620
      DATA(I2+1)=DATA(I2+1)-TEMPI                                       TES05630
      DATA(I2CNJ)=DATA(I2CNJ)+TEMPR                                     TES05640
      DATA(I2CNJ+1)=DATA(I2CNJ+1)-TEMPI                                 TES05650
      IF (IFORM) 160,180,180                                            TES05660
  160 DATA(I2CNJ)=DATA(I2CNJ)+DATA(I2CNJ)                               TES05670
      DATA(I2CNJ+1)=DATA(I2CNJ+1)+DATA(I2CNJ+1)                         TES05680
  170 DATA(I2)=DATA(I2)+DATA(I2)                                        TES05690
      DATA(I2+1)=DATA(I2+1)+DATA(I2+1)                                  TES05700
  180 CONTINUE                                                          TES05710
      TEMPR=ZR-.5                                                       TES05720
      ZR=ZSTPR*TEMPR-ZSTPI*ZI+ZR                                        TES05730
  190 ZI=ZSTPR*ZI+ZSTPI*TEMPR+ZI                                        TES05740
C     RECURSION SAVES TIME, AT A SLIGHT LOSS IN ACCURACY.  IF AVAILABLE,TES05750
C     USE DOUBLE PRECISION TO COMPUTE ZR AND ZI.                        TES05760
```

```
  200 IF (IFORM) 270,210,210
C     UNPACK THE REAL TRANSFORM VALUES (TWO PER COLUMN)
  210 I2=IP2+1
      I1=I2
      J1=IP0*(N/2+1)*NREM+1
      GO TO 250
  220 DATA(J1)=DATA(I1)
      DATA(J1+1)=DATA(I1+1)
      I1=I1-IP0
      J1=J1-IP0
  230 IF (I2-I1) 220,240,240
  240 DATA(J1)=DATA(I1)
      DATA(J1+1)=0.
  250 I2=I2-IP1
      J1=J1-IP0
      DATA(J1)=DATA(I2+1)
      DATA(J1+1)=0.
      I1=I1-IP0
      J1=J1-IP0
      IF (I2-1) 260,260,230
  260 DATA(2)=0.
  270 RETURN
      END
C
C
      SUBROUTINE PRPLOT(DATA,DR,IMAX,JMAX,R0)
C
C ***********************************************************************
C     THIS SUBROUTINE PLOTS THE |P(R)| VS R CURVE, STARTING AT THE
C     SOURCE AND MOVING IN A POSITIVE DIRECTION OF RANGE.
C ***********************************************************************
C
      DIMENSION DATA(4096),PMOD(2048),R(2048)
C
      IMARK = INT(IMAX/5.) + 1
      KMAX = JMAX - 1
      JMAX2 = JMAX - 2
C
      DO 30 I = 1,JMAX
      FLY = FLOAT(I)
      R(I) = R0 + FLY * DR
C      R(JMAX-I) = -R(KMAX+I)
   30 CONTINUE
C
      RMIN = R0
      RMAX = R(JMAX)
C
      WRITE(6,100)
```

```
100   FORMAT(/,3X,'I',6X,'RANGE',7X,'REALP',7X,'IMAGP',5X,'MODULUS OF P'TES06250
     1,/)                                                                   TES06260
C                                                                           TES06270
      DO 10 I = 1,JMAX                                                      TES06280
      PMOD(I) = SQRT((DATA(2*I-1))**2 + (DATA(2*I))**2)                     TES06290
C      WRITE(6,200)I,R(I),DATA(2*I-1),DATA(2*I),PMOD(I)                     TES06300
10    CONTINUE                                                              TES06310
C200   FORMAT(2X,I4,2X,F10.2,3(2X,F10.7))                                   TES06320
C                                                                           TES06330
      PMAX = -1.0                                                           TES06340
      DO 20 I = 1,JMAX                                                      TES06350
      IF(PMOD(I).GT.PMAX)PMAX = PMOD(I)                                     TES06360
20    CONTINUE                                                              TES06370
C                                                                           TES06380
      CALL COMPRS                                                           TES06390
      CALL AREA2D(4.0,6.0)                                                  TES06400
      CALL XNAME('RANGE (M)$',100)                                          TES06410
      CALL YNAME('MAGNITUDE OF PRESSURE, P(R)$',100)                        TES06420
      CALL LINESP(0.5)                                                      TES06430
      CALL HEADIN('MAGNITUDE OF PRESSURE AS A FN OF RANGE $',100,1.0,1)     TES06440
      CALL NOCHEK                                                           TES06450
      CALL GRAF(RMIN,'SCALE',RMAX,0.0,'SCALE',PMAX)                         TES06460
      CALL CURVE(R,PMOD,JMAX,IMARK)                                         TES06470
      CALL ENDPL(1)                                                         TES06480
      RETURN                                                                TES06490
      END                                                                   TES06500
C                                                                           TES06510
C                                                                           TES06520
      SUBROUTINE WTHPLT(IMAX,GM,CKM,Q,AK,BE)                                TES06530
C                                                                           TES06540
C***********************************************************************TES06550
C     THIS SUBROUTINE PLOTS THE ACOUSTIC PRESSURE SPECTRUM AS A FUNCTIONTES06560
C     OF THE HORIZONTAL WAVENUMBER                                          TES06570
C********************************************************************** TES06580
C                                                                           TES06590
      DIMENSION GM(4096),CKM(4096),Q(4096),BE(4096)                         TES06600
C                                                                           TES06610
      IMARK = INT(IMAX/5.) + 1                                              TES06620
      GMIN = GM(1)                                                          TES06630
      GMAX = AK                                                             TES06640
      PMAX = -1.0                                                           TES06650
      QMAX = -1.0                                                           TES06660
      BMAX = 0.0                                                            TES06670
      DO 10 I = 1,IMAX                                                      TES06680
      IF(CKM(I).GT.PMAX)PMAX = CKM(I)                                       TES06690
10    CONTINUE                                                              TES06700
C                                                                           TES06710
      DO 15 I = 1,IMAX                                                      TES06720
```

```
      IF(Q(I).GT.QMAX)QMAX = Q(I)
15    CONTINUE
C
      IF(PMAX.GE.QMAX)SMAX = PMAX
      SMAX = QMAX
C
C ********************************************************************
C    GMAX IS THE MAXIMUM VALUE KH CAN TAKE ON BASED ON THE EQUATION
C            ((DELTA K) * (DELTA R)) = (2 * PI/IMAX)
C
C    GMAX IS THE MAXIMUM VALUE KH CAN TAKE ON AND STILL PRODUCE "REAL"
C    THEORETICAL Q AND BETA VALUES.  KZ < SQRT(AK**2 + KH**2) => Q REAL.
C
C    SCALE THE HORIZONTAL AXIS IN KH (GM)
C ********************************************************************
C
C
      CALL COMPRS
      CALL AREA2D(4.0,6.0)
      CALL XNAME('HORIZONTAL WAVENUMBER, 1/M$',100)
      CALL YNAME('PRESSURE SPECTRUM MAGNITUDE$',100)
      CALL LINESP(0.5)
      CALL HEADIN('PRESSURE SPECTRUM VS KH$',100,1.0,1)
      CALL NOCHEK
      CALL GRAF(GMIN,'SCALE',GMAX,0.0,'SCALE',SMAX)
      CALL CURVE(GM,CKM,IMAX,IMARK)
C      CALL DOT
C      CALL CURVE(GM,Q,IMAX,IMARK)
C      CALL RESET('DOT')
      CALL ENDPL(2)
      RETURN
      END
C
C
      SUBROUTINE WTVPLT(IMAX,CKM,Q,AK,BE)
C
C ********************************************************************
C     THIS SUBROUTINE PLOTS THE PRESSURE SPECTRUM AS A FUNCTION OF THE
C     VERTICAL WAVENUMBER (BE).
C ********************************************************************
C
      DIMENSION CKM(4096),Q(4096),BE(4096)
C
      IMARK = INT(IMAX/5.) + 1
      BMAX = BE(1)
      BMIN = BE(IMAX)
      PMAX = -1.0
      QMAX = -1.0
```


6,108 Blank

LIST OF REFERENCES

1. Lauer, R. B., Signal Transmission in the Wavenumber Domain, Technical Memorandum, Naval Underwater Systems Center, New London Laboratory, New London, CT, 5 June 1979.

2. Naval Underwater Systems Center Report 4103, Fast Field Program for Multilayered Media, by F. R. DiNapoli, 26 August 1971.

3. Stamey, B. B., Preliminary Investigation of the Environmental Sensitivity of Acoustic Signal Transmission in the Wavenumber Domain with Respect to Source Depth Determination, Masters Thesis, Naval Postgraduate School, Monterey, CA, 1982.

4. Blanchard, J., A Comparison of Two Acoustic Parabolic Equation Transmission Loss Models for Compatibility with the Wavenumber Technique in the Determination of Source Depth, Masters Thesis, Naval Postgraduate School, Monterey, CA, 1984.

5. Kinsler, L., and others, Fundamentals of Acoustics, 3rd ed., John Wiley and Sons, 1982.

6. Urick, R. J., Principles of Underwater Sound, 3rd ed., Mcgraw-Hill, 1983.

7. Officer, C. B., Introduction to the Theory of Sound Transmission, McGraw-Hill, 1958.

8. Coppens, A. B., Mathematical Derivation of the Acoustic Pressure Spectrum of the Lloyds' Mirror, Naval Postgraduate School, Monterey, CA, January 1985.

9. IMSL Library Reference Manual, 9th ed., v. 2, IMSL, 1982

10. Gabrielson, T., Mathematical Derivation of the Acoustic Pressure Spectrum for the Lloyds' Mirror, Naval Postgraduate School, Monterey, CA, February 1985.

BIBLIOGRAPHY

Bergland, G. D., "A Guided Tour of the Fast Fourier Transform," IEEE Spectrum, v.6, July 1969.

Blackman, R. B. and Tukey, J. W., The Measurement of Power Spectra, Dover Publications, Inc., 1958.

Brigham, E. O., The Fast Fourier Transform, Prentice-Hall, Inc., 1974.

DiNapoli, F. R. and Deavenport, R. L., "Numerical Models for Underwater Acoustic Propagation," Ocean Acoustics, v. 1, Springer-Verlag, New York, NY, 1979.

DiNapoli, F. R. and Deavenport, R. L., "Theoretical and Numerical Green's Function Field Solution in a Plane Multilayered Media," Journal of the Acoustic Society of America, v. 67(1), January 1980.

International Series of Monographs on Electronics and Instrumentation, v.9, Pergamon Press, Inc., 1960.

Naval Surface Weapons Center Report 75-18, A Statistical Model for the Fluctuation of Sound Transmission in the Sea, Urick, R. J., 11 February 1975.

Naval Underwater Systems Center Technical Memorandum 781054, A Simplified Derivation of a Quadrature Subsampling Technique, Lackoff, M. R., 14 March 1978.

Stanton, T. K. and Beyer, R. T., "The Interaction of Sound with Noise in Water," Journal of the Acoustic Society of America, v.64(6), December 1978.

Thomas, G. B. and Finney, R. L., Calculus and Analytic Geometry, 5th ed., Addison-Wesley Publishing Company, 1979.

Urick, R.J., "Models for the Amplitude Fluctuations of Narrow-Band Signals and Noise in the Sea," Journal of the Acoustic Society of America, v. 64(6), December 1978.

INITIAL DISTRIBUTION LIST

		No. Copies
1.	Defense Technical Information Center Cameron Station Alexander, VA 22314	2
2.	Library, Code 0142 Naval Postgraduate School Monterey, CA 93943	2
3.	Chairman (Code 55Fo) ASW Academic Group Naval Postgraduate School Monterey, CA 93943	1
4.	Prof. A. B. Coppens (Code 61Cz) Department of Physics Naval Postgraduate School Monterey, CA 93943	4
5.	Prof. C. R. Dunlap (Code 68Du) Department of Oceanography Naval Postgraduate School Monterey, CA 93943	3
6.	Prof. Suk Wang Yoon (Code 61Yo) Department of Physics Naval Postgraduate School Monterey, CA 93943	3
7.	Prof. T. Gabrielson (Code 61Gt) Department of Physics Naval Postgraduate School Monterey, CA 93943	1
8.	LCDR P. B. King 425 Pine Shadows Drive Slidell, LA 70458	3
9.	Commanding Officer Naval Ocean Research and Development Activity NSTL, MS 39522	1
10.	Commanding Officer Naval Ocean Research and Development Activity (ATTN: Code 223) NSTL, MS 39522	1
11.	Office of Naval Research ATTN: Mr. R. B. Lauer Naval Ocean Research and Development Activity 800 N. Quincy Street Arlington, VA 22217	1
12.	Commanding Officer Naval Eastern Oceanography Center ATTN: LCDR J. Blanchard McAdie Bldg. (U-117) Naval Air Station Norfolk, VA 23511	1

13. LCDR B. Stamey 1
5508 Buskirk Street
North Charleston, SC 29406

14. Ms Catherine Smith 2
P. O. Box 58
Carmel Valley, CA 93924

END

FILMED

8-85

DTIC